

REPUBLIQUE ALGERIENNE DEMOCRATIQUE ET POPULAIRE

MINISTERE DE L'ENSEIGNEMENT SUPERIEUR ET DE LA RECHERCHE SCIENTIFIQUE

UNIVERSITE DES SCIENCES ET DE LA TECHNOLOGIE HOUARI BOUMEDIENE

Faculté d'Electronique et d'Informatique



Thèse De Doctorat En Sciences

Présentée pour l'obtention du grade de Docteur

En: ELECTRONIQUE

Spécialité : Contrôle de Processus et Robotique

Par : LATI Abdelhai

Sujet :

Visions et Vidéos pour les UAVs

Soutenue publiquement le 24/10/2019. Devant le jury composé de :

M. LARABI Slimane	Professeur à l'USTHB	Président
M. BELHOCINE Mahmoud	Directeur de Recherche au CDTA	Directeur de thèse
Mme. ACHOUR Nouara	Professeur à l'USTHB	Codirectrice de thèse
Mme. KOURGLI Assia	Professeur à l'USTHB	Examinatrice
M. HAMERLAIN Mustapha	Directeur de Recherche au CDTA	Examineur
M. NEMRA Abdelkrim	MCA à l'EMP	Examineur

PEOPLE'S DEMOCRATIC REPUBLIC OF ALGERIA

MINISTRY OF HIGHER EDUCATION AND SCIENTIFIC RESEARCH

UNIVERSITY OF SCIENCE AND TECHNOLOGY HOUARI BOUMEDIENE

Faculty of Electronics and Informatics



Thesis of Doctorate in Sciences

Presented for obtaining the degree of Doctor

In: ELECTRONICS

Speciality: Process Control and Robotics

By: LATI Abdelhai

Title:

Visions and Videos for UAVs

Publicly graduated on 24/10/2019 in front of the jury composed of:

Mr. LARABI Slimane	Professor at USTHB	President
Mr. BELHOCINE Mahmoud	Director of Research at CDTA	Director of Thesis
Mrs. ACHOUR Nouara	Professor at USTHB	Co-director of Thesis
Mrs. KOURGLI Assia	Professor at USTHB	Examiner
Mr. HAMERLAIN Mustapha	Director of Research at CDTA	Examiner
Mr. NEMRA Abdelkrim	MCA at EMP	Examiner

ACKNOWLEDGEMENT

I would like to thank God Almighty for giving me the strength, knowledge, ability and opportunity to undertake this research study and to persevere and complete it satisfactorily.

I would like to express my sincere gratitude to my supervisor Prof. *BELHOCINE MAHMOUD* and my co-supervisor Prof. *ACHOUR NOURA* for the continuous support of my doctorate study and related research, for their patience, motivation, and immense knowledge. Their guidance helped me in all the time of research and writing of this thesis.

I would like to thank a lot my president of jury: *Mr. LARABI SLIMANE*, Professor at USTHB for accepting to preside the jury of my graduation. I express my sharp gratitude and my respect to the members of jury: *Mrs. KOURGLI ASSIA*, Professor at USTHB, *Mr. HAMERLAIN MUSTAPHA*, Director of research at CDTA and *Mr. NEMRA ABDELKRIM*, MCA at EMP, for agreeing to examine this work.

I have great pleasure in acknowledging my gratitude to my colleagues at Ouargla University "UKMO", Prof. Benhellal Belkhir and Prof. Chaa Mourad in ensuring that the fire keeps burning and being there at times when I required motivation and also for assisting me in different ways for my research. Their support, encouragement and credible ideas have been great contributors in the completion of the thesis.

I would especially thank my wife and all my family members in particular my mother and my father for their constant support and encouragement during all my years of studies in university.

LATI ABDELHAI

Table Of Contents

Table of Contents

ACKNOWLEDGEMENT	
TABLE OF CONTENTS	I
LIST OF FIGURES	IV
LIST OF TABLES	VII
LIST OF ABBREVIATIONS	VIII
General Introduction	1
■ Introductory Descriptions	1
■ The Problems Statement	2
■ The Proposed Solutions	2
■ Thesis Organization	3
CHAPTER I: UAVs and Vision Systems	4
I.1. Introduction	4
I.2. Brief History about UAVs	5
I.3. Classifications of UAVs	6
I.4. Uses of UAVs	8
I.4.1. Aerial Reconnaissance	8
I.4.2. Scientific Research	10
I.4.3. Logistics and Transportations	11
I.5. Vision System for UAVs	11
I.6. State of the Art of Vision System for UAVs	13
I.6.1. Vision – Based Target Acquisition and Targeting	13
I.6.2. Vision – Based Flight Control	15
I.6.3. Vision – Based Navigation	16
I.6.3.1. Obstacle Detection and Avoidance	17
I.6.3.2. Simultaneous Localization And Mapping	18
I.6.3.3. Image Mosaic Construction	19
I.7. Conclusion	20
CHAPTER II: State of the Art about Image Mosaicing	21
II.1. Introduction	21
II.2. Image Mosaicing	21
II.2.1. Features Detection	22
II.2.1.1. Features from Accelerated Segment Test “FAST” detector	24
II.2.1.2. Harris corner detector	25
II.2.1.3. Scale Invariant Feature Transformation (SIFT)	27

II.2.1.4. Speed-Up Robust Features (SURF).....	29
II.2.2. Features Matching	31
II.2.2.1. Correlation based features matching.....	31
II.2.2.2. Descriptors based features matching.....	32
II.2.2.3. Features tracking based matching	33
II.2.3. Image Transformation Models	34
II.2.3.1. Geometric Transformations.....	34
II.2.3.2. Homography Matrix.....	35
II.2.3.3. Homography Estimation using DLT	36
II.2.3.4. RANSAC for Homography Refinement	37
II.2.4. Image Re-projection	37
II.3. Related Works about Image Mosaicing.....	39
II.3.1. Correlation Based Methods	39
II.3.1. Descriptors Based Methods.....	41
II.4. Conclusion	47
CHAPTER III: The Proposed Fuzzy Matching Algorithms	48
III.1. Introduction	48
III.2. Proposed Contributions	48
III.3. Fuzzy Correlation Based Features Matching	49
III.3.1. Correlation Measures.....	49
III.3.1.1. Sum of Absolute Difference (SAD)	49
III.3.1.2. Zero-Mean Sum of Square Difference (ZSSD).....	49
III.3.1.3. Normalized Cross Correlation (NCC).....	50
III.3.2. Fuzzy Correlation Inference System	50
III.4. Fuzzy ILBP Based Features Matching.....	51
III.4.1. LBP Technique	51
III.4.1.1. Improved LBP Descriptor	52
III.4.1.2. Hamming Matching Distance.....	53
III.4.2. Fuzzy ILBP Inference System	53
III.5. Fuzzy RANSAC Based Outliers Rejection Method	54
III.5.1. RANSAC Technique	54
III.5.2. Bidirectional Technique.....	55
III.5.3. Fuzzy RANSAC Inference System.....	56
III.6. Fuzzy Image Mosaicing Algorithm.....	56
III.6.1. Points Based Features Detection	57
III.6.1.1. Harris Algorithm.....	57
III.6.1.2. SIFT Algorithm	58
III.6.2. Fuzzy Features Matching	58

III.6.2.1. Fuzzy Correlation.....	58
III.6.2.2. Fuzzy ILBP	60
III.6.2.3. Fuzzy RANSAC	61
III.6.3. Homography Estimation.....	63
III.6.4. Image Warping and Blending	63
II.7. Conclusion	64
CHAPTER IV: Results and Evaluations	65
IV.1. Introduction	65
IV.2. Simulation Results	66
IV.2.1. Image Acquisition	66
IV.2.2. Evaluations of Harris/ SIFT based features detection	67
IV.2.3. Evaluations of Fuzzy Features Matching	69
IV.2.3.1. Performance Measures.....	72
IV.2.4. Linear Estimation of Homography Parameters	74
IV.2.5. Backward Image Warping and Interpolation Blending	74
IV.3. Tests of Mosaicing Aerial Images.....	75
IV.4. Tests of Mosaicing Different Images.....	77
IV.5. Comparison with Literatures	78
IV.6. LabVIEW Implementation	81
IV.6.1. LabVIEW Platform.....	81
IV.6.2. Implementation of image mosaicing on LabVIEW	83
IV.6.2.1. Test 1: Smart phone images.....	85
IV.6.2.2. Test 2: Medical images	87
IV.6.2.3. Test 3: UAV images	88
IV.6.2.4. Test 4: Satellite images	89
IV.6.3. Implementation of Features based object tracking on LabVIEW.....	91
IV.6.3.1. State of the Art about Object Tracking.....	91
IV.6.3.2. Results of Object Tracking on LabVIEW	92
IV.7. Conclusion	95
General Conclusion.....	96
■ Conclusions about Thesis	96
■ Perspectives for Futures Works	97
References	98
Scientific Products	
Appendix : Non-Linear Algorithms for homography estimation	

List Of Figures

List of Figures

Figure I-1: The most important applications of UAVs.....	4
Figure I-2: An MQ-9 Reaper, a hunter-killer surveillance UAV	9
Figure I-3: The DRS RQ-15 Neptune	9
Figure I-4: Aerial photograph of an alligator near Lake Okeechobee taken from the Nova 2.1 UAV	10
Figure I-5: The AR-Drone quad copter	10
Figure I-6: Mini-drone delivers a parcel	11
Figure I-7: (a) PTZ camera, (b) stereo-vision camera	12
Figure I-8: Window being tracked during UAV flight.....	13
Figure I-9: Flight Test of the Glider (a) image taken during flight, (b) image processing results.....	14
Figure I-10: DJI M100 quad copter	16
Figure I-11: UAV for obstacle detection for obstacle avoidance	18
Figure I-12: The quad rotor with embedded vision system.	18
Figure II-1: Principle of FAST corner detection.....	25
Figure II-2: Types of features with Harris algorithm, (a) Region, (b) edge, (c) corner	25
Figure II-3: Principle of Difference of Gaussian (DoG)..	27
Figure II-4: SIFT descriptor generation.....	28
Figure II-5: The approximations of Gaussian second order partial derivatives by box filters.....	30
Figure II-6: Description of SURF features.	31
Figure II-7: Searching for candidates matches in template image using correlation method.	31
Figure II-8: Homography between three overlapped images..	36
Figure II-9: Mosaic rendering by re-projection onto a cylindrical and planar manifold..	38
Figure II-10: Categories of image mosaicing algorithms..	39
Figure II-11: a) Two overlapped images captured by the UAV. b) The obtained image mosaic [77].	41
Figure II-12: Image mosaic of two successive images seen by a camera embedded on an UAV [23].	42
Figure II-13: The developed EsiReg Interface [78].....	42
Figure II-14: A planar mosaic of Keble College, Oxford automatically generated from 60 images captured using a handheld video camera [57].....	43

Figure II-15: (a) Mosaic before mismatch elimination, (b) mosaic effect after mismatch elimination.	44
Figure II-16: Illustration of UAV-based applications with computer and Google Earth.	44
Figure II-17: Image registration result of the UAV image sequence onto the satellite image	45
Figure III-1: The used Fuzzy correlation algorithm.....	51
Figure III-2: Construction of LBP descriptor.....	52
Figure III-3: ILBPDs for different values of points (P) and radius (R).....	52
Figure III-4: The used Fuzzy ILBPDs algorithm.....	54
Figure III-5: Illustrating example of checking the bidirectional condition	55
Figure III-6: Diagram of the proposed Fuzzy RANSAC based algorithm.	56
Figure III-7: Flow chart for the proposed image mosaicing algorithm.	57
Figure III-8: Algorithm for detecting SIFT features	58
Figure III-9: (a) The first input membership function (MF) ‘hamming distance’(d _h). (b) The second input membership function ‘Belongingness to R1 or R2’. (c) The output MF ‘match/ no match’.....	60
Figure III-10: Backward image warping.....	63
Figure III-11: Blending based on interpolation	64
Figure IV-1: The various stages of image mosaicing algorithm	65
Figure IV-2: Capturing aerial images by UAV	66
Figure IV-3: (a) and (b) Two successive images seen by a camera embedded on an UAV	66
Figure IV-4: a) and b) Features detected in both images by Harris detector.....	67
Figure IV-5: a) and b) Features detected in both images by SIFT detector	67
Figure IV-6: Evaluation of SIFT and Harris detectors under different scale changes.....	69
Figure IV-7: Feature matching using correlation method (SAD).....	70
Figure IV-8: Outliers rejection using fuzzy correlation based method.....	70
Figure IV-9: Feature matching using Improved LBP descriptor.....	71
Figure IV-10: Outliers rejection using fuzzy based LBP method.....	71
Figure IV-11: Feature matching using LBP descriptor	72
Figure IV-12: Outliers rejection using fuzzy RANSAC based method	72
Figure IV-13: Image mosaic (a) after geometric registration, (b) after blending	74
Figure IV-14: a) Left side of montain, b) Right side of montain, c) Image mosaic of the two images.....	75

Figure IV-15: a) Lower side of road, b) Upper side of road, c) Image mosaic of the two images of road ...	76
Figure IV-16: a) Left side of bridge, b) Right side of bridge, c) Image mosaic of the images of bridge	76
Figure IV-17: a) Left image inside laboratory, b) Right image inside laboratory, c) Obtained mosaic	77
Figure IV-18: a) Left image in front of faculty, b) Right image in front of faculty, c) Obtained mosaic.....	78
Figure IV-19: Front panel of LabVIEW of image compression algorithm.	81
Figure IV-20: General block diagram of LabVIEW	82
Figure IV-21: Necessary steps for performing LabVIEW-FPGA embedded system	82
Figure IV-22: Acquisition of the overlapped satellite image.....	83
Figure IV-23: Features detection by Harris detector	84
Figure IV-24: Features matching using FREAK descriptors	84
Figure IV-25: Image mosaic by applying backward warping	85
Figure IV-26: (a) overlapping smart phone images, (b) features detection by Harris detector, (c) finding correspondences using FREAK descriptors, (d) the obtained image mosaic and details.....	86
Figure IV-27: (a) overlapping medical images, (b) features detection by Harris detector, (c) finding correspondences using FREAK descriptors, (d) the obtained image mosaic and details.....	88
Figure IV-28: (a) overlapping images of drone, (b) features detection by Harris detector, (c) finding correspondences using FREAK descriptors, (d) the obtained image mosaic and details.....	89
Figure IV-29: (a) overlapping satellite images, (b) features detection by Harris detector, (c) finding correspondences using BRISK descriptors, (d) the obtained image mosaic and details	90
Figure IV-30: The method proposed for object tracking flowchart.....	92
Figure IV-31: Interface of features based object tracking	93
Figure IV-32: Car tracking (detected object within green trapezium).	93
Figure IV-33: object (Arduino) detection and tracking.	94

List Of Tables

List of Tables

Table I-1. Possible classification of UAVs.....	7
Table I-2. UAV build types [12].....	7
Table II-1. Different types of image transformations.....	34
Table III-1. Parameters of inputs fuzzy MFs	58
Table III-2. Fuzzy rules for correlation based matching	59
Table III-3. Fuzzy RANSAC rules base.....	62
Table IV-1. Effect of Harris threshold on detected corners.....	68
Table IV-2. Effect of window size value on features matching	70
Table IV-3 Important statistics of the obtained ILBP results.....	71
Table IV-4. Important statistics of the obtained fuzzy RANSAC results	78
Table IV-5. Comparison of RMSE values of some related works	79
Table IV-6. Comparison of recall values with literatures.	79
Table IV-7. Comparison of time cost of the proposed algorithm with other methods	80

List Of Abbreviations

List of Abbreviations

BRIEF	Binary Robust Independent Elementary Features
BRISK	Binary Robust Invariant Scalable Key points
CS-LBP	Centre Symmetric Local Binary Pattern
DLT	Direct Linear Transformation
DoG	Difference of Gaussians
ERAST	Environmental Research Aircraft and Sensor Technology
FANNS	Fast Approximate Nearest Neighbor Search
FAST	Features from Accelerated Segment Test
FOV	Field Of View
FPGA	Field Programmable Gate Array
FREAK	Fast RETinA Key points
GA-ASI	General Atomics Aeronautical Systems
GCS	Ground Control Station
GPS	Global Positioning System
HALE	High Altitude Long Endurance
INS	Inertial Navigation System
KLT	Kanade Lucas Tomasi tracker
LabVIEW	Laboratory Virtual Instrumentation Engineering Workbench
LBPD	Local Binary Patterns Descriptor
LoG	Laplacian of Gaussians
LSE	Least Squares Estimation
MALE	Medium Altitude Long Endurance
MATLAB	MATrix LABoratory
MI	Mutual Information

MLE	Maximum Likelihood Estimate
MTOW	Maximum Take-Off Weight.
MUAV	Micro and Mini UAV
NASA	National Aeronautics and Space Administration
NCC	Normalized Cross Correlation
NND	Nearest Neighbor Distance
PC	Personal Computer
PTZ camera	Pan – Tilt- Zoom camera
RAM	Random Access Memory
RANSAC	RANdom SAmples Consensus
RGB	Red Green Blue
RMSE	Root Mean Squared Error
SAD	Sum of Absolute Differences
SLAM	Simultaneously Localization and Mapping
SSD	Sum of Square Differences
SURF	Speed Up Robust Features
SVD	Singular Value Decomposition
UAV	Unmanned Aerial Vehicle
UK	United Kingdom
USA	United State of America
USAF	United States Air Force
VI	Virtual Instrument
VTOLUAV	Vertical Take-off Landing UAV
ZSSD	Zero Sum of Squared Differences
2D	2 Dimensions
3D	3 Dimensions

General Introduction

General Introduction

➤ Introductory Descriptions

In recent years, scientific research and commercial investment on Unmanned Aerial Vehicles (UAVs) have increased considerably, and have led to the design of several types of aerial aircrafts. The main challenge of most aerial applications is to develop self-operating air agents capable of performing tasks independently of human interaction. For that, optical sensor techniques have been integrated into the UAV structure to enhance its missions. The vision based applications of UAVs can be categorized into different types according to the research topics; however they mostly share some basic image processing operations.

Due to lower cost of UAV imaging in some critical tasks, when compared to the conventional imaging techniques, it has become more common in many engineering domains and applications, but, the use of low-resolution non-metric digital cameras for this technology has significant problems in image processing automation. In the image acquisition phase, the camera display criteria (shutter speed and aperture value) and weather conditions have significant effects on the quality of the acquired images. Other factors that determine the geometry accuracy are the effects of the motion angle and the tilt of the image. The latter mainly results from vehicle stability, which can be influenced by engine vibration, turbulence and sudden wind flow [1].

Aerial image collection and processing methods provide a broad range of research in terms of creating new solutions and improving existing solutions for the accuracy of imaging tools. Today, professional tried to prevent UAV camera movement during acquiring data. Unfortunately, UAVs rarely give a stable camera position because of internal and external conditions. Thus, the obtained sequence of images can contain unclear and blurred images that cause confusion in the automatic processing of aerial data. These blurred images should be filtered manually, which is cumbersome to the eyes and prone to errors and time. By eliminating blurry images, the number of images is reduced and can adversely affect the result of aerial data processing [2].

In computer vision and image processing, several methods have been developed in previous works to detect whether the images are clear or not. A widely used application for automatic blur detection is the "auto focus" system in cameras, which should prevent the user from taking blurry images resulting from inappropriate focus setting or camera motion [3].

➤ The Problems Statement

For aerial imaging, small UAVs are very receptive to changes in air currents; and fast movements of them with a reduced field of view make it difficult for user to follow causing disorientation. In other applications, it is often required to enlarge an area to display details of objects of interest, thereby reducing the field of view, thereby reducing the environmental awareness of the operator. Most of the proposed approaches for image blur elimination and improving resolution are affected by some camera parameters or UAV speed, thus, they cannot guarantee obtaining good results in most cases.

Stitching overlapping views captured from aerial platform is known as image mosaicing, this algorithm is being used to enhance quality of UAV images, but mosaic techniques require that terrain features be matched to adjacent images as much as possible. Because, overlapping images can be taken at different orientations and displacement, it is a real difficulty to match the corresponding features with adjacent images when mosaic is assembled.

➤ The Proposed Solutions

Image mosaicing is based mainly on the used technique for features matching, in which a good performance of this stage ensures getting good mosaic. Our main contributions are:

- 1) Using Local Binary Patterns (LBP) technique in image mosaicing algorithm, this approach was frequently used for face recognitions and textures classifications. And improving the performances of the used LBP approach, either in term of execution time or in term of number of good matches.
- 2) Enhancing the performance of RANdom SAmple Consensus (RANSAC) algorithm for removing outliers by imposing a bidirectional condition technique, and proposing a fuzzy inference system for eliminating most of false matches.
- 3) Improving the performance of correlation based features matching by proposing fuzzy inference system that links different correlation measures, and other inference system to enhance the performance of LBP based features matching.
- 4) Creating a practical execution interface on LabVIEW platform, this allowed the user to upload overlapping images and get the result with one order; also this interface can be used to implement our algorithms on embedded systems.

For understanding clearly our project, after introducing the main interests of our research; we have divided our thesis into four main chapters; which are clearly defined in the next section.

➤ **Thesis Organization**

□ Chapter I is a general description of UAVs types and classifications, and a state of the art about the important applications of aerial vision systems, these applications were classified into: target acquisition, flight control, and navigation.

□ Chapter II covers the important steps of image mosaicing algorithm with related works about existing approaches for performing aerial mosaics construction, in which we have focused on works that used some outliers rejection techniques.

□ Chapter III presents the proposed fuzzy based outliers rejection methods for ensuring good mosaic results, these methods are: fuzzy correlation based technique, fuzzy LBP based technique and fuzzy RANSAC based technique.

□ Chapter IV focuses on methodology and steps that we followed to perform for obtaining the Matlab simulation results. After evaluating the results of the different proposed approaches, LabVIEW implementation of image mosaicing was detailed in this chapter. At the end, we finish our report by general conclusions and future works.

Chapter I :

UAVs and Vision Systems

I. UAVs and Vision Systems

I.1. Introduction

UAVs are commonly used in both military; and civilian applications .This applications can be categorized as “the dull, the dirty, and the dangerous missions”; where the risk of sending a human piloted aircraft is unacceptable or impractical [4]. When compared to manned aerial vehicles, UAVs are believed to provide important benefits - they do not contain, or need a qualified pilot on board, and they reduce the exposure risk of the aircraft operator. Also they are able to stay in the air for much longer as they are not constrained by a human’s (pilot’s) physical limits. However, losing a UAV costs millions, and computer systems or software could break down; resulting in loss of UAV mission. Thus, improved safety and reliability for UAVs are still required.

Unmanned aircrafts can fly autonomously, or be piloted remotely; however, modern UAVs are controlled with both autopilots, and human controllers in ground stations [5]. This allows them to fly long, uneventfully flights under their own control, and fly under the command of a human pilot during complicated phases of mission; such missions are shown in **Figure I-1**.

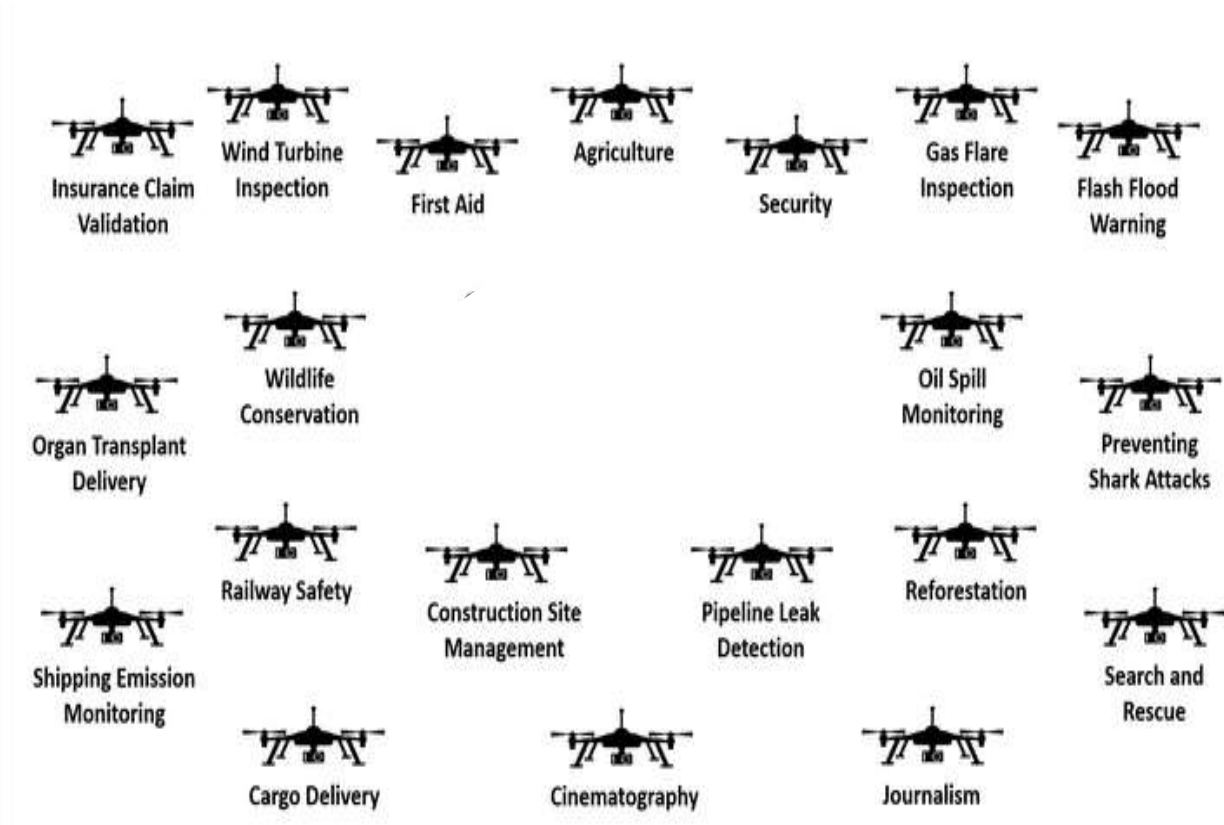


Figure I-1: The most important applications of UAVs.

Despite UAVs systems have no on-board human pilots; they require a high amount of human development and involvement, to accomplish successful operations. A typical modern UAV system involves a launch crew (1-3 people), a mission crew (2-5) people [6]. Thus, there is a significant amount of human-human and human-vehicle interaction involved in UAV system operations. Much of this collaboration is done between geographically distributed people (e.g. the mission crew may be in the United States while the launch crew and information consumers may be in Afghanistan).

Growth in the UAV industry has been increased and the use and capabilities of UAVs have grown rapidly. This is due to increased military and civilian usage, as well as the availability of better sensors, lighter and stronger aircraft structures, more powerful and smaller computers, better aircraft-to-ground communications. Besides, with the advances in technology, futuristic UAVs are expected to become increasingly autonomous, in current UAV missions, it is usual to have multiple operators responsible for a single UAV, however, futuristic UAV missions are expected to have single operators controlling multiple UAVs.

I.2. Brief History about UAVs

Historically; the first pilotless aircrafts, called aerial torpedoes, were developed shortly after the First World War and resembled modern cruise missiles. The current UAVs originate mostly from radio controlled pilotless target aircrafts built in the US and UK in the 1930s [7]. The first UAVs developed for surveillance were not utilized until the Vietnam War, where many Fire bee drones were introduced for simple reconnaissance activities. Initially, these drones were equipped with simple cameras and later fitted with communications, night photo and electronic intelligence.

In the late 1970s and early 1980s, the Israeli Air force successfully utilized UAVs in war [8]. Since then, UAVs have been playing a critical role in US military operations and continue to expand, covering a wide range of mission capabilities [9]. In addition, innovative technologies in areas such as UAV control, communication technology, processors, data link systems, payload technologies, sensors, propulsion and weaponry are ongoing at major military and aerospace organizations. The American Environmental Research Aircraft and Sensor Technology (ERAST) project was a very important research project which promoted and enabled the use of UAS in the civilian sphere early on. This National Aeronautics and Space Administration (NASA) project sought to develop unmanned aircraft that could be employed for extended scientific missions [10].

A recent study of the worldwide UAV market concluded that U.S. spending on UAVs amounted to about 73% of worldwide research and production spending in 2003 [10-11]. The U.S. dominated this market in recent years due, in part, to the depth of research and wide range of production programs. UAV development has been spotty, with clear leadership in endurance UAVs but laggard performance in fielding tactical UAVs, especially compared with Europe.

Europe currently represents the second-largest UAV market. While quite a bit of research has been funded in Europe over the past decade, procurement has been modest and mostly confined to small numbers of tactical UAV systems [11]. Non-European countries also have a significant UAV role. Israel, which was the pioneer for many of the current tactical UAV efforts, has continued to be a major player in UAV sales to smaller armed forces around the globe. Israel continues to innovate in the UAV field.

I.3. Classification of UAVs

The unmanned aircrafts come in different sizes, from the size of an insect to that of a commercial airliner. They can range from full-sized (and costly) aircraft to ones that weigh a few ounces, the unmanned aircraft of interest need to be large enough to carry cameras and other sensors that can be used for roadway monitoring and surveillance but also portable enough to be carried in some vehicles for some applications.

UAVs can be classified into different functional categories, either for military or non-military tasks; however they can also be categorized in terms of these four characteristics:

- Range.
- Flight altitude.
- Endurance.
- Maximum Take-Off Weight (MTOW).





Table I-1 classifies UAVs into several categories. The ranges of values given for each characteristic are examples which need not necessarily to be strictly applied to all systems in a defined category [10]. Based upon the values listed for each of the four characteristics, it is clear that a strict separation between different categories or classes is not possible, as certain characteristics overlap one another or are identical.

Table I-1: Possible classification of UAVs [10].

Category	Range (Km)	Flying Altitude (m)	Endurance (h)	MTOW (Kg)	Example
Micro and Mini UAV (MUAV)	< 10	300	< 2	< 30	Md4-200
Medium Altitude Long Endurance (MALE)	> 500	15000	24 - 48	1500 - 7000	Talarion Predator
High Altitude Long Endurance (HALE)	> 2000	20000	24 - 48	4500-15000	Global Hawk
Vertical Take-off Landing UAV (VTOLUAV)	x - 204	x - 6100	-0.18 - 8	0.019 - 1400	MQ-8 Fire Scout

Other major distinctions are the build type and the used engine. **Table I-2** gives a brief overview of the advantages and disadvantages of different build types of UAVs:

Table I-2: UAV build types [12].

Type	Advantages	Disadvantages	Example
Fixed Wing	*Long range *Endurance	*Horizontal take-off, requiring substantial space or support. *Inferior manoeuvrability compared to VTOL (Vertical Take-Off and Landing).	 Indra
Tilt –Wing	*Combination of fixed-wing and VTOL advantages	*Technologically complex *Expensive	 SUAS News
Unmanned Heli-copter	* VTOL *Manoeuvrability *High payloads possible	*Expensive *Comparably high maintenance requirements	 Swiss UAV
Multi-copter	*Inexpensive * Easy to launch * Low weight	*Limited payloads *Susceptible to wind due to low weight	 Micro-drones

I.4. Uses of UAVs

Since their creation, UAVs have found many uses in police, military, and also in civilian applications. Currently, most of UAVs are used for the following tasks:

- Aerial reconnaissance.
- Logistics and transportation.
- Scientific research.

I.4.1 Aerial Reconnaissance

Reconnaissance or surveillance can be defined as the near observation of person's behaviors or buildings, for managing, influencing, directing, or protecting them. There are different surveillance methods, such as GPS tracking, camera surveillance and biometric monitoring. Some problems are associated with the mentioned techniques, and UAVs gave the ideal solution to overcome the limitations faced by other surveillance methods, in which they present an easier, faster, and cheaper method of acquiring data.

The UAVs can enter narrow and confined spaces, produce minimal noise, and can be equipped with night vision cameras and thermal sensors, allowing them to provide imagery that the human eye is unable to see [13]. Aerial reconnaissance, surveillance, and other observation tasks have been primary aircraft applications since the early days of powered flight. They remain key activities in domains from military and security operations. However, airborne observation is typically a deadly dull process that strains the vigilance and morale of human pilots and makes poor use of their costly, hard-won skills. Thus, following the rule of “dull, dirty or dangerous,” it is considered an excellent application for autonomous vehicles. UAVs have been employed in this capacity for decades, though almost exclusively for reconnaissance [14].

Technological improvements combined with increasing investment and interest in UAVs promise to increase their capabilities and availability, thus enabling more diverse and demanding missions. Of particular interest to several operational communities are missions using UAVs to maintain “situation awareness” by continuous or periodic surveillance [12]. UAVs are often used to get aerial video of a remote location, especially where there would be unacceptable risk to the pilot of a manned aircraft. UAVs can be equipped with high resolution still, video and even infrared cameras. The information obtained by the UAV can be streamed back to the control center in real time [15], **Figure I-2** shows example of this UAV called MQ-9 Reaper.



Figure I-2: An MQ-9 Reaper, a hunter-killer surveillance UAV.

MQ-9 Reaper is surveillance UAV; it is developed by General Atomics Aeronautical Systems (GA-ASI) for the United States Air Force (USAF). It is being used by US Air force and NASA. MQ-9 Reaper is the first hunter killer UAV designed for long-endurance, high-altitude surveillance. It has fast speed, strong engine and great capability of carrying payload and cruise; it can be monitored and controlled by aircrew in the Ground Control Station (GCS). All of these properties makes it especially useful for long-term loitering operations, both for surveillance and support of ground troops [16]. **Figure I-3** shows other type of mobile, low-footprint tactical surveillance UAV called RQ-15 Neptune.



Figure I-3: The DRS RQ-15 Neptune.

The RQ-15 Neptune is developed in the United States and it can be operated from land or sea. It can be pneumatically auto launched in a matter of minutes. It specifically addresses tactical operations over land or water where formal runway systems are unavailable. The six-foot launcher allows the aircraft to be deployed from utility vehicles or small surface vessels supporting operations day or night, on land or at sea [17].

I.4.2 Scientific Research

In many cases, scientific research necessitates obtaining data from hazardous or remote locations, as shown in **Figure 1-4**. A good example is hurricane research; which involves sending a large manned aircraft into the center of a storm to obtain meteorological data. A UAV can be used to obtain this data, with no risk to a human pilot [18]. The growing use of UAVs for research now is due partly to the miniaturization of scientific instrumentation, which is opening up new applications as the aircraft can be outfitted with a wider array of sensors. The growth has also been spurred by the retirement of military equipment, which several government agencies have gladly repurposed and redeployed.



Figure 1-4: Aerial photograph of an alligator near Lake Okeechobee taken from the Nova 2.1 UAV.

The AR-Drone quad copter shown in **Figure 1-5** caught attention of universities and research institutions, and nowadays is being used in several research projects.



Figure 1-5: The AR-Drone quad copter.

The AR-Drone has been used for experiments in aerial visual autonomous navigation in structured environments [19]. Moreover, some machine learning approaches were involved to predict the position errors of the UAV following desired flight trajectories.

Other researchers used the drone as experimental platforms for human-machine interaction [20], and even as a sport assistant, by providing external imagery of athletes' actions.

I.4.3 Logistics and Transportation

Logistics is a key competitive factor for companies. To be successful in the competition, one is reliant on dependable, efficient and innovative logistics. Logistics involves management, storage and supervision of the transport of goods. Outstanding logistics means customer satisfaction. Speed is still an important factor for a successful logistics process. For logistics, especially at close range, the quick delivery and pickup by drone from the air is a future option in addition to the standard transport of products and goods.

The areas of application are firstly the internal and external transportation and shipping, as well as the distribution of goods. In the area of spare part transport (spare part logistics) speed is the decisive factor. Machine failures often lead to loss of production and thus revenue. The fast and efficient transport of spare parts by drone (**Figure I-6**) within large plants is the first segment of the huge field of transportation on which scientists concentrated [21].



Figure I-6: Mini-drone delivers a parcel.

Small UAVs have found their way to civil applications. A broad variety of UAV models has been developed and commercialized in the past few years and is available today for end users. UAVs fly routes in an autonomous manner, carry cameras for aerial photography, and may transport goods from one place to another. UAVs can be used to carry and deliver a variety of payloads. Helicopter type UAVs are well suited to this purpose, because payloads can be suspended from the bottom of the airframe, with little aerodynamic penalty.

I.5. Vision Systems for UAVs

Since a long time, integrating vision systems in UAVs became an exciting field in academic research and industrial applications. Vision sensors with other avionic sensors can greatly extend functions of unmanned vehicles to variety of tasks, such as vision-based reconnaissance, surveillance and target acquisition. Vision's sense plays a very important

role in our daily lives. It is a great evolutionary advantage gained to make moving or hunting more efficient. Similarly, a vision sensor for UAV is as its pair of eyes to obtain information of designated targets and environments. Vision sensing technologies for UAVs have the following advantages [22]:

1. The capability of providing rich information of objects of interest and the surrounding environments, including geometry of the scene, photometry of the object.
2. They require only natural light and do not depend on any other signal source, such as beacon stations or satellite signals.
3. They are generally of low cost and light weight compared to other related sensing systems such as radars.
4. They do not emit any energy, so that the whole system is almost undetectable and safer in special conditions, such as battlefields.

Aerial vision is a sensor, which is capable to give the most complete information “what” and “where” of objects that is likely to be faced by an aerial robot. People have an active vision system, therefore; we are able to focus on certain areas of interest in a scene through eye and head movements or just by diverting attention to the different parts of the seen images. Vision system for UAV can choose some aerial information for some aerial applications using different types of visual sensors as shown with figure (Figure I-7).



Figure I-7: (a) PTZ camera, (b) stereo-vision camera.

Figure I-7 shows two cameras with different characteristics, these cameras can acquire visible aerial images that are clearer than infrared or thermal ones, because they can be displayed in the same colors, shadows, and intensity as seen by the human eye [23]. Visual cameras have demonstrated a strong cognitive ability, making them highly used in navigation and mapping in robots, but they still have a number of drawbacks. The images taken by the camera need a large storing memory, and for detecting interest regions, numerous image processing algorithms should be processed and implemented.

I.6. State of the Art of vision systems for UAVs

Depending on how to use extracted vision information, the applications of vision systems for UAVs can be roughly divided into several categories:

I.6.1 Vision-based Target Acquisition and Targeting

Vision information is used to search and identify the target of interest, and estimate the relative distance and orientation of the target with respect to the UAV. The estimated information is used to guide the UAV to follow the target. Several interesting works were done in this domain. To detect and track a specified building, a vision system for an unmanned helicopter was presented in [24], in which two feature tracking techniques were applied and analyzed. A model-based tracking algorithm was proposed based on a second order kinematic model and Kalman filtering technique. Visual sensing was used for estimating the position and velocity of features in the image plane (urban features like window) in order to generate velocity references for the flight control. These visual-based references were then combined with GPS-positioning references to navigate towards these features and then track them. **Figure I-8** shows result of an implementation of the algorithm, which was used to track four points corresponding to four corners of a window. A gray level version of the captured image is used for this purpose.



Figure I-8: Window being tracked during UAV flight.

The implemented vision system in this project, allowed such robots to serve as intelligent eyes-in-the-sky suitable for numerous important applications; including law enforcement, search and rescue, aerial mapping and inspection, and movie making.

In [25], the authors presented a real-time visual tracking approach based on a geometric active contour method, which was capable of realizing air-to-air tracking of a fix-wing airplane. Using a single onboard vision sensor for relative navigation itself is an important contribution in that it significantly reduces the cost and complexity of airborne navigation systems that rely on GPS, INS and related communication systems.

In [26-27], a small-size glider was developed to fly automatically to a specified target with information from an on-board vision sensors only. A fast image processing algorithm, executed in a ground station, was proposed to detect the target. An extended Kalman filtering technique was also used to estimate the states of the glider with information extracted from the captured images. Based on desired flying characteristics and the payload requirements, a 2-meter 2-axis glider was chosen. The glider is equipped with elevator and rudder, and the two meter wing span provides sufficient payload capacity to ensure a very slow stall speed with the additional weight from the video system. **Figure I-9** shows a photo taken during the flight depicted in the following plots and onboard images with the results of the image processor. During this flight the image processor tracked the window all the way to the end of the flight process, and the glider hit the center of the window. The glider was launched by hand, from an altitude of 15 ft above the window, and the window was approximately 100 ft from the launch site.

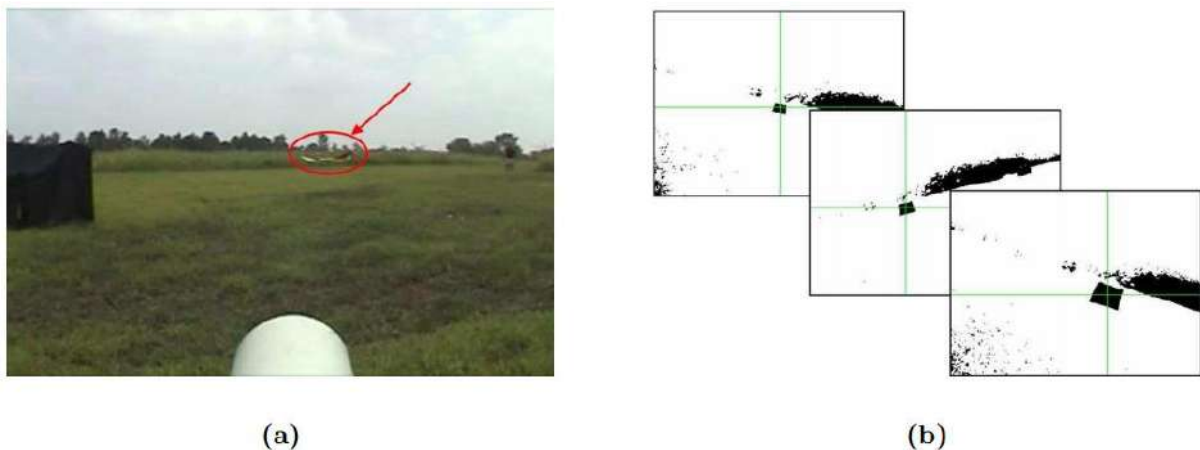


Figure I-9: Flight Test of the Glider (a) image taken during flight, (b) image processing results.

As a special case of target acquisition and targeting; vision-based landing represents a recent research issue. Vision-based system for landing a UAV on a ground pad was reported in [28]. A differential ego-motion estimation approach was employed to observe the states of the UAV with known initial values, including the relative position and velocity. These estimates were integrated with the flight control as a state observer to realize autonomous landing. However, this work was mostly focused on simulation.

In the literature [29], for determining the location of a ground based target viewed from an UAV; an interesting method was proposed. This method was based on using a range finder, and determining the pixel coordinates on the video frame; the target's geo-location was determined in the North-East-Down (NED) frame. The contribution of this method was that the target could be localized to within 9m when view from an altitude of 2500m and down to 1m from an altitude of 100m. This method offered a highly versatile tracking and geo-localization technique that had very good number of advantages over the previously suggested methods, such as; operating day and night in all weather conditions.

Another work [30] dealt with visual tracking for a camera embedded in a drone. The main idea of this project was to transmit video to the ground where images were processed on a PC, and sending back commands to the drone. The objective was to track any fixed object on the ground without knowledge about shape or texture and to keep it centered in the image. In order to achieve this task an algorithm that combines feature-based and global motion estimation was proposed. This algorithm provided a good robustness to very strong video transmission noise and works at a frame rate close to 25 fps. The control of the system is based on a double closed loop, which achieves a fast convergence to the desired position. Experimentation in real conditions showed the effectiveness of the proposed scheme. Despite several works were done in vision-based detection and tracking, real time processing and the complex environment surrounding UAVs are still the main constraints of implementing vision-systems for UAVs [31].

I.6.2 Vision-based Flight Control

The purpose of the vision-based flight control is to use vision information to estimate relative motion of a UAV to the surrounding environment. Normally, such estimated motion is integrated with inertial sensors to obtain the displacement and velocity of the UAV, which are used in the feedback control to stabilize the UAV.

In one work [32], various ideas and approaches were explored to deal with the inherent uncertainty and image noise in motion analysis, and develop a low complexity, accurate and reliable scheme to estimate the motion fields from UAV navigation videos. The motion field information allowed the authors to accurately estimate ego-motion parameters of the UAV and refine the motion measurements from other sensors. Based on the motion field information, they computed the range map for objects in the scene. Once they had accurate knowledge about the vehicle motion and its navigation environment, control and guidance laws could be designed to navigate the UAV between way points and avoid obstacles.

In [33], authors proposed a new control method that allows a micro UAV of **Figure I-10** to land autonomously on a moving platform in the presence of uncertainties and disturbances.

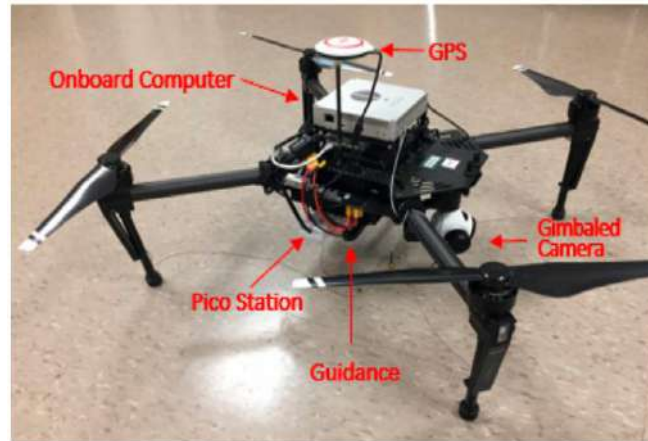


Figure I-10: DJI M100 quad copter.

The suggested control method was implemented in a low-cost, lightweight embedded system that could be integrated into micro UAVs. The presented method consisted of vision-based target following, optimal target localization, and model predictive control, for optimal guidance of the UAV. The obtained results demonstrated the efficiency and robustness of the algorithm with wind disturbances and noisy measurements.

In [34], an implementation of an aircraft poses and motion estimator was presented; using visual systems as the principal sensor for controlling an unmanned aircraft or as a redundant system for an Inertial Measure Unit (IMU) and gyros sensors. First, the authors explored the applications of the united theory for central cameras for attitude and heading estimation, explaining how the skyline is projected on the image and how it is segmented and used to calculate the UAV's attitude. Then they used appearance images to obtain a visual compass, and they calculated the relative rotation and heading of the aerial vehicle. Additionally, they also showed the use of a stereo system to calculate the aircraft height and to measure the UAV's motion. Finally, they presented a visual tracking system based on Fuzzy controllers working in both a UAV and a camera pan and tilt platform. Every part was tested using the UAV COLIBRI platform to validate the different approaches, which include comparison of the estimated data with the inertial values measured onboard the helicopter platform and the validation of the tracking schemes on real lights

I.6.3 Vision-based Navigation

Vision-based navigation aims to estimate and control the location and motion of a UAV flying from one place to another by integrating vision sensing technologies with measurements of other navigation sensors.

I.6.3.1 Obstacle Detection and Avoidance

In some GPS denied regions and in regions where remote controlled UAV navigation was impossible, it was necessary to make the UAV effectively more versatile and fully autonomous. In [35], a vision based navigation and obstacle detection mechanism for UAVs was developed. A fixed single onboard video camera on the UAV was used to extract images of the environment of a UAV. These images were then processed to detect an obstacle in the path if any. This method was effective in detecting dark as well as light colored obstacles in the vicinity of the UAV. Authors developed two algorithms. The first one was to detect the horizon and land in the images extracted from the camera and to detect an obstacle in its path. The second one was specifically to detect a light colored obstacle in the environment, thus making their method more precise. The time taken for processing of the images and generating a result was very small, thus this algorithm was also fit to be used in real time applications. These Algorithms were more effective than previously developed methods in this field, because this algorithm did the detection of any obstacle without knowing the size of it beforehand. This algorithm was also capable of detecting light colored obstacles in the sky which otherwise might be missed by an UAV or even a human pilot sometimes. Thus it made the navigation more precise.

A vision-based navigation system was addressed in [36] to guide a UAV fly through urban canyons. Optic-flow was proposed to work together with a stereo vision algorithm. Optic flow from a pair of sideways-looking cameras was used to keep the UAV centered in a canyon and initiate turns at junctions, while the stereo vision sensing from a forward-facing stereo head was used to avoid obstacles in front. They claimed that the combination of stereo and optic-flow was more effective at navigating urban canyons than either technique alone.

In [37], authors proposed a visual servoing approach for controlling a micro aerial vehicle; which was based on monocular camera input and a fuzzy logic controller. The developed system was well suited for important inspection tasks, because the camera's pitch angle can be arbitrarily defined and is not restricted to nadir views. The including of a fuzzy logic controller allowed to quickly vary payloads as no model knowledge about the MAV was required, and it tolerates quickly changing velocity measurements which were commonly observed in visual pose estimation.

In another work [38], during the aerial vehicle motion, changes in the size of the area of the approaching obstacles were estimated as illustrated in **Figure I-11**:

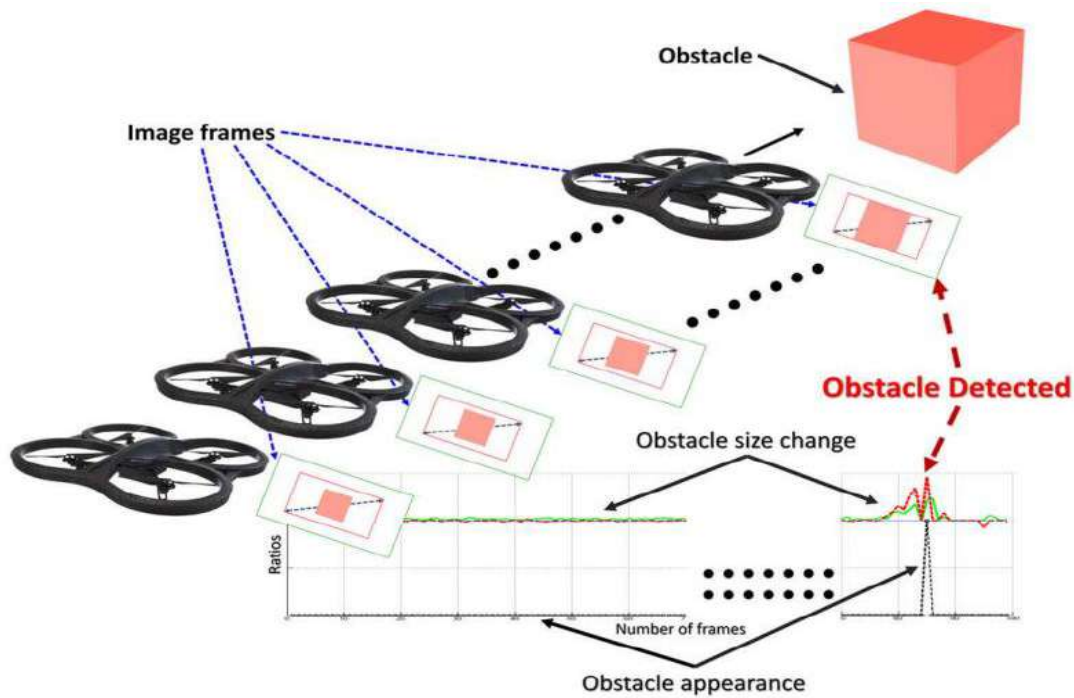


Figure I-11: UAV for obstacle detection for obstacle avoidance.

The proposed method detected the key points of the obstacles, and then extracted the obstacles that were likely to approach the UAVs. By comparing the ratio of the area to the obstacle and the position of the UAV, the method decided whether the detected obstacle could cause a collision or not. Finally, by estimating the 2D obstacle position in the image and combining with the tracked road points, UAV carried out avoidance.

I.6.3.2 Simultaneously Localization and Mapping

Simultaneously Localization and Mapping (SLAM) is one solution of navigation in a GPS denied environment, this type of navigation system typically made use of vision sensor. In [39], SLAM vision system for micro aerial vehicle is shown in **Figure I-12**:

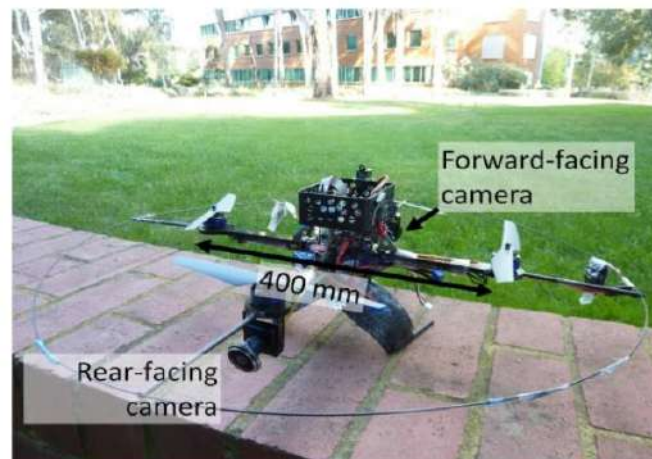


Figure I-12: The quad rotor with embedded vision system.

By the embedded camera on UAV, low quality visual information was acquired with no dependence on tracking features between frames. The approach was inspired by the observation that a flying robot equipped with appropriate local movement behaviors tends to follow similar “safe” paths through the constraints of a typical GPS-denied environment. The proposed algorithm gave good localization results in terms of evaluation metrics for cluttered outdoor environments where GPS is generally not available.

I.6.3.3 Image Mosaic Construction

Since a long time and even before the age of digital computers, image mosaicing was known in the mankind practice . In the past ,all images that were made from hilltops or balloons, were manually pieced together ,but after the development of airplane technology in 1903 , and due to the limited flying heights of the first airplanes and the need for large photo maps, professionals were forced to create image mosaics from overlapping photographs [40]. The research on image mosaic technology is widely common in many research fields such as; space exploration, remote sensing image processing, medical image analysis and other fields, that is why it has become the focus of computer graphics research in recent years.

An Image Mosaic is a synthetic composition generated from a sequence of images and it can be obtained by understanding geometric relationships between images. The geometric relations are the coordinate systems that relates the different image coordinate systems [41]. The basis of the image mosaicing technique is to find the common part in the two images which are going to be mosaiced.

Constructing image mosaics is an active area of research in the field of computer vision, image processing, and computer graphics. Since many years, image mosaics were used for various applications, and the most traditional application was and still until now; the construction of large aerial and satellite photographs from collections of overlapped images [42]. Today, there exist more recent modern applications for image mosaicing including; scene stabilization, change detection, video compression, increasing the field of view and resolution of a camera. The performance of an image mosaicing algorithm depends mainly on features detection and matching, because robust features detector and robust method for features matching ensure robust geometric and photometric image registrations, which are very important for an image mosaicing algorithm.

I.7. Conclusion

Scientific uses for UAVs, including for weather reconnaissance, aerial surveying of natural resources or hazard monitoring, have been envisioned since early entrepreneurs began developing these types of aircraft more than two decades ago. And beginning, UAVs were used infrequently as novel platforms for atmospheric observations. The growing use of UAVs for research now is due partly to the miniaturization of scientific instrumentation, which is opening up new applications as the aircraft can be outfitted with a wider array of sensors. Some of these sensing systems, which deal with computer vision, offered solutions to data acquisition and exploitation challenges in defense, security, robotics, training, and the medical marketplace [43-44]. Cameras are one type of UAV's sensors which are useful for extracting meaningful information from acquired images in real time and in real world applications.

The UAV is widely applied to the private sector such as exploration, aerial photography, and agricultural and disaster observation as well as to the military sector such as military surveillance, urban combat environment. In the area to which it is difficult for people to access such as disaster areas or much crowded downtowns, the UAV image processing can properly assist people to perform their tasks without actually accessing the areas [43-45]. Vision systems in UAVs have a great applicability to the aerial surveillance rather than to the ground where there is limitation in movement. As UAVs are becoming more compact, it is expected that the image processing in UAV will become more popular in many areas including disaster control, public service, surveillance and reconnaissance.

Compared with traditional ways of obtaining images, the UAV based platform for photogrammetric and remote sensing is a more flexible and easy way to provide high-resolution images with lower cost. So building UAV based platforms is becoming a hot field throughout the whole world. However, there are also some problems with UAV images, e.g. the views of UAV images from UAV are smaller than those of traditional aerial images, so these images with small views should be pasted together in order to increase the visual field [46]. Thus, mosaicing UAV image are a critical task. Different procedures are required for combining UAV sequence images, to achieve image mosaics with a large field of view.

Chapter II :

State of the Art about Image

Mosaicing

II. State of the Art about Image Mosaicing

II.1. Introduction

Due to the precise set of information that may be provided by digital images about the scene, they are widely used in many domains such as robotics, medicine ...etc., but in some cases, a single image cannot provide all the required details for good analysis. However, the information contained within many overlapping views of a scene may be combined to produce single image with superior quality, extended field of view and reduced noise. In the past ,all images that were made from hilltops or balloons, were manually pieced together ,but after the development of airplane technology , professionals thought about aerial imaging for creating large photo maps. We have seen that aerial images may suffer from different problems such as difference in illumination, distortion and low resolution. The common solution is to acquire several aerial images of parts of the scene from different sides at high magnification and assemble them into a composite single image mosaic which preserves the high resolution. Mosaic originates from an old Italian word “mosaico” which means a picture or pattern [47] produced by arranging together small pieces of stone, tile, glass, etc. image mosaicing technology is used in important applications; such as:

- Construction of extended aerial maps.
- Tracking and controlling moving objects.
- 3D reconstructions of a scene.
- Simultaneous Localization And Mapping.
- Surveillance, teleportation, maintenance and inspection.

II.2. Image Mosaicing

In order to create an image mosaic, it is necessary to study the following techniques:

- 1- **Features Detection:** Detecting special distinguishable objects in images.
- 2- **Features Matching:** Finding correspondences between overlapping images.
- 3- **Homography Estimation:** Estimating mapping through correspondences.
- 4- **Image Warping:** Projecting images on each other by special mapping.

The performance of an image mosaicing algorithm depends mainly on the performance of the first and the second stages, because if features are extracted using a robust detector, and matching guarantees that the points which represent the same element of the scene in both images are correctly matched, the work which remains to create the mosaiced image is only finding an image transformation model by which images can be warped on each other.

II.2.1. Features Detection

The term of features is being used in for different applications in computer vision domain such as image registration, and image classification. Detecting features in an image means selecting special parts in it; and performing some operations on them to decide if they are features or not, these features should be covariant to a class of transformations. Two different classes of image features can be detected in image; namely global features and local features. Global features are used to describe an image as a whole and can be interpreted as a particular property of the image involving all pixels; color and texture are common example of this type. Local features aim to detect key points or interest regions in an image.

i) Classifications of Features

Different classifications of features were stated in the literatures, as global and local categories, but; the following classes are suitable for most image processing algorithms:

➤ Points

The points are ideal primitives for image mosaicing algorithm because their coordinates can be used directly to estimate the parameters of transformation matrix, and also because of their stability in image translation and rotation. Points can easily be detected by a human monitor. This kind of features is the most desirable in computer's vision and it can be easily seen and can be detected using simple algorithms [48].

➤ Regions

Areas or regions can be defined as projections of closed surfaces, water tanks, lakes, buildings, or shades. They are often represented by centers of gravity, which are invariant to rotation, expansion and deviation, and stable under a random noise and gray level change. These areas were detected by some segmentation methods; therefore, the accuracy of the segmentation can affect the result of the detected regions. More recently, researchers have been interested in selecting areas that do not change with scaling. For example, Alhichri and Kamel suggested the whole idea of virtual circuits, using the distance transformation [49].

➤ Lines (or curves)

Lines features can be segments of lines, contours or edges of objects, such as borders of regions, roads or rivers. They can be detected using standards methods of edges detection like Canny detector, or a detector based on Laplacienne of Gaussian (LoG). The lines are often represented by pairs of points of extremities, or by their points of medium [50].

ii) Properties of good features

Since, feature is an image pattern which differs from its immediate neighborhood, it should have some properties, in which; the effect of these characteristics depends on the performed applications and compromises need to be made. In computer vision application image features should satisfy some characteristics in order to be good features [51]:

---**Repeatability**: Given two images of the same object or scene, taken under different viewing conditions, a high percentage of the features detected on the scene part visible in both images should be found in both images.

-- **Accuracy**: The detected features should be accurately localized, both in image location, as with respect to scale and possibly shape.

--- **Locality**: Features should be local, so as to reduce the probability of occlusion and to allow simple model approximations of the geometric and photometric deformations between two images taken under different viewing conditions (e.g., based on a local planarity assumption).

--- **Quantity**: The number of detected features should be sufficiently large, such that a reasonable number of features are detected even on small objects. However, the optimal number of features depends on the application. Ideally, the number of detected features should be adaptable over a large range by a simple and intuitive threshold. The density of features should reflect the information content of the image to provide a compact image representation.

-- **Efficiency**: Preferably, the detection of features in a new image should allow for time-critical applications.

--- **Invariant to geometric transformations**: Which means scaling, rotation and translation transformations.

--- **Invariant to photometric transformations**: If the image is viewed in different light conditions, the same features must be detected.

For image mosaicing, repeatability is an important condition in the matching process (association), because the matching should be performed between the repeated features in the two overlapped images, and if one feature is not found in one of the two images, a false association error may occur; which will lead to deformed image transformation model, thus a deformed image mosaic can be obtained. Different feature detectors were proposed in the literatures with a variety of definitions for what type of features in an image, each detector has some advantages but at the same time has some drawbacks.

Several algorithms of feature detectors were developed, in which; they are based on detecting and isolating desired features of the image or pattern for identifying or interpreting meaningful information from the image data. Thus, different features detectors have been involved in active topics for image representation in computer vision community. In the next section, we state the most important developed approaches to detect invariant and distinctive features from an image.

II.2.1.1. Features from Accelerated Segment Test “FAST” corner detector

FAST is a simple and fast corner detector; it is based on detecting local invariant points in an image by comparing pixel-gradients in a neighbourhood of pixels. FAST algorithm defines corner point as pixel which has intensity value greater or less than that of the surrounding pixels. The reason behind the work of the FAST algorithm was to develop an interest point detector for use in real time frame rate applications like SLAM on a mobile robot (e.g. UAVs), which have limited computational resources. Each one of the surrounding pixel can have one of the following three states as given by Corner Response Function (CRF) in **equation II-1**. Depending on these states, it is judged whether a pixel is a corner point [53].

$$CRF = \begin{cases} d & I_x \leq I_p - t \\ s & I_p - t < I_x < I_p + t \\ b & I_p + t \leq I_x \end{cases} \quad (\text{II-1})$$

Where:

d: darker, s: similar, b: brighter.

I_p : the gray value of candidate pixel;

I_x : the gray value of the neighbour pixel;

t :is a given threshold value.

As shown in **Figure II-1**, a high speed test was proposed to exclude a large number of non-corners. This test examines only the four pixels at 1, 9, 5 and 13 (First 1 and 9 are tested if they are too brighter or darker. If so, then checks 5 and 13). If pixel candidate is a corner, then at least three of these must all be brighter than or darker than . If neither of these is the case, then pixel candidate cannot be a corner. The chosen threshold serves as parameter for controlling the total numbers of extracted corners in a given image [52].

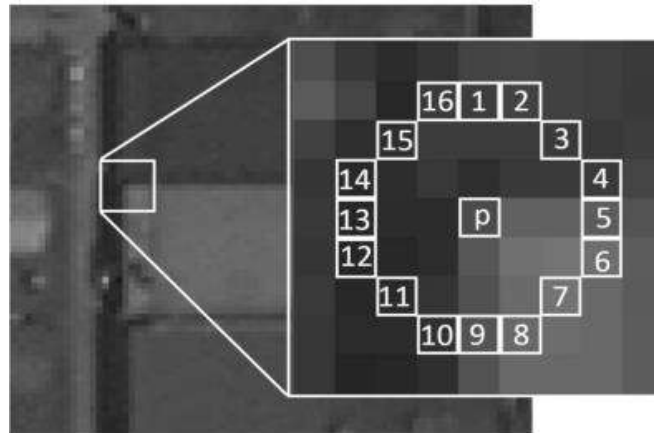


Figure II-1: Principle of FAST corner detection.

II.2.1.2. Harris Corners Detector

Since it is simple to compute, and fast enough to work on computers, Harris corner detector is a popular key point detector, it is popular because it is rotation, scale and illumination variation independent and also invariant to image noise. It is based on the local auto correlation function of a signal for find little patches of image that generate a large variation when moved around [53]. Since a long time, corners features were used in different computer vision application, because they are discrete, reliable and meaningful. As shown in **Figure II-2**, the main idea of Harris detector is the necessity of simply recognizing the point by searching for intensity values within a small patches and by shifting the windows in any direction, we should have a large change in appearance [54].

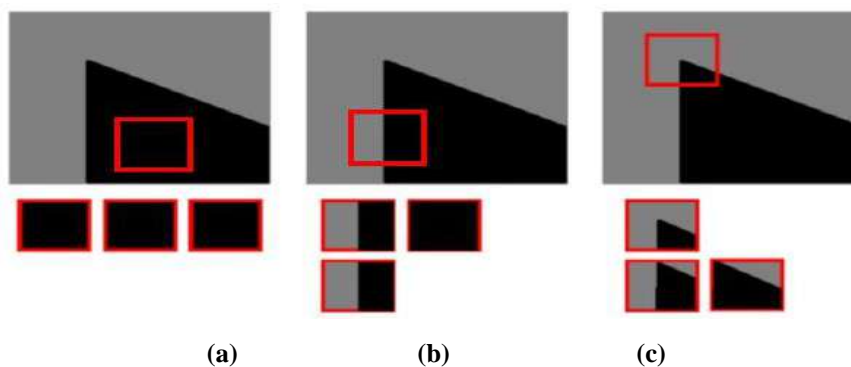


Figure II-2: Types of features with Harris algorithm, (a) Region, (b) edge, (c) corner.

In Harris detection algorithm, for a point to be considered as a corner, all shifts (in at least one of the opposite directions) should produce a significant intensity change. The following points give the mathematical operations for Harris algorithm [53-54]:

i. Applying Corner Operator:

For each pixel in the image, the corner operator is applied to obtain a cornerness measure for this pixel. The cornerness measure is simply a number indicating the degree to which the

corner operator believes this pixel is a corner. Interest point corner detection algorithms differ on how the corner operator makes this measurement, but all algorithms consider only pixels within a small window centered on the pixel a measurement is being made for. The output of this step is a cornerness map. Since for each pixel in the input image the corner operator is applied to obtain a cornerness measure, the cornerness map has the same size as the image.

ii. Thresholding Cornerness Map

Interest point corner detectors define corners as local maximum in the cornerness map. However, at this point the cornerness map will contain many local maxima that have a relatively small cornerness measure and are not true corners. To avoid reporting these points as corners, the cornerness map is typically thresholded. All values in the cornerness map below the threshold are set to zero. Choosing the threshold is application dependent and often requires trial and error experimentation. The threshold must be set high enough to remove local maxima that are not true corners, but low enough to retain local maxima at true corners. In practice there is rarely a threshold value that will remove all false corners and retain all true corners so a trade-off must be made based on the requirements of the application.

iii. Non-maximal Suppression

The thresholded cornerness map contains only non-zero values around the local maxima that need to be marked as corner points. To locate the local maxima, non-maximal suppression is applied. For each point in the thresholded cornerness map, the suppression sets the cornerness measure for this point to zero if its cornerness measure is not larger than the cornerness measure of all points within a certain distance. After non-maximal suppression is applied, the corners are simply the nonzero points remaining in the cornerness map.

❖ Properties and limitations

Corners detectors are generally simple to implement and update. They are invariant to image rotation and translation and partially invariant to affine intensity change. But these types of detectors are sensitive to noises and non-invariant to large image scale. However, corners detectors are improved and adopted in many computer vision algorithms.

An adaption of corner detectors can be made on the threshold parameter; this will control effective property of features detector which is repeatability. To guarantee good corners detection with high repeatability, it was proposed to give a low threshold value; and compute recall value, if this value is higher or equal to predefined value, the threshold is kept, otherwise we increase it till we get the mentioned recall value.

II.2.1.3. Scale Invariant Feature Transformation (SIFT)

SIFT is features detector and descriptor, it was proposed in 2004 by Lowe [55]. This detector uses a scale-space extrema to efficiently detect the location of those stable key points in the scale and space that are invariant to intensity, and viewpoint change. Then, an orientation histogram based on the gradient in different directions is formed around the key point and the dominant orientation is used to represent the key point orientations. A gradient histogram is constructed as a very distinctive descriptor of that key point. Thus, each key point is represented by the scale and orientation. SIFT descriptors uses a simple processing algorithm to extract from an image a set of descriptors that are invariant to translations, rotations and zoom-outs.

i. SIFT detector

Difference of Gaussian (DoG) method which is shown in **Figure II-3** is used for features' selections, locations of the detected features are invariant to scale change of the image; this can be done by looking for stable features across all possible scales, using a continuous scale space function. The algorithm for key point's location is given in the following stages [23]:

a) Scale-space extrema detection

The initial computation stage searches over all scales and image positions. It can be implemented easily by using a Difference-of-Gaussian function to identify potential interest points that are invariant to scale and orientation, as illustrated by **equation II-2**:

$$D(x, y, \sigma) = (G(x, y, k\sigma) - G(x, y, \sigma)) * I(x, y) = L(x, y, k\sigma) - L(x, y, \sigma) \quad (\text{II} - 2)$$

Where

* is the convolution operation in x and y,

$L(x, y, \delta) = G(x, y, \delta) * I(x, y)$ defines the scale space representation of an image, with:

$$G(x, y, \sigma) = \frac{1}{2\pi\sigma^2} e^{-(x^2+y^2)/2\sigma^2} \quad (\text{II} - 3)$$

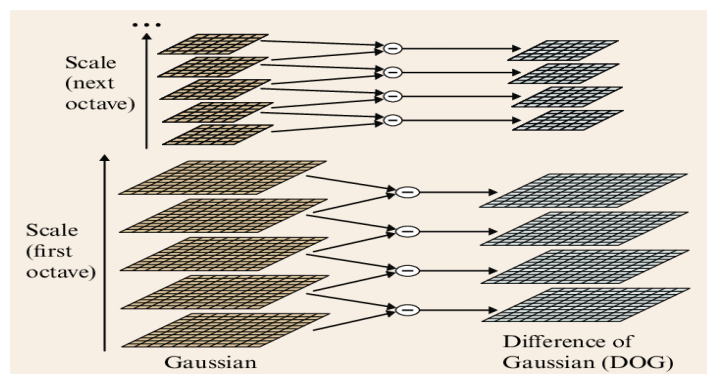


Figure II-3: Principle of Difference of Gaussian (DoG).

b) Key point localization

At each candidate pixel location, a detailed model is fit to determine location and scale. Interest points can be chosen based on measures of their stability, in which features situated on edges are not stable and cannot be selected.

ii. SIFT Descriptor

To describe the detected SIFT key points, the local gradient values and orientations of pixels around the key point should be used. A describing vector is constructed for each feature by following these steps [23, 55]:

a) Orientation assignment

Based on directions of local image gradient, orientations can be assigned to each key point location. The assigned orientation for each feature makes it invariant different transformations and reduces the effect of photometric changes.. This operation is mathematically complicated and computationally heavy.

b) Feature descriptor

The measured local image gradients at the selected scale in the region around each detected interest point. These are transformed into a representation that allows for significant levels of local shape distortion and change in illumination. **Figure II-4** summarizes the two important stages for building SIFT descriptors:

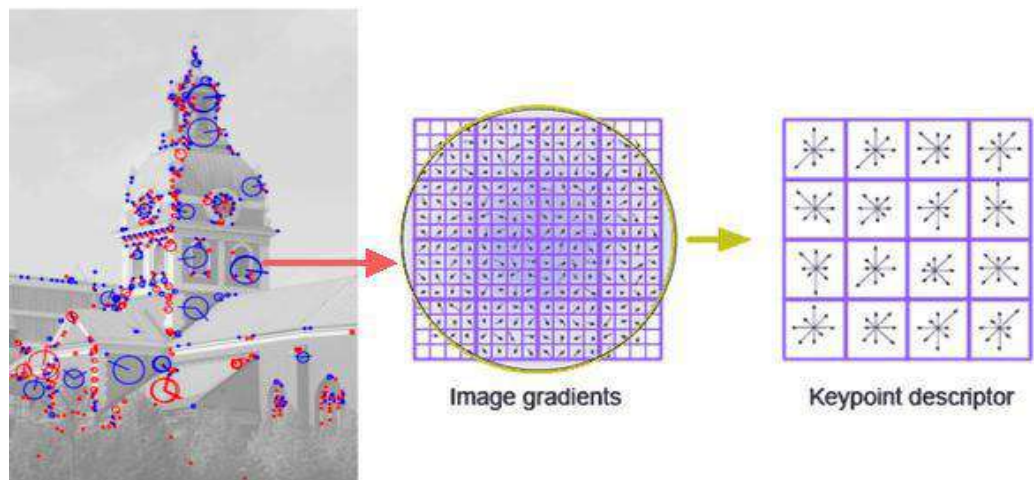


Figure II-4: SIFT descriptor generation.

➤ Properties and limits of SIFT

- It detects suitable number of invariant and distinctive features.
- Extracted features face robustly with significant image changes (large image translation and rotation, scale change and photometric changes).

- SIFT uses a constant factor k between the scales. However, a big value of k implies few key points and small values of k implies detection of lot of key points.

II.2.1.4. Speed-Up Robust Features (SURF)

SURF was developed by Herbert Bay [56] as an improved variant of SIFT which is widely used in the computer vision applications. It was developed to speed up the detection of features that are invariant to good properties. Thus, SURF exceeds many features detectors in terms of speed and accuracy. Key point's detection is based on the approximation of the Hessian matrix by using the image integral in order to reduce calculation time. The SURF algorithm is comprised mainly of the following steps [57]:

a) Key points localization

To localize SURF features, integral image is used for fast and easy implementation of box type convolution filters, the value of an integral $I_{\Sigma}(p)$ at a location $p = (x, y)$ represents the sum of all pixels intensities in the input image I of a formed rectangular region, this is given by **equation II-4**:

$$I_{\Sigma}(P) = \sum_{i=0}^x \sum_{j=0}^y I(x, y) \quad (\text{II} - 4)$$

The integral given in equation takes only 3 additions/subtractions to get the sum of the pixels intensities over an upright rectangular region ($\Sigma = I_{\Sigma}(D) - I_{\Sigma}(C) - I_{\Sigma}(B) + I_{\Sigma}(A)$) This makes the calculation time of image integral the independent of the box size.

Rather than using a different measure for selecting the location and the scale, SURF algorithm relies on the determinant of the Hessian matrix which is defined as stated in **equation II-5** [56]:

$$H(P, s) = \begin{pmatrix} L_{xx}(P, s) & L_{xy}(P, s) \\ L_{xy}(P, s) & L_{yy}(P, s) \end{pmatrix} \quad (\text{II} - 5)$$

Where

$L_{xx}(P, s)$ denotes the convolution of Gaussian second- order derivative in x direction with input image in point P at scale s , and the same thing for $L_{xy}(P, s)$ and $L_{yy}(P, s)$.

Using the integral image simple box filters are used to approximate the second-order Gaussian partial derivation and yielding less computation cost. One big advantage of this approximation is that, convolution with box filter can be easily calculated with the help of integral images. And it can be done in parallel for different scales. Also the SURF relies on determinant of Hessian matrix for both scale and location (see **Figure II-5**).

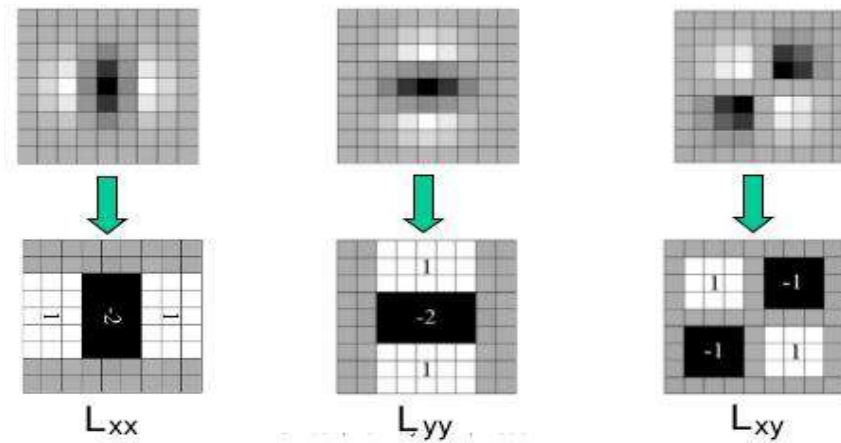


Figure II-5: The approximations of Gaussian second order partial derivatives by box filters.

The problem thus is reduced from calculating Gaussian second-order derivative responses to the box filter responses. Denoting the blob responses by D_{xx} , D_{yy} and D_{xy} , then the determinant of the original Hessian matrix in SURF is approximated by **equation II-6** [58]:

$$\det(H_{approx}) = D_{xx}D_{yy} - (0.9D_{xy})^2 \quad (\text{II} - 6)$$

Where:

0.9 is used to balance the Hessian determinant.

For achieving scale invariance features, SURF algorithm applies box filters of different sizes on the original image to search and compare key points. Box filters of different sizes create the scale space, which is divided into octaves. The local maxima of box filter responses larger than a pre-defined threshold in image and scale space are chosen as interest point candidates. Non-maximum suppression in a 3x3 neighborhood is applied to screen out “false” candidates with position correction elements above 0.5 and localize interest points [58].

b) Key point description

SURF is more preferable method as it is faster and easier to compute and produces smaller feature descriptors compared to SIFT. The SURF algorithm builds a descriptor around the neighborhood of each detected key point by rotating the neighborhood according to the calculated orientation of the feature and then dividing this area into 4x4 square sub-regions. Then, Haar wavelet responses represented by box filter responses in horizontal and vertical direction at 5x5 equally spaced sampling points within each of the sub-regions are calculated [59]. These responses and their absolute values are summed up separately for each sub-region. The 4-dimensional descriptor vectors $v = (\sum d_x, \sum d_y, \sum |d_x|, \sum |d_y|)$ of all 16 sub regions are concatenated and form a 64-dimensional feature vector as illustrated by **Figure II-6**.

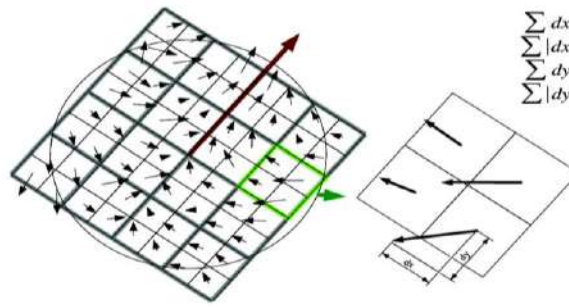


Figure II-6: Description of SURF features.

➤ Properties of SURF detector

SURF detector is invariant for the change of scale, orientation changes; also it has a high repeatability. It is faster compared to other algorithms (e.g. SIFT, Harris- Laplace, etc.). However; SURF is invariant to photometric transformations (e.g. illumination change).

II.2.2. Features matching

The matching is to find for each point of an image, its correspondent in the other image knowing that the image points are projections of the real 3D points of the same scene. In order to match two images, it is needed to look for technique that compares each pair of features from each image based on similarity measures of their respective descriptions strategy. Several matching methods were proposed in the literatures [57]:

- ✓ Correlation based methods.
- ✓ Descriptors based method.
- ✓ Tracking based methods.

II.2.2.1. Correlation based features matching

Correlation algorithms are easier to implement when compared to other feature-based matching algorithms. This method requires a measure of similarity for find the point correspondences between the two overlapping views of a scene. As shown in **Figure II-7** each pixel key-point in one image has a lot of possible candidates in the other image to be examined in order to determine the best correspondence pixel key-point [60].

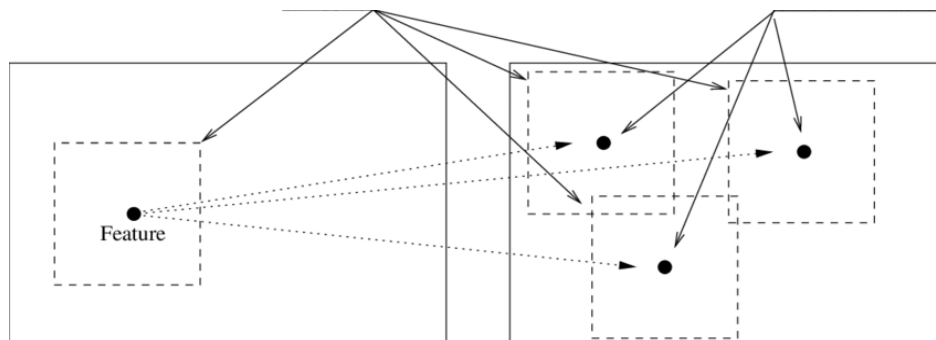


Figure II-7: Searching for candidates matches in template image using correlation method.

Several similarities measures have been suggested in the literatures as matching criterions like sum of absolute difference (SAD), sum of square difference (SSD) and normalized cross correlation (NCC). An experimental study on the different similarity measures in the presence of various image distortions has found that NCC provides the best performance [61]. NCC is also more robust against illumination changes than the widely-used SAD and SSD. Thus NCC is a most suitable measure to efficiently determine the location of a template in gray scale image. Due to its effectiveness, NCC has been used in many applications, however, because of its high computational cost; it is impractical for real time applications.

The main problem associated with all correlation matching algorithms is that the size of the correlation windows must be carefully chosen. If the correlation windows are too small, the intensity variation in the windows will not be distinctive enough, and many false matches may result, however, if the correlation window is too high, only few matches can be found.

II.2.2.2. Descriptors Based Features Matching

In this method, the best candidate match for each key-point is found by identifying its nearest neighbor in the database of key-points from training images. The nearest neighbors are defined as the key-points with minimum Euclidean distance from the given descriptor vector. The probability that a match is correct can be determined by taking the ratio of distance from the closest neighbor to the distance of the second closest [62]. Lowe rejected all matches in which the distance ratio is greater than 0.8, which eliminates 90% of the false matches while discarding less than 5% of the correct matches.

Using the Nearest-neighbor algorithm, the similarity score between two key points is the magnitude of the difference of their descriptors, so a lower score indicates a closer match. For each feature u in image 1, we compute the difference between u and every feature v in image 2, keeping track of the best and second-best matches. We accept a match between u and v if the difference between them is less than the difference between u and its second-best match from image 2. Additionally, to prevent points in image 2 from being matched to more than one feature in image 1, we output only the best match for each feature in image 2.

Using **equation II-7**, the Euclidean distance between two descriptors can be calculated:

$$d(u, v) = \left(\sum_i (u_i - v_i)^2 \right)^{1/2} \quad (\text{II} - 7)$$

Where

d is the calculated Euclidean distance.

u and v are the descriptors of image 1 and 2 respectively.

This matching algorithm is suitable when good features can be extracted from the scene, also it is faster than correlation-based methods and it is widely used for visual robotic navigation algorithms, but it is relatively insensitive to illumination changes.

II.2.2.3. Features Tracking Based Matching

This feature-matching method is extensively used for different image processing applications such as image registrations and video tracking, it is based on searching for features in a set of overlapping images and then matching these features by looking for a set of likely key points locations in each successive images where the amount of motion the appearance deformation is expected to be small. Kanade-Lucas-Tomasi (KLT) is an important tracking algorithm; which was used for features matching purpose, it was suggested by Tomasi and Kanade [63] in 1981. This method is largely used in computer vision systems to track features in a series of images. KLT relies on detecting key points in the first image, and then tracking these features in the images sequence.

Assuming that the camera moves slowly so that the variation between images is small, so that the neighbor of a point $f(x, y)^T$ tracked in the image I_1 can be found in image I_2 by a simple translation d as given by **equation II-8** :

$$I_2 = I_1(x - dx, y - dy) + n(x, y) \quad (\text{II} - 8)$$

Where

- $d(dx, dy)^T$ is the vector of translation between the image I_1 and the image I_2 .
- $n(x, y)$ is the noise in the position (x, y) .

The estimation of the distance d can be performed through minimizing the quadratic error ε in neighbor window w according to an optimization criterion given by **equation II-9**:

$$\varepsilon = \sum [I_1(f - d) - I_2(f)]^2 \omega(f) \quad (\text{II} - 9)$$

Where

$w(f)$ is a weighting function, generally $w(f) = 1$, but it can also take a Gaussian form if we want to give more importance to the center of the window.

Equation II-10 gives the Taylor series development to first order of the intensity function I_1 :

$$I_1(p - d) = I_1(p) - J^T d \quad \text{with } J = \left[\frac{\partial I_1(p)}{\partial x} \quad \frac{\partial I_1(p)}{\partial y} \right]^T \quad (\text{II} - 10)$$

Where

J is the Jacobian matrix of I_1 .

The development gives a solution of the form $Ad=b$ with **equation II-11**:

$$\begin{cases} A = \sum JJ^T W(p) \\ b = \sum_{P \in Q} [I_1(P) - I_2(p)] J(p) W(p) \end{cases} \quad (\text{II} - 11)$$

These equations, a least squares approach can be used to estimate d . The drawback of KLT based features matching is that it is valid only when the pixel displacement is small. Therefore, improved versions of it are necessary.

II.2.3. Image Transformation Models






II.2.3.1. Geometric Transformations

Geometric transformations of the image are basic functions of graphic design as well as computer visions algorithms. The main transformations of graphics are translation, rotation and change of scale; in addition, the affine and projective parameters are used to model a wider range of transformations, especially for texture mapping. The mentioned transformations yield to important types of linear models as [64]:

- Isometric transformation.
- Similarity transformation.
- Affine transformation.
- Projective transformation.

Table II-1 shows the main differences between the main types of image transformations models, with showing the effect of them on the original image.

Table II.1: Different types of image transformations.

<i>Name of Image model</i>	<i>Symbolic Matrix</i>	<i>Example Matrix</i>	<i>Example</i>
Original	$\begin{pmatrix} 1 & 0 & 0 \\ 0 & 1 & 0 \\ 0 & 0 & 1 \end{pmatrix}$	$\begin{pmatrix} 1 & 0 & 0 \\ 0 & 1 & 0 \\ 0 & 0 & 1 \end{pmatrix}$	
Isometric	$\begin{pmatrix} \cos \theta & \sin \theta & t_x \\ -\sin \theta & \cos \theta & t_y \\ 0 & 0 & 1 \end{pmatrix}$	$\begin{pmatrix} 0.707 & 0.707 & 0 \\ -0.707 & 0.707 & 0 \\ 0 & 0 & 1 \end{pmatrix}$	
Similarity	$\begin{pmatrix} s * \cos \theta & s * \sin \theta & t_x \\ -s * \sin \theta & s * \cos \theta & t_y \\ 0 & 0 & 1 \end{pmatrix}$	$\begin{pmatrix} 1.5 & 0 & 0 \\ 0 & 1.5 & 0 \\ 0 & 0 & 1 \end{pmatrix}$	
Affine	$\begin{pmatrix} \alpha_{00} & \alpha_{01} & t_x \\ \alpha_{10} & \alpha_{11} & t_y \\ 0 & 0 & 1 \end{pmatrix}$	$\begin{pmatrix} 1.5 & 0 & 0 \\ 1 & 1.5 & 0 \\ 0 & 0 & 1 \end{pmatrix}$	
Projective	$\begin{pmatrix} h_{00} & h_{01} & h_{02} \\ h_{10} & h_{11} & h_{12} \\ h_{20} & h_{21} & h_{22} \end{pmatrix}$	$\begin{pmatrix} 1 & 0 & 0 \\ 0 & 1 & 0 \\ 0 & 0.005 & 1 \end{pmatrix}$	

An isometric model is a simple geometric transformation that preserves Euclidian distance, in other words; after applying isometric transformation; the distance between two key points in one image will be the same as the distance between their corresponding key points in the mapped image, the same principle goes for the angles between lines and areas. The only difference between a similarity transform and an isometric transform is that the latter contains a factor called isotropic scaling which is invariant with respect to direction. An affine transformation is similar to a similarity transform, but it is composed of two rotations angles and two non-isotropic scaling factors and it does not preserve the distance ratios or the angles between lines or areas. Projective or homography transformation will be illustrated in details in the next section.

II.2.3.2. Homography Matrix

The form of the projective transformation matrix H determines the type of geometric transformation represented. With a rotation angle θ , and translations (t_x and t_y) and making use of the “1” in the homogeneous coordinate, we can add translation to get relation given in **equation II-12 [65]**

$$H = \begin{bmatrix} \cos(\theta) & -\sin(\theta) & t_x \\ \sin(\theta) & \cos(\theta) & t_y \\ 0 & 0 & 1 \end{bmatrix} = \begin{bmatrix} R & t \\ 0^T & 1 \end{bmatrix} \quad (\text{II} - 12)$$

Multiply the rotation matrix by s to get scaling, this is stated in **equation II-13**:

$$H = \begin{bmatrix} s * \cos(\theta) & -s * \sin(\theta) & t_x \\ s * \sin(\theta) & s * \cos(\theta) & t_y \\ 0 & 0 & 1 \end{bmatrix} = \begin{bmatrix} s * R & t \\ 0^T & 1 \end{bmatrix} \quad (\text{II} - 13)$$

Skewing can be introduced by multiplying a and b parameters, as shown in **equation II-14**:

$$H = \begin{bmatrix} s * a * \cos(\theta) & -s * b * \sin(\theta) & t_x \\ s * a * \sin(\theta) & s * b * \cos(\theta) & t_y \\ 0 & 0 & 1 \end{bmatrix} = \begin{bmatrix} s * R & t \\ 0^T & 1 \end{bmatrix} \quad (\text{II} - 14)$$

While perspective is adjusted in the final row, homography can be written and encoded in the H -matrix as illustrated in **equation II-15**:

$$H = \begin{bmatrix} s * a * \cos(\theta) & -s * b * \sin(\theta) & t_x \\ s * a * \sin(\theta) & s * b * \cos(\theta) & t_y \\ p_0 & p_1 & 1 \end{bmatrix} = \begin{bmatrix} H_{00} & H_{01} & H_{02} \\ H_{10} & H_{11} & H_{12} \\ H_{20} & H_{21} & 1 \end{bmatrix} \quad (\text{II} - 15)$$

The matrix H works on homogeneous coordinates, so dividing it on an arbitrary non-zero constant does not change its function. If we want to rotate an image around its center at $(x_c; y_c)$. We can express that operation as shifting the image upward and to the left, until its center lies on the origin, rotating the image and then translating it back to its original position.

There are many situations in computer vision where estimating a one of the mentioned transformation may be required. In our case, for image mosaicing; we need a transformation model to project two overlapped image on each other to create an image mosaic, therefore; the projective transformation (homography) is the most suitable model for our purpose.

II.2.3.3. Homography Estimation Using DLT

Estimating the homography relating two views is an essential step in many image processing applications that include multiple view geometry [66]. This transformation exists between images of planar scene; which are captured by arbitrary camera motion, also it is verified when the scene is almost planar such as images of UAV flying at high altitude, the last case is when images are taken by purely rotating camera about its optical center. **Figure II-8** shows how homographies link three overlapped views of a scene.

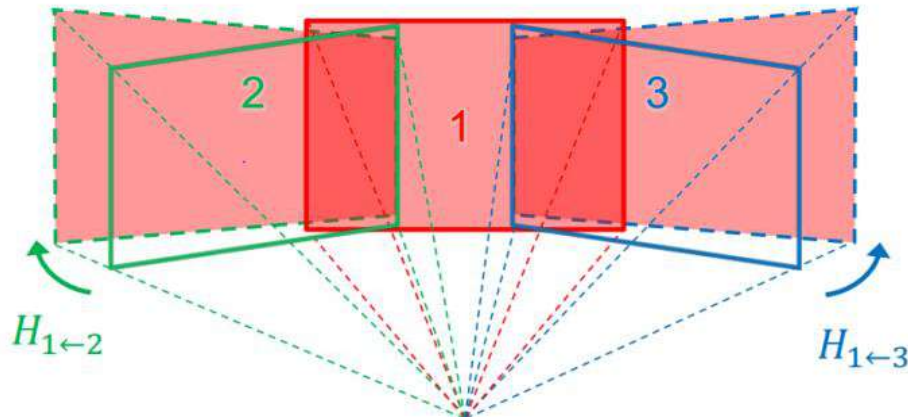


Figure II-8: Homography between three overlapped images.

Several techniques have been proposed for estimating the homography matrix between two overlapping views of a scene. These algorithms depend mainly on primitives; either simple key points or complex ones like non-parametric curves. The different techniques make different assumptions on the imaging setup and what is known about the scene.

The Direct Linear Transform (DLT) algorithm is a simple algorithm used to estimate the homography matrix H using a sufficient set of point correspondence. Letting a point and its correspondent that can be written respectively as $(x, y, 1)$; $(u, v, 1)$, we get **equation III-8**:

$$\begin{cases} -h_1x - h_2y - h_3 + (h_7x + h_8y + h_9)u = 0 \\ -h_4x - h_5y - h_6 + (h_7x + h_8y + h_9)v = 0 \end{cases} \quad (\text{III} - 8)$$

These two equations can be written in matrix form as given by **equation (III-9)**:

$$Ah = 0 \quad (\text{III} - 9)$$

Where

$$A = \begin{pmatrix} -x & -y & -1 & 0 & 0 & 0 & ux & uy & u \\ 0 & 0 & 0 & -x & -y & -1 & vx & vy & v \end{pmatrix}$$

$$h = (h_1 \quad h_2 \quad h_3 \quad h_4 \quad h_5 \quad h_6 \quad h_7 \quad h_8 \quad h_9)^T$$

Since N pairs of correspondences provide 2N equations, 4 pairs are sufficient to solve for the 8 degrees of freedom of H. For N>4 pairs of points, this equation will not have an exact solution. In this case, a solution which minimizes the algebraic residuals, $r = AH$, in a least-squares sense may be obtained, by taking the singular vector corresponding to the smallest singular value. The estimation of homography matrix using the minimum number of correspondences is useful for many applications.

After estimating homography matrix from the set of found matched key-points using the mentioned techniques above, this matrix may be incorrect and would introduce excessive error; because of false associations problem, one most commonly used method to correct homography is RANSAC which is a general technique to take data, fit an initial model made of a random sample of the provided data, test for consensus among the rest of the data (i.e., find data that is ‘close’ to the model), produce a new model using the data in consensus, and if the stopping conditions are not met, start over.

II.2.3.4. RANSAC for Homography Refinement

Homography estimation using RANSAC is a key step in feature matching; as it improves the stability of image registration [67-68]. It can estimate the parameters of homography matrix with a high degree of accuracy. In this method, for a number of iterations, a random sample of 4 correspondences is selected and a homography H is computed from those four correspondences by the direct method. Each pair of correspondence is then classified as an inlier or outlier depending on its concurrence with H. After all of the iterations are done, the iteration that contained the largest number of inliers is selected. H can then be recomputed from all of the correspondences that were considered as inliers in that iteration.

II.2.4. Image Re-projection

After homography estimation, every point in every image can be transformed to a point in the global frame. In order to render an image mosaic from the set of all overlapping images and homographies, it is necessary to map points of every image to points in the rendered image using one of the projection manifolds shown in **Figure II-9** [57].

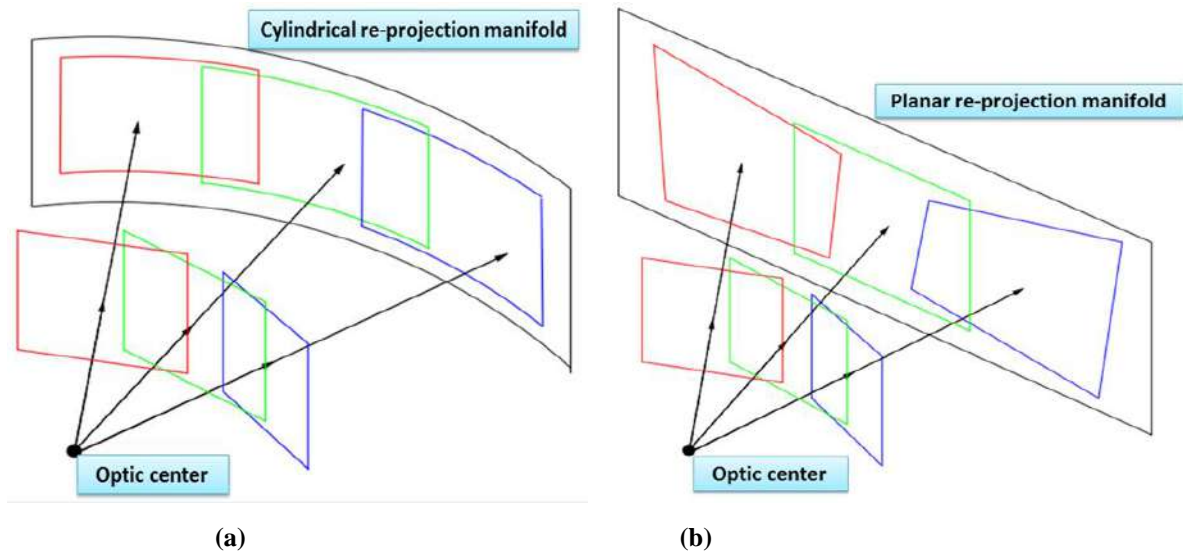


Figure II-9: Mosaic rendering by re-projection onto a) Cylindrical manifold , b) planar manifold.

Cylindrical manifold is used when image sequence is obtained from camera rotates about a single axis with very large angle of rotation (possibly a full 360 degree sweep). Since the projective distortion of the back-projected images increases toward the periphery of the mosaic, the resulted image mosaic will have form similar to the classic “bow-tie”. Planar manifold is suitable for both general-scene/rotating- camera and planar-scene/general-motion cases. But with image sequences which sweep a large angle (> 90 degrees), the projective distortion means that the mosaic image becomes infinite in size, and the planar manifold cannot be useful any more. When the homography is computed, we can transform an image to the coordinate frame of the other one. And that can be done in two different ways:

i. Forward warping

Here, we find the coordinates of pixels of the second image in the frame of the first image using the forward application of the homography as given by **equation II-16**:

$$x' = H * x \quad (\text{II} - 16)$$

ii. Backward warping

Here, we find the coordinates of pixels of the first image in the frame of the second image with the backward application of the homography as given by **equation II-17**:

$$x = H^{-1} * x' \quad (\text{II} - 17)$$

Where

x is the coordinate of pixel in the first image.

x' is the coordinate of pixel in the second image.

H is the homography relating the two images.

II.3. Related Works about Image Mosaicing

As shown in **Figure II-10**, image mosaicing techniques can be mainly classified into two classes: Direct or intensity based methods and feature based methods [69]. Direct methods use the whole pixels of image for constructing the mosaic and they are found to be useful for mosaicing images that have large overlapping regions with translations and small rotations. Feature based methods use distinctive pixels in image and they can be used in the case of small overlapping regions and tend to be more accurate and useful in different domains.

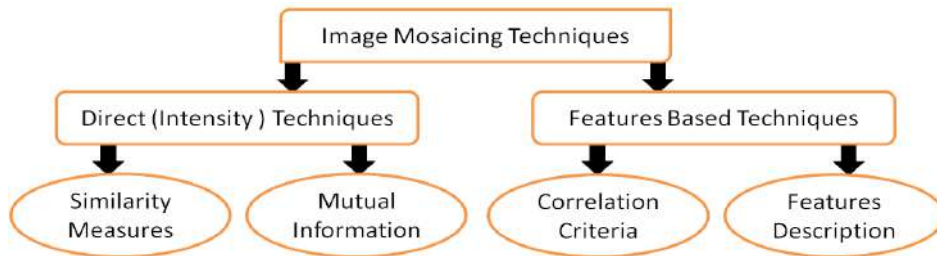


Figure II-10: Categories of image mosaicing algorithms.

The main advantages of feature-based methods over the intensity based methods are their speed, robustness, and the availability of creating image mosaics of a non-planar scene with unrestricted camera motion [70]. Various methods were adopted for achieving features based image mosaicing, and those methods can be classified according to the used detectors for features extraction, the approach included for features matching, methodology of homography matrix estimation and the used blending function; all of those processes can be achieved in different ways. In this section, we state some previous correlation based methods and other descriptors based methods for image mosaicing.

II.3.1. Correlation Based Methods

In order to attain a high field of view of a scene, two different approaches of creating image mosaic were developed in [69]; the first method was based on the property of phase correlation by involving featureless registration technique, which used the translation and rotation parameters between the two overlapping images for image alignment. The second method was based on some correlation measures, in which outliers elimination approach was needed to estimate parameters of projective transformation. A comparative analysis [71] showed that panorama creation based on correlation does not need feature extraction. It was just based on the weighted average relation between the overlapping images. The study proved that correlation method took less time but the quality of the mosaic is not very good, however; feature descriptors method consumes more time but produce high quality of image mosaic, and the two studied methods required removing false associations from matches.

In [72], two different images mosaicking techniques were compared; the first one was based on NCC criterion for registering overlapping images of a scene, while the second one was based on Mutual Information (MI). The obtained results showed that to get good results when working with NCC measure, the size of template window should be carefully chosen. Image mosaicing was also involved in clinical studies for acquiring high resolution sections of images; cross-correlation based mosaic construction was used in [73] in order to correctly register the images onto composite image. The proposed method was fast, effective and gave considerable improvements in visual effects of the stitched images compared to the existing methods. NCC optimization algorithm based on minimum spanning tree was used for stitching overlapping images [74], the proposed method generated normalized correlation matrix for matching feature points, and the minimum spanning tree was used in the matching process to eliminate false matches. The obtained results showed that the proposed algorithm had higher accuracy and convenience, and easy to implement.

Theoretically, to be able to estimate the homography relating the two images, only four corresponding points in two images are required. In practice, a large number of points are detected on the two images and thus, more than four correspondences can be found. If one of the found correspondences is not correct, it will lead to deformed image mosaic. That is why various approaches were developed to solve the problem of false correspondences. In another project [75], key-points were detected by Harris corner detector, then; a modified version of the correlation algorithm proposed in [76] was used for features matching. Through applying similarity measure between the detected corners in the two images, there could be multiple candidate matches with different match strength. The assumption in the modified version of correlation is that the match strength for a particular match is more if, in a small neighborhood of that match, there exist other matches, which are related by a similar transform as the match in question. Homography relating the two images was estimated using RANSAC technique and the result of RANSAC implementation was better over that of Least Squares Estimation of homography matrix.

Through our deep researches in literatures; we have found that correlation methods for creating image mosaic was not widely used, because they are non-invariant to large image rotation and translations, and this invariance leads to problem of false associations that needs to be overcome, otherwise; it produces false estimation to the transformation models and to deformed image mosaic, therefore; several outliers rejection techniques were needed.

II.3.2. Description Based Methods

Since sending the first satellites to send back pictures to earth, and because the new UAVs are low cost and they can be very useful to rapidly obtain updated images; the need of image mosaicing increased. In the work presented in [77], the Harris-Laplace method was used to first find scale-invariant key-points; then, the descriptor of each key-point was found by applying Gaussian-weighting around a square window using the same techniques as the used with SIFT descriptors. RANSAC method, together with DLT algorithm were used to robustly estimate the projective transformations between two images from a set of putative correspondences. To find the putative correspondences between key-points, the ratio of the Euclidean distances of the first over the second nearest neighbor of each key-point was used. Computed homographies were then used to build the mosaic of images as shown with **Figure II-11 (a, b)**.

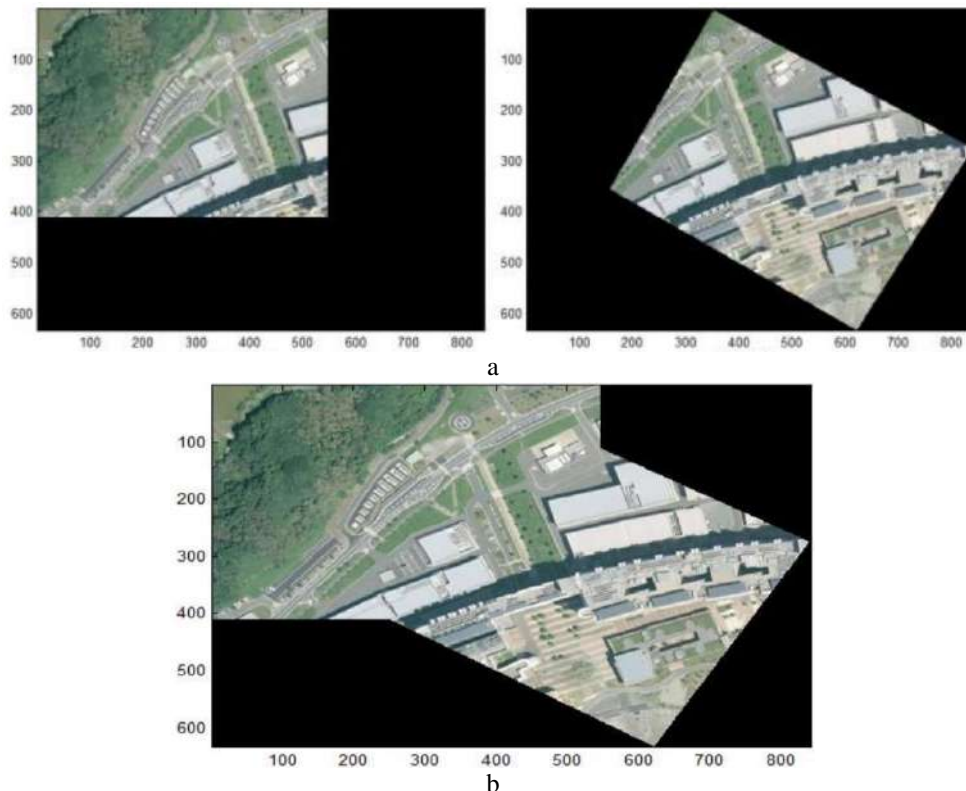


Figure II-11 a) Two overlapped images captured by the UAV. b) The obtained image mosaic [77].

The researched method showed to be invariant to translations, rotations, scale variations, perspective transformations, contrast and brightness changes and even to the presence of some noise. The obtained results showed the importance of the following things:

- The minimization of the tilt angles of the quad-rotor.
- The necessity for high overlapping percentages between images.
- The images should be taken at high flight altitudes.

Author in [23] presented robust solutions to technical problems of airborne 3D Visual SLAM. These solutions were developed based on a stereovision system available onboard UAVs. The proposed airborne Visual SLAM enables UAVs to construct a reliable map of an unknown environment and localize themselves within this map without any user intervention. To construct such large map for the UAV environment (image mosaic) using a camera embedded on the aircraft, Adapted SIFT detector was used to extract and match features between all the images and by DLT technique; homography was estimated in order to project every two successive images on each other as shown in **Figure II-12**.

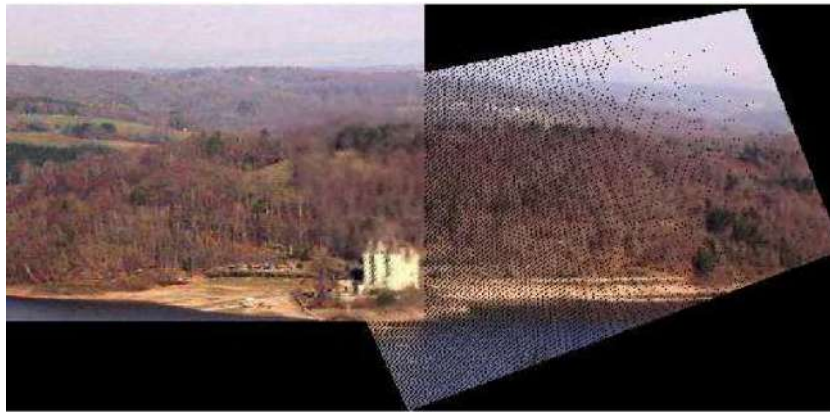


Figure II-12: Image mosaic of two successive images seen by a camera embedded on an UAV [23].

In [78], a general purpose image mosaicing system; for video mosaicing and panoramic views creation named EsiReg was presented. This system was based on a feature-point stitching approach to perform the registration of overlapping images. A robust SIFT algorithm was used to extract and match the feature points in the images, and to have a smooth resulting image, seamless weighted blending methods was also implemented to give good mosaic results as given in **Figure II-13**.

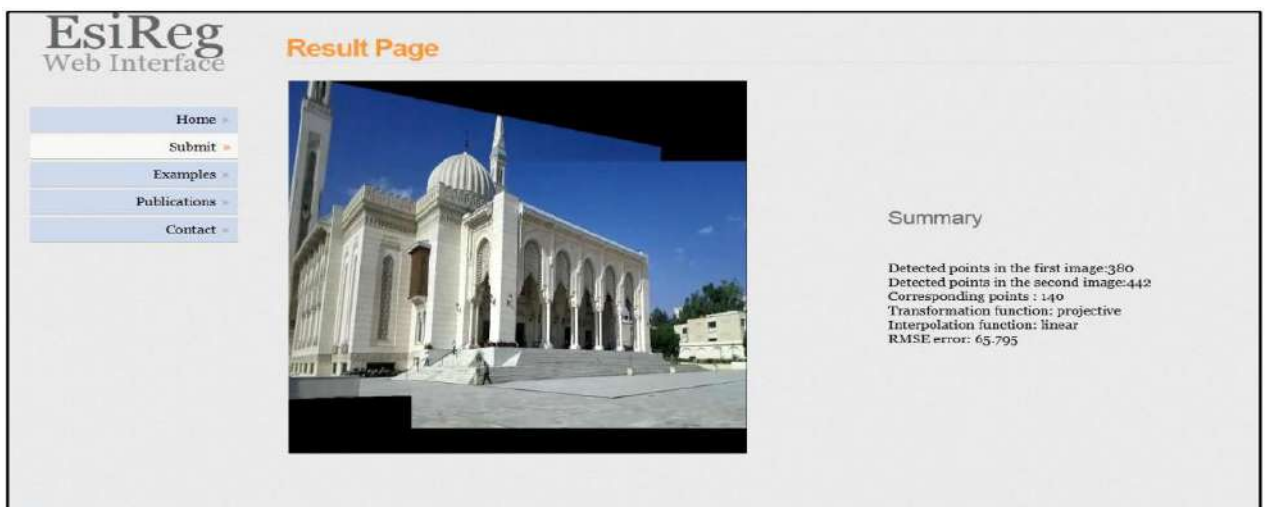


Figure II-13: The developed EsiReg Interface [78].

In another work [57], a Maximum Likelihood Estimate (MLE) was used for estimating homography, that technique is based on matched image features. After detecting features from pair of images using Harris corners detector, localized correlation score approach was used to discriminate between possible multiple matches between every successive images. Even though this modified correlation technique decreased the number of outliers, a set of matches contained many outliers which were inconsistent with the desired homography. Thus; RANSAC robust estimation algorithm was then applied to simultaneously estimate a homography and a set of matches consistent with the homography. Finally the estimation was refined using a non-linear optimizer (MLE).

The ML estimate of the homography H and the correspondences $\{x_i \leftrightarrow x_i'\}$ is the homography \hat{H} and corrected correspondences $\{\hat{x}_i \leftrightarrow \hat{x}_i'\}$ which minimize **equation II-18**:

$$C = \sum_i d^2(\hat{x}_i, x_i) + d^2(\hat{x}_i', x_i') \quad (\text{II} - 18)$$

- Where $d(x_i, x_i')$ is the Euclidean image distance between the points x_i and x_i' ,
- C The cost function is minimized using the Levenberg- Marquardt algorithm.

Figure II-14 shows the obtained planar image mosaic using MLE algorithm of Keble College, Oxford University which is generated from 60 overlapping images captured using a handheld video camera device.



Figure II-14: A planar mosaic of Keble College, Oxford automatically generated from 60 images captured using a handheld video camera [57].

In the literature [79], a novel and fast strategy was proposed for registering and mosaicing UAV images. Firstly, the original images will not be zoomed in to be 2 times larger ones at the initial course of SIFT operator, and the total number of the pyramid octaves in scale space is reduced to speed up the matching process; sequentially, RANSAC issued to eliminate the mismatching tie points. Then, bundle adjustment is introduced to solve all of the camera geometrical calibration parameters jointly. Finally, the best seam line searching strategy based on dynamic schedule was applied to solve the dodging problem arose by aero plane's side-

looking. Beside, a weighted fusion estimation algorithm is employed to eliminate the “fusion ghost” phenomenon. It was concluded from the obtained results, that the UAV panorama has a high accuracy, and didn’t take much time. That means UAV image mosaic system was able to meet the requirements for disaster emergencies and could be used in cities with paroxysmal disasters. **Figure II-15** is the mosaic rendering with 12 images in the first air strip. The achieved panorama images were of acceptable accuracy and robust to unstable camera poses. Meanwhile, noisy and illumination change were eliminated to some degree.

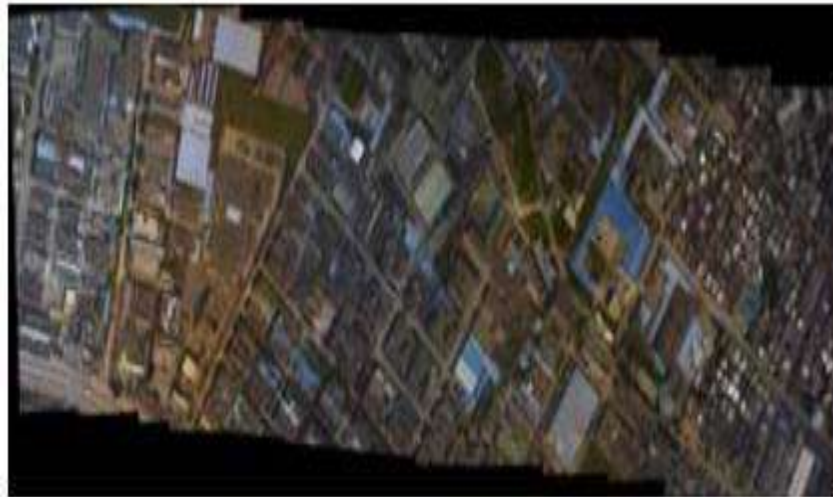


Figure II-15: mosaic effect after mismatch elimination.

UAV has been increasingly employed in various applications with computer and Google Earth/map, as shown in **Figure II-16**. Moreover, a major task of UAV is to capture the image sequence of video surveillance regions and geo-localize the objects of interest. To achieve this goal, the core technique is an image registration system between a video stream and an orthophotograph as shown below.

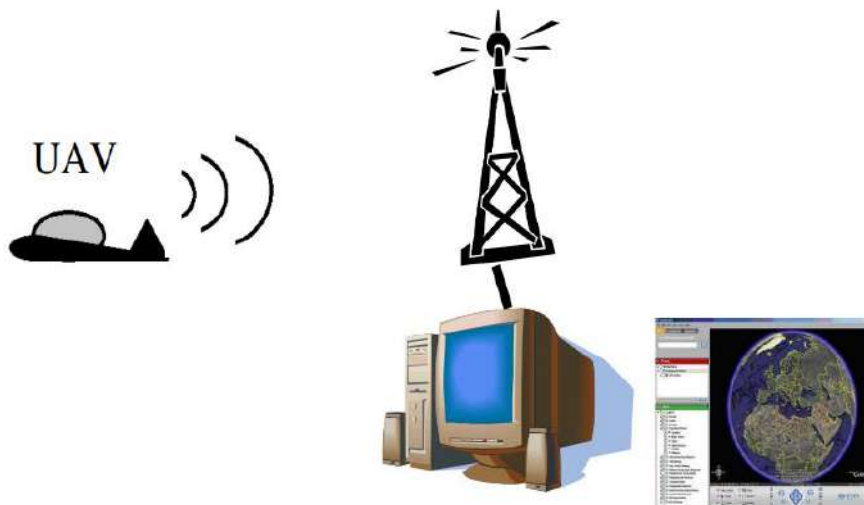


Figure II-16: Illustration of UAV-based applications with computer and Google Earth.

In [80], the goal of this research was to estimate the homography matrices that can precisely register UAV images onto the Google satellite map with less distortion. It may perform image registration between consecutive UAV images by using SIFT techniques. In contrast, for UAV-to-Google image registration, it was a great challenging task due to quality mismatch. It should be noted that the quality of mismatch addressed in this work includes different illumination conditions and qualities due to images from different sensors, and even low resolution in the Google satellite image. Moreover, it is worth noting that since the goal of the work was to register the UAV image sequence onto the Google satellite image correctly, the critical problem was how to estimate the homography between each UAV image and Google satellite image. Even though a good image registration among consecutive UAV images could be achieved, a good registration between each aerial image and Google satellite image still cannot be promised because of quality mismatch. Two UAV image sequences were used to evaluate the performance. Each UAV sequence includes five UAV images. The obtained results were compared to results of other registration system. **Figure II-17** shows the results of the first UAV image sequence to Google satellite image registration.



Figure II-17: Image registration result of the UAV image sequence onto the satellite image.

In literature [81], authors proposed constructing a 2D map from the sequence of aerial images taken by UAV. The proposed method were comprised of SURF approach for feature detection and extraction, feature matching using Fast Approximate Nearest Neighbor Search (FANNS) with automatic algorithm tuning, then, estimation of the optimal transform between images using RANSAC technique and finally creating a mosaic by stitching images together using the obtained transformations. The method described in [82] enabled the mosaicing of images captured from an aerial platform, for providing a larger field-of view for the operator. Overlapping aerial views were registered and combined together seamlessly in real-time. The real-time performance of the algorithm was achieved by using simple oriented image patches chosen around FAST corners for features matching. Then, the BaySAC technique [68] was used to enable an accurate perspective transformation.

In [83] a robust global features based image mosaicing algorithm was proposed for combining high resolution remote sensing images of urban areas, the proposed method improved three essential steps: tonal adjustment for making the mosaicked image appear to be a natural single image, seam line detection for finding the optimal seam line where the images share the most similarity, and image blending for providing a smooth transition near the seam line. Most of recent image mosaicing algorithms are based on using local features rather than global ones, due to their robustness against different geometric and photometric transformations. Points based image mosaicing [84] was used to assemble several overlapping images in order to constitute the global frame, in which a robust feature-point matching method was involved to perform the mosaicing. For all of these images, Scale Invariant Feature Transform (SIFT) detector [85] was used to detect and match features between images. Then RANSAC technique was used to reject outliers and estimate the homography between images for image re-projection purpose.

In other recent work [86], a real-time approach for fusing GPS information into Simultaneous Localization and Mapping (SLAM) processing for mosaicing a large-scale aerial images incrementally was proposed, FAST detector and Binary Robust Independent Elementary Features (BRISF) descriptor were used for features extraction, and RANSAC approach was used to fit a plane from sampled map-points. The method described in [87] was proposed for construction of mosaic image from an underwater video sequence, DoG technique, which is part of SIFT was used for feature detection, then; for each interest point, a texture descriptor was constructed using Centre Symmetric Local Binary Pattern (CS-LBP) technique to describe the key point, then feature descriptors were matched using Nearest Neighbor Distance (NND) ratio to measure the similarity between features. This binary descriptors based matching method rejected most of produced false matches.

By looking for the stated works in the related works of image mosaicing, we can obviously notice that for most of the proposed algorithms, false associations cause practical problem. A classical solution to the correspondence problem is the RANSAC algorithm. It permits the estimation of parameters of a mathematical model by random sampling. The basic assumption is that the resulted matches consist of inliers that can be used for estimating parameters of transformation model, and outliers that do not fit the model. However, RANSAC and several variants do not handle a proportion of inliers inferior to 50% [88]. Different improvements have been made to this technique [89], such as proposing to iteratively use RANSAC to detect parts of the image that have sustained different geometrical transforms.

Most of the related works were based either on correlation measures or on features descriptors for constructing image mosaic, but these two methods requires furthermore processing algorithms (i.e. RANSAC) to guarantee estimating homography from a set of good matches.. Therefore, efficient enhancements are proposed in our work for correlation and descriptors based image mosaicing algorithms, through involving fuzzy logic theory.

II.4. Conclusion

In this chapter, we presented a very wide application of image registration which is image mosaicing. We stated the various necessary steps to create an image mosaic in which different approaches were discussed in details. The image mosaic is obtained by fusing the overlapped split images of a large split, but the most important task before mosaicing is to find out the overlap region or correspondence points between the split images. The overlap region is found by matching similar features present in the given split images. Even if there are many approaches for achieving image mosaicing, we can hardly tell which is the easy way or the best way to achieve it. Because of the wide spread of fuzzy logic system in different scientific domains; we propose using it for performing image mosaicing as discussed in next chapter.

Chapter III :

The Proposed Fuzzy Matching
Algorithms

III. The Proposed Fuzzy Matching Algorithms

III.1. Introduction

In the previous chapter, we have synthesized different works concerning features based image mosaicing algorithms in the literatures, and we have concluded that most of these works depend mainly on some outliers rejection techniques, these refinement approaches showed good performance in most works; but they still need more improvements. In our thesis; we have proposed novel enhancements to those approaches, and we have involved other techniques to image mosaicing algorithms as illustrated in the next sections:

III.2. Proposed Contributions

We have proposed to use Local Binary Patterns technique in order to create binary descriptors around the detected corners based key points for features matching purpose, and we have compared our results with SIFT/SURF descriptors based matching. The obtained results were visually and numerically efficient [90]. We have enhanced the performance of the proposed LBP based matching technique; which is based on some interpolations, by concatenating eight elements LBP descriptors to create long descriptors, these improved LBP technique gave better results than the classical LBP approaches [91]. We have also proposed to use adapted features detection algorithm, this adaption can control the number of detected features in the overlapped region between the two images, because high repeatability in that region makes things easier for features matching. We have also investigated the performance of novel approaches for outliers rejection. These novel techniques were more capable of dealing with problems of false associations, and they can be developed by incorporating fuzzy logic [92], in the features matching methodologies. We have started by the classical matching techniques then, we have passed to descriptors based matching approaches as follows:

- Fuzzy correlation based features matching.
- Fuzzy ILBP based features matching [93].
- Fuzzy RANSAC based features matching [94].

Most of the proposed methods have been recently published as scientific papers. For each method; we are going to present theoretical and mathematical descriptions, the used fuzzy inputs and outputs, and the implemented fuzzy inference systems, finally the considered defuzzification technique for removing false matches. All of the proposed fuzzy methods will be used as critical stage in image mosaicing algorithms.

III.3. Fuzzy Correlation Based Features Matching

III.3.1. Correlation Measures

Once the feature points of the two image are detected separately by any type of features detector , correlation based matching algorithm is certainly easier to implement and debug as compared to feature descriptors matching algorithms . This matching algorithm requires a measure of similarity [60] between the two overlapped images. For each pixel key point in one image, there are a lot of possible candidates in the other image to be examined in order to determine the best correspondence pixel key point [61]. The effective parameter of these matching criteria is the size of correlation window. Three different correlation measures will be used as fuzzy inputs in our case.

III.3.1.1. Sum of Absolute Difference

Sum of Absolute Differences (SAD) is one of the simplest of the measures which is calculated by subtracting pixels within a square neighborhood between the reference image I_1 and the target image I_2 followed by the aggregation of absolute differences within the square window; as given by the **equation III-1**:

$$SAD = \sum_{(i,j) \in W} |I_1(i,j) - I_2(x+i, y+j)| \quad (III-1)$$

Where:

W : the chosen correlation window.

i,j : size of correlation window (1→n).

$I_1(i,j)$: values of intensities in I_1 .

$I_2(x+i,y+j)$: values of intensities in I_2 .

III.3.1.2. Zero-Mean Sum of Square Difference

In Zero-Mean Sum of Square Difference (ZSSD) method the cost is determined as in Sum of Square Difference (SSD) also by subtracting the mean of the match area from each intensity value. However, subtracting the mean from the squared intensities adds to the computational complexity of the aggregation method as given by **equation III-2**:

$$ZSSD = \sum_{(i,j) \in W} [(I_1(i,j) - M_1) - (I_2(x+i, y+j) - M_2)]^2 \quad (III-2)$$

Where:

M_1 : Mean of first image intensity over window.

M_2 : Mean of second image intensity over window.

If the left (I_1) and right (I_2) images exactly match, the resultant will be zero.

III.3.1.3. Normalized Cross Correlation

In Normalized Cross Correlation (NCC) method of cost aggregation a window of suitable size is determined and moved over the entire image or the cost matrix. The correspondence is thus obtained by dividing the normalized summation of the product of intensities over the entire window by the standard deviation of the intensities of the images over the entire window [95], as illustrated in **equation III-3**:

$$NCC = \left(\frac{\sum_{(i,j) \in W} [I_1(i,j)I_2(x+i,y+j)]}{\sum_{(i,j) \in W} \left[I_1(i,j)^2 \sum_{(i,j) \in W} I_2(x+i,y+j)^2 \right]} \right) \quad (III - 3)$$

NCC is even more complex to both SAD and SSD algorithms. In which for a feature point in the first image, cross correlation can be built with each feature point of the second image, and choosing the corresponding features as the ones with the highest correlation values in the interval $[-1; +1]$ with a value of $+1$ for identical features in both overlapped images. In practice, a value greater than 0.8 is considered to be a good match [61].

III.3.2. Fuzzy Correlation Inference System

Fuzzy logic is much more than a logical or classical system. It includes several composing sides. The principal sides are: logical, fuzzy-set-theoretic, epistemic and relational. Most of the practical applications of fuzzy logic are associated with its relational sides. Fuzzy logic resembles human decision making, with ability for finding precise solutions in approximate datasets collection. The use of fuzzy logic with the correlation approach includes the transformation of the input variables to respective fuzzy variables, according to a set of fuzzy rules. Our proposed algorithm, which is presented in **Figure III-1**, is based on three fuzzy variables sets and 27 fuzzy rules, each one of these rules depend mainly on the calculated correlation measures using SAD, ZSSD and NCC criteria.

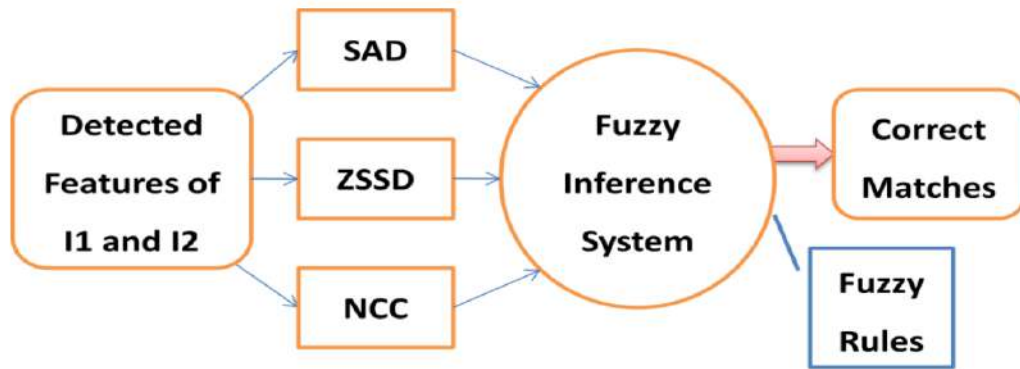


Figure III-1: The used Fuzzy correlation algorithm.

Using correlation window of size (3×3) , the three similarity measures, SAD, ZSSD and NCC inherent to each feature pixel are used as input fuzzy sets and submitted to a fuzzy inference system that determines the inliers among all the matched features. In the proposed fuzzy inference system, input membership functions determine the degree of truth to the fuzzy sets good, medium and bad, that represent the degree of similarity between the pixels of the left and right images, being a good value of similarity, a bad value of similarity and medium value between good and high similarities.

In the proposed method; in order to assign output values, three fuzzy output sets are proposed good, medium and bad, where good represents the major numerical output values, descending to the values pertaining to the medium set and finally the values from the bad set that represents the maximum numerical values that can define the output.

III.4. Fuzzy ILBP Based Features Matching

III.4.1. LBP Technique

Classical algorithm for Local Binary Patterns (LBP) is a binary system description which expresses the relationship of size of a gray image pixel point and its neighborhood pixels points; it was originally used to describe image texture information. Nowadays, research workers put forward a lot of improved LBP algorithms that have been applied in features matching; face recognition, etc.; and that because of its simple computation complexity and partial scale, rotation, and illumination invariance [96]. LBP method provides a robust way for describing pure local binary patterns in textures. The original (3×3) neighborhoods are thresholded by the value of central pixel. The threshold neighborhood pixel values are concatenated to form long binary descriptors. This algorithm can be easily combined with simple features detector for image features matching.

III.4.1.1 Improved LBP Descriptor

From the description of LBP technique, it is clear that it involves only simple arithmetic operations, since we are looking for good matching results with less calculation time; we have proposed to use a novel modified version of this technique; which satisfies our desires. **Figure III-2** illustrates the necessary steps to create eight elements LBP vector around a feature pixel of gray level of value 65.

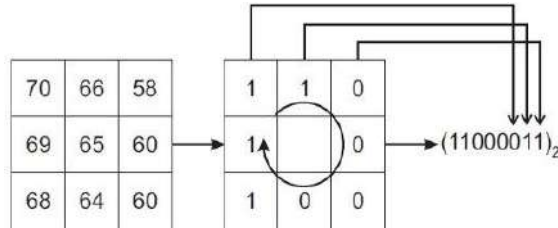


Figure III-2: Construction of LBP descriptor.

For key point defined by its coordinates (x,y), the elements of each ILBPD; for given radius R and number of surrounding points N can be expressed simply by **equation III-4**:

$$ILBP_{N,R}(x, y) = [S(z_0), S(z_1), \dots, S(z_{p-1})] \tag{III-4}$$

In which
$$S(z_i) = \begin{cases} 1, & z_i \geq 0 \\ 0, & z_i < 0 \end{cases} \text{ and } z_i = (g_i - g_c)$$

Where:

g_c is the detected interest point.

$g_{p,i}$ is one of the eight pixels around g_c .

By concatenating N eight elements LBP vector, we can get a long (8 × N) binary vector called Improved LBP descriptor [91], in which N depends on the chosen radius from the detected point features to the central feature pixel (**Figure III-3**).

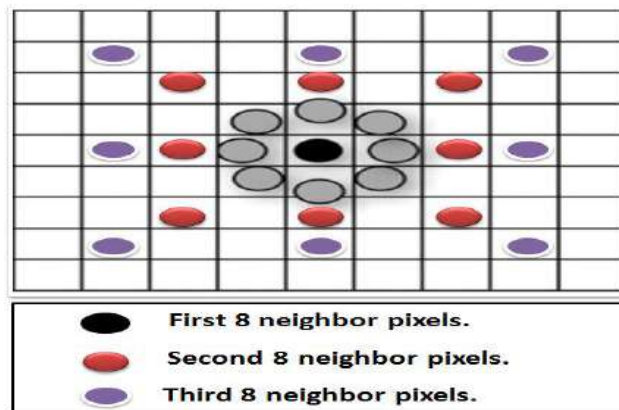


Figure III-3: ILBPDs for different values of points (P) and radius (R).

We take at each step only eight neighbor pixels with exact pixel values instead of taking all neighbor pixels and interpolating values of some pixels.

III.4.1.2 Hamming Matching Distance

Improved LBPDs depend only on increasing radius; and keeping at each time eight pixels in the neighbors. If two ILBPDs are compared, small distance value context between them is a sign of good match ability, the distance between two ILBDs is measured using the Hamming distance, which is a simple bitwise exclusive or (XOR) instruction [97]. Hence, computation and matching of ILBDs can be implemented efficiently. For two feature points, p_{ij} and $p_{i'j'}$ from images i and i' respectively, we can compute the matching distance as **equation III-5**:

$$d_s(p_{ij}, p_{i'j'}) = d_{ham}(\widehat{h}_{ij}, \widehat{h}_{i'j'}) \quad \text{(III-5)}$$

Where

$\widehat{h}_{ij}, \widehat{h}_{i'j'}$: refers to *ILBPD1 and ILBPD2*.

d_{ham} : Hamming distance between ILBPDs.

In the ideal case; the Improved LBP descriptors of the matched features should be completely coinciding, in other words, the distance between them should be zero. Some relation should be made to avoid mismatching due the noise in the binary vectors. For that, we have imposed to use fuzzy logic theory to eliminate some false association.

In LBP algorithm, every feature pixel in an image generates a single binary code. Then a decimal value is calculated for the different codes. These codes form the LBP feature vector, which characterize the image features. The LBP is based on hard thresholding of surrounding pixels, which makes features description sensitive to noise.

III.4.2. Fuzzy ILBP Inference System

In order to improve the LBP approach, we have considered fuzzy logic theory. Fuzzy logic resembles human decision making, with ability for finding precise solutions in approximate datasets collection. The use of fuzzy logic in the LBP approach includes the transformation of the input variables to respective fuzzy variables, according to a set of fuzzy rules. Our proposed algorithm [93], which is presented in **Figure III-4**, is based on three fuzzy variables sets and four fuzzy rules, each one of these rules depend mainly on Hamming distance between the Improved LBP Descriptors.

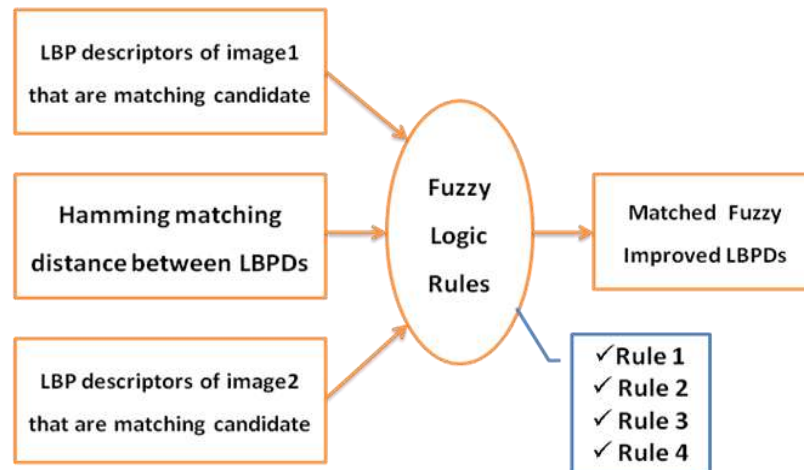


Figure III-4: The used Fuzzy ILBPDs algorithm.

The fuzzy Improved LBPDs can be created by following these steps :

- 1) Detect key-points based features for each image using one of the robust detectors (FAST, Harris, SIFT, SURF ... etc.).
- 2) Create LBP descriptors around the detected features using the first nearest eight neighborhoods pixels, with distance of one pixel from the center pixel.
- 3) Recreate LBP descriptors around the detected features using the second nearest eight neighborhoods pixels with distance of two pixels from the center pixel.
- 4) Repeat procedure (3), till the n^{th} nearest neighborhoods pixels is reached, where n is the predefined distance of pixels from the central one.
- 5) Put the obtained eight elements vectors from step (4) in one long binary vector of $(n \times 8)$ elements; and label them as Improved LBP Descriptors.
- 6) Apply Hamming distance to find the matching candidates, among the created Improved LBPDs of image 1 and the created Improved LBPDs of image 2.
- 7) Based on the calculated Hamming distances, and the matching candidates, apply fuzzy rules to choose the final matched Improved LBP descriptors among descriptors of image 1 and two respectively.

III.5. Fuzzy RANSAC Based Outliers Rejection Method

III.5.1. RANSAC Technique

The basic idea of RANSAC algorithm is that all the inliers must follow the same image transformation, while outliers do not have any overall behavior. We can use RANSAC idea [89] to perform a statistical analysis of the samples to discard outliers. Having a set of matched features between overlapping images; RANSAC algorithm can be summarized in the following five points:

- 1) Randomly; select the minimum number of pairs required to determine the transformation parameters (For image mosaicing; we need at least four pairs).
- 2) Solve for the parameters of the transformation (Estimating homography parameters).
- 3) Determine how many points from the set of all matched points fit with a predefined tolerance ($|x' - x * H|$).
- 4) If the fraction of the number of inliers over the total number points in the set exceeds a predefined threshold τ , consider the identified inliers and terminate.
- 5) Otherwise, repeat steps 1 through 4 (maximum of N iterations can be pre-defined).

III.5.2. Bidirectional Condition

Imposing the bidirectional condition is for keeping only pairs which verify matching in both directions, as shown in **Figure III-5**, this condition helps for removing most of the false associations. To illustrate this approach; we suppose that after applying features matching technique; we got two matched pairs of features between image 1 and image 2; which are pair (A, A') and pair (B,B'), now we check if these matches are consistent in both directions. From figure 1, point A in image 1 corresponds to point A' in image 2 when matching from the left to the right and point A' in image 2 corresponds to point A in image 1 when matching from the right to the left, so it is consistent in both direction and considered as good match (inlier). However; pair (B,B') verifies only matching from the left to the right and doesn't verify the matching from the right to the left; so it is considered as a bad match (outlier).

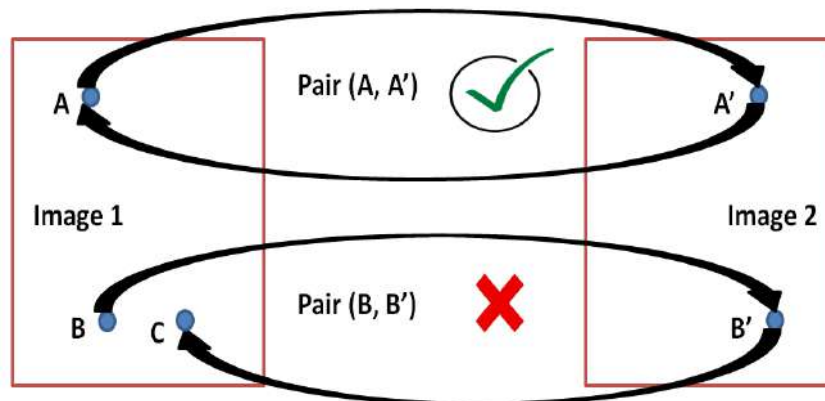


Figure III-5: Illustrating example of checking the bidirectional condition.

This approach of correspondence search identifies correspondences of more confident features and expands to other features, also helps reducing the chance of having incorrectly matched features, thus; combining this approach with RANSAC technique in fuzzy inference system using logical rules removes approximately most of false matches.

III.5.3. Fuzzy RANSAC Inference System

Sometimes, RANSAC technique for outliers rejection is certainly affected by the matches, resulting in inaccurate estimations when the majority of the matches are incorrect; therefore, we propose a simple fuzzy method for brute force outliers rejection according to human perception. The proposed method refines matching between overlapping images. Firstly, SIFT detector is involved for detecting salient locations in an image, then, Local Binary Patterns (LBP) technique is used for extracting descriptors that are distinctive and invariant to changes in viewpoint, illumination, scale, noise and local geometric distortion, after that, hamming distance can be applied to get a set of matched features, which is composed of inliers and outliers, in order to eliminate these outliers, we have proposed to use two inputs membership functions; RANSAC technique and bidirectional condition, these inputs will be controlled by six different fuzzy rules, in order to get finally the set of inliers. The overall architecture of the proposed fuzzy method is given in **Figure III-6**.

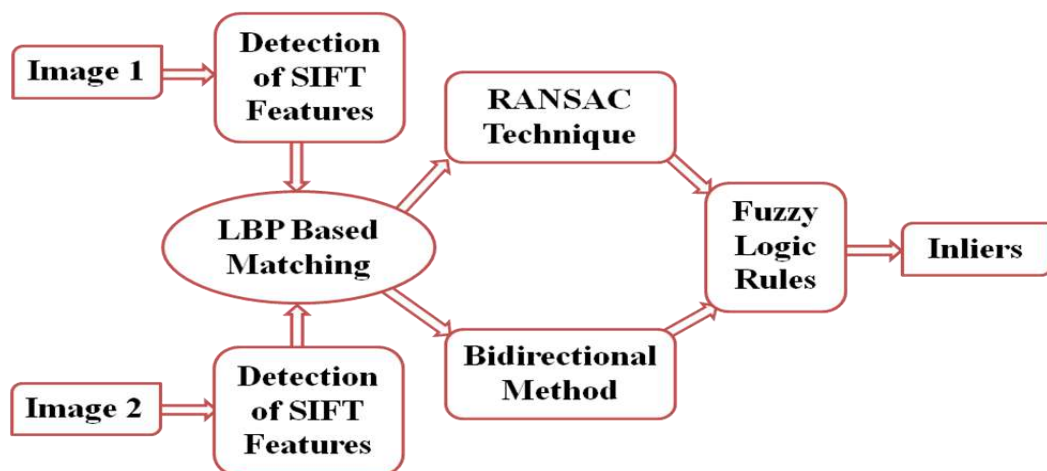


Figure III-6: Diagram of the proposed Fuzzy RANSAC based algorithm.

To define the overlapping between image 1 and 2, SIFT detector locates interest points in each image, then, binary descriptors (LBPDs) can be simply constructed around every key point in the two images, in order to find a set of matches relating the overlapped images by applying hamming distance operation. After that, we take the set of matches and apply bidirectional checking method and RANSAC algorithm, then; we link them by fuzzy rules to keep only inliers and reject outliers.

III.6. Fuzzy Image Mosaicing Algorithm

Various algorithms were proposed for aerial image mosaicing. Since we are looking for robust algorithm, we have proposed efficient features detection and matching techniques.

Figure III-7 shows the flow chart of our proposed algorithm:

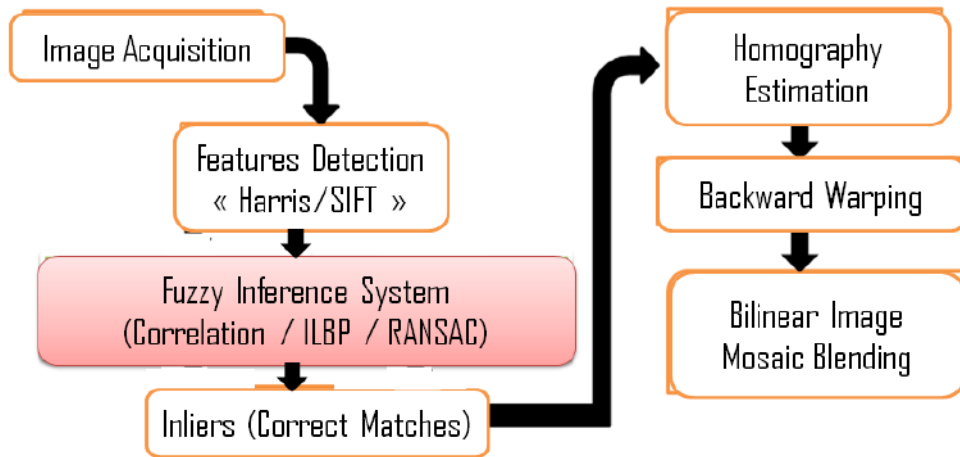


Figure III-7: Flow chart for the proposed image mosaicing algorithm.

III.6.1. Points Based Features Detection

III.6.1.1. Harris Algorithm

The adaption of Harris detector can be made on the threshold parameter; this will control effective property of features detector which is repeatability. To guarantee good corners detection with high repeatability, we have proposed adaption of threshold parameter.

The algorithm behind the Harris Corner Detector is as follows:

1. Computing derivatives I_x and I_y for the image (Sobel Filter).
2. Constructing cornerness map for each pixel as follows:
 - (a) Computing autocorrelation matrix using **equation (III-6)**:

$$M = \begin{pmatrix} A & C \\ C & B \end{pmatrix} \quad (III - 6)$$

Where: “For all i in the window”

$$A = \left(\sum_i \frac{\partial I_i}{\partial x} \right)^2, \quad B = \left(\sum_i \frac{\partial I_i}{\partial y} \right)^2 \quad \text{and} \quad C = \left(\sum_i \frac{\partial I_i}{\partial x} \frac{\partial I_i}{\partial y} \right) .$$

- (b) Computing cornerness measure MSc using **equation (III-7)**:

$$MSc(x, y) = \det(M) - k (\text{trace}(M))^2 \quad (III - 7)$$

Where

k is a constant (usually 0.04), $\det(M) = \lambda_1 \lambda_2 = AB - C^2$ and $\text{trace}(M) = \lambda_1 + \lambda_2 = A + B$

3. Constructing threshold cornerness map

✓ if $MSc(x,y) < \text{pre-defined threshold}$ then $MSc(x,y) = 0$

Where $MSc(x,y)$ is the cornerness measure of the pixel (x,y) .

4. No-maximal suppression

- ✓ if $MSc(x,y) < MSc(i,j)$ for all (i,j) in the window centered at (x,y) Then $MSc(x,y)=0$
- ✓ All pixels with a cornerness measure $MSc(x,y) > 0$ are Harris corners.

III.6.1.2. SIFT Algorithm

After filtering the input image; the difference of Gaussian images are performed, then; stable key points can be identified based on the local maxima or minima of the difference of Gaussian pyramids. **Figure III-8** shows the main steps for SIFT detection.

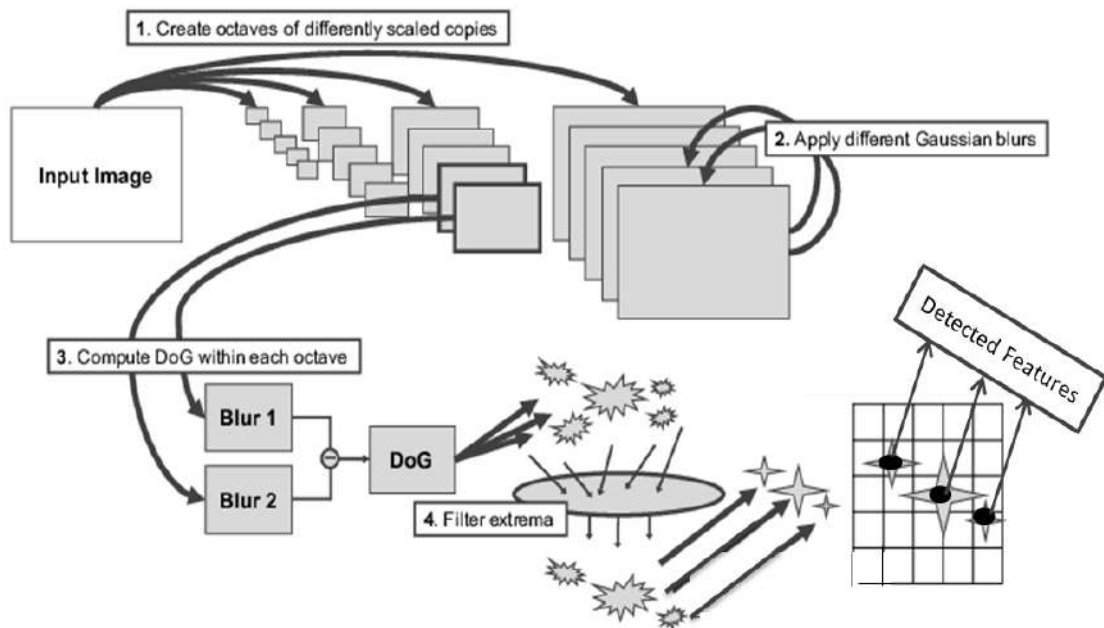


Figure III-8: Algorithm for detecting SIFT features.

III.6.2. Fuzzy Features Matching

III.6.2.1. Fuzzy Correlation

After detecting features on each overlapped images, three different correlation measures were calculated using **equations (III-1,III-2 and III-3)** with (3×3) neighbor pixels, then; the obtained scores were submitted to the inference system to be processed through twenty seven rules. We have described the input fuzzy sets with trapezoidal membership functions (MFs) using the following parameters of **Tables III-1**:

Table III-1: Parameters of inputs fuzzy MFs.

Fuzzy sets			Fuzzy variables
SAD score	ZSSD score	NCC score	
$0 \rightarrow 6$	$0 \rightarrow 30$	$0.5 \rightarrow 0.8$	Good
$4 \rightarrow 15$	$20 \rightarrow 50$	$0.3 \rightarrow 0.55$	Medium
≥ 13	≥ 45	otherwise	Bad

In order to relate the input sets to the output sets, we have used rules IF-THEN type and the AND operator of Zedah [92]. The designed rules are shown in the **Table III-2**.

Table III-2: Fuzzy rules for correlation based matching.

Rules	SAD	ZSSD	NCC	Outputs
1	Good	Good	Good	GM
2	Good	Good	Medium	GM
3	Good	Good	Bad	BM
4	Good	Medium	Good	GM
5	Good	Medium	Medium	MM
6	Good	Medium	Bad	BM
7	Good	Bad	Good	BM
8	Good	Bad	Medium	BM
9	Good	Bad	Bad	BM
10	medium	Good	Good	GM
11	medium	Good	Medium	MM
12	medium	Good	Bad	BM
13	medium	Medium	Good	MM
14	medium	Medium	Medium	MM
15	medium	Medium	Bad	BM
16	medium	Bad	Good	BM
17	medium	Bad	Medium	BM
18	medium	Bad	Bad	BM
19	Bad	Good	Good	BM
20	Bad	Good	Medium	BM
21	Bad	Good	Bad	BM
22	Bad	Medium	Good	BM
23	Bad	Medium	Medium	BM
24	Bad	Medium	Bad	BM
25	Bad	Bad	Good	BM
26	Bad	Bad	Medium	BM
27	Bad	Bad	Bad	BM

The outputs in our case describe the matched features as follows:

- Good Match -> GM,
- Bad Match -> BM,
- Medium Match -> MM.

We have proposed to keep only matched features which are good, and we have considered both medium and bad matches as outliers, the good outputs depend on having at least two good inputs among the three inputs, this assumption will make things easier in programming fuzzy rules stage.

The result of the fuzzy inference system was determined using the Sugeno type. The obtained set of pairs of matched features from fuzzy based correlation can be used for finding an appropriate projective transformation.

III.6.2.2. Fuzzy ILBP

The fuzzy logic theory is used in our work; to determine the correct matches between two overlapped images. The inputs to the fuzzy logic for every pair of matched key points which are defined by ILBP descriptors are as follows:

- 1) The measured Hamming distance (d_h) between every two ILBP descriptors.
- 2) Belongingness of the ILBP descriptor to its region (R1) in image 1.
- 3) Belongingness of the ILBP descriptor to its region (R2) in image 2.

The membership functions for input variable 'Hamming distance " d_h "' is defined by trapezoid functions for 'low' and 'high' (see **Figure III-9 (a)**). The input variable 'belongingness' is defined by sigmoid function, shown in **Figure III-9 (b)**. Output variable is defined using Sugeno type by 'match' and 'no match' (see **Figure III-9 (c)**).

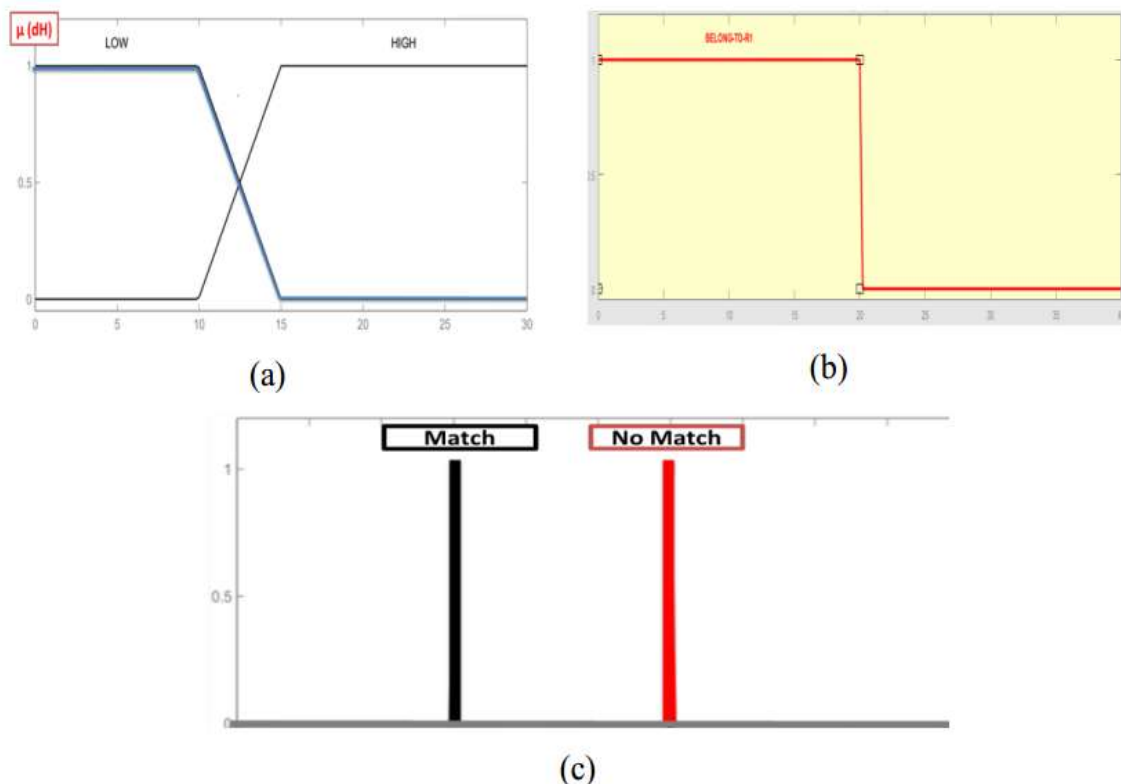


Figure III-9: (a) The first input membership function (MF) 'hamming distance' (d_h). (b) The second input membership function 'Belongingness to R1 or R2'. (c) The output MF 'match/ no match'.

For each matched features of overlapped images using ILBP descriptors, a Hamming measure and correlation criterion (in our case we have used Sum of Absolute Difference) are calculated, then, fuzzy logic which is discussed in previous section is used to find if the key points are said to be semantically matched or not.

In our case; constant Sugeno output membership functions are used to identify the matching status by “0 or 1” for ‘match’ or “no match” respectively. The following are the fuzzy rules used for the proposed system to determine the matching decision.

1. If (d_H is low) and (r1 is belong) and (r2 is belong) then (ILBPDs match).
2. If (d_H is high) and (r1 is not belong) and (r2 is not belong) then (ILBPDs do not match).
3. If (d_H is low) and (r1 is not belong) and (r2 is belong) then (ILBPDs do not match).
4. If (d_H is high) and (r1 is belong) and (r2 is not belong) then (ILBPDs do not match).

During the matching process, the distance between the ILBP descriptors for two image features is computed with Hamming distance and the correlation score is calculated to determine the belongingness of ILBPDs. Then these distance and scores are used as the crisp inputs of the fuzzy system. The membership values of the measured hamming distance is found for two fuzzy set Low and High, and the membership values for the calculated correlation scores is found for two fuzzy set either belong or not. The rules are evaluated and finally the output decision is obtained from the zero order Sugeno type output membership function (singleton) as a Match or No Match.

III.6.2.3. Fuzzy RANSAC

Fuzzy sets are more general than classical set, in which they try to act the way humans represent and reason with real world knowledge in fuzzy manner. Fuzzy logic is a form of many valued logic; it deals with reasoning that is approximate rather than fixed and exact. The membership function defines the fuzziness of different significant set of information. Fuzzy logic has been extended to handle the concept of partial truth, where the truth value may range between completely true and completely false. In our case, we have used two fuzzy sets; which are RANSAC error and bidirectional check, these sets can be either completely true or false, and we will select randomly four pairs of matched features and apply bidirectional condition. So, if it is verified for all of the selected pairs, then we apply RANSAC technique with predefined error, finally; if the obtained RANSAC error is less or equal to the predefined error, the selected four pairs will be considered as inliers, otherwise, they will be outliers, this procedure will be applied on all the found matches.

We first apply the bidirectional check; if it is verified; then we can apply RANSAC check with predefined threshold value (we choose $\tau = 4$ in our case), if the pairs give value less or equal to the threshold; we consider them as inliers, otherwise pairs are classified as outliers. It should be noted that in [98], a similar type of fuzzy base rules were conducted to enable a robot to autonomously identify all landmarks inside an office, but with normalized fuzzy inputs. **Table III-3** illustrates the used fuzzy rule base of inputs and outputs.

Table III-3 Fuzzy RANSAC rules base.

Inputs		Outputs
Bidirectional Check	RANSAC Check	Pairs Types
Verified	Less	Inliers
Verified	Equal	Inliers
Verified	More	Outliers
Not Verified	Less	Outliers
Not Verified	Equal	Outliers
Not Verified	More	Outliers

The following conditional sentences illustrate the relation between inputs and outputs:

- 1) **If** “*Bidirectional Condition Check*” is Verified, **And** “*Calculated RANSAC score*” is Less than predefined threshold, **Then** Pairs are considered as Inliers.
- 2) **If** “*Bidirectional Condition Check*” is Verified **And** “*Calculated RANSAC score*” is Equal to predefined threshold **Then** Pairs are considered as Inliers.
- 3) **If** “*Bidirectional Condition Check*” is Verified **And** “*Calculated RANSAC score*” is More than predefined threshold **Then** Pairs are considered as Outliers.
- 4) **If** “*Bidirectional Condition Check*” is Not verified **And** “*Calculated RANSAC score*” is Less than predefined threshold **Then** Pairs are considered as Outliers.
- 5) **If** “*Bidirectional Condition Check*” is Not verified **And** “*Calculated RANSAC score*” is Equal to predefined threshold **Then** Pairs are considered as Outliers.
- 6) **If** “*Bidirectional Condition Check*” is Not verified **And** “*Calculated RANSAC score*” is More than predefined threshold **Then** Pairs are considered as Outliers.

One of the most important advantage of our proposed fuzzy system; is its adaption to different predefined fuzzification threshold (RANSAC error) for inliers selection, in which; selecting a small threshold value guarantees obtaining few pairs of matches but these pairs are robust inliers, however; selecting a large threshold value guarantees obtaining numerous pairs of matches but these pairs are mixture of inliers and outliers. For our algorithm, we need at least four robust inliers to estimate homography matrix for obtaining good mosaic.

III.6.3. Homography Estimation

Homography or projective transformation is the suitable image mapping model for image mosaicing purpose, which is a planar transformation with 8 degrees of freedom, in which 4 correspondences are enough to solve for the homography directly.

As illustrated in the second chapter, homography can be estimated using linear method; however some non-linear algorithms which are based on minimizing some cost functions may be used. These cost functions are given in the appendix.

III.6.4. Image Warping and Blending

Using homography matrix, overlapping images were warped; we have determined bounds of the new combined image where the corners of left image would fall in the coordinate frame of the right image. This was done by multiplying homography on the corner point coordinates. Then we have attempted to lookup colors for any of these positions we got from the left image as given by equation 10 and illustrated in **Figure III-10**:

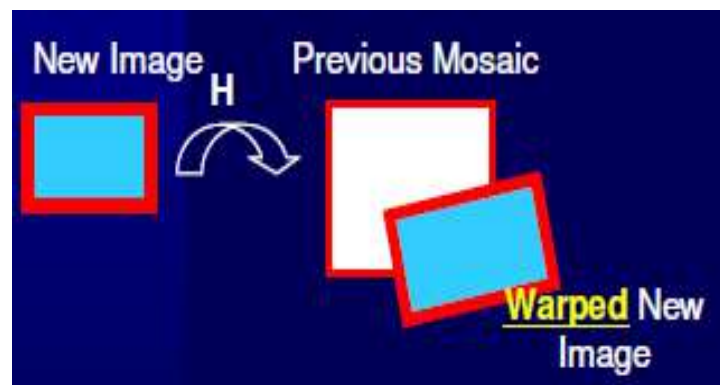


Figure III-10: Backward image warping.

When overlapping images contain mobile objects, or if the parameters of the homography matrix are not very precise, then, it is more likely to have an undesirable effect of difference in intensity. Interpolation blending technique is a simple approach, in which; the pixel values in the blended regions are weighted average from the two overlapping images. Sometimes, it is better to take more than two neighbor pixels in interpolation process. In our case, we have used the bilinear interpolation algorithm; which is slightly more sophisticated interpolation method, it interpolates pixel value from the nearest surrounding mapped source pixels, and this simple algorithm produces excellent results. So, to eliminate this effect, we should take into account the intensity value of the two images as shown in **Figure III-11**:

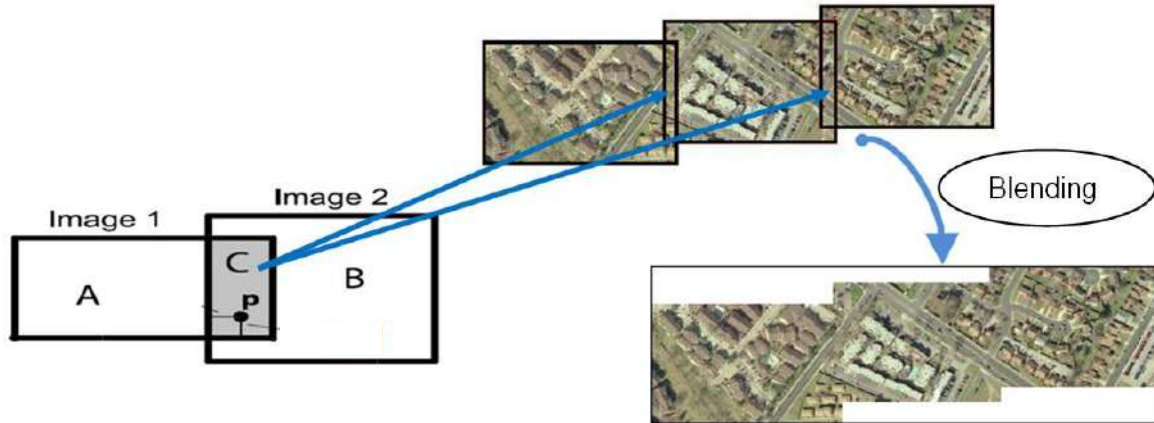


Figure III-11: Blending based on interpolation.

A continuous blending of intensities could be obtained by taking the weights of the pixels in the region C for images inversely proportional to the distances of the pixels to nearest boundaries of the two images. The intensity of pixel p will be obtained by **equation (III-10)**:

$$I_p = \frac{I_p^A + I_p^B}{2} \quad (\text{III} - 10)$$

Where

- I_p^A : Intensity of image 1 at point p .
- I_p^B : Intensity of image 2 at point p .

III.7. Conclusion

Fuzzy based matching systems for outliers rejection have been included in our image mosaicing algorithms. The objective of those techniques was to ensure estimating good homography matrices for image warping. The ideas were to extract images' features, then to describe those using robust fuzzy rules for controlling the matching quality. For all fuzzy techniques; each matched key points of overlapping image is obtained using fuzzy logic systems discussed in previous sections. The key points are said to be semantically matched if they verify some necessary associations conditions, and unmatched otherwise. In the next chapter; we will apply our proposed fuzzy approaches for constructing image mosaic, and check some evaluations metrics to validate our algorithms.

Chapter IV :
Results and Evaluations

IV. Results and Evaluations

IV.1. Introduction

This chapter is composed of two parts; in the first part, we will discuss the obtained simulation results of the proposed image mosaicing algorithms using Matlab software. In the second part; we are going to discuss the implementation results of the different stages of image mosaicing and object tracking algorithms on LabVIEW platform. **Figure IV-1** shows the main followed steps of image mosaic construction from multiple overlapping images.

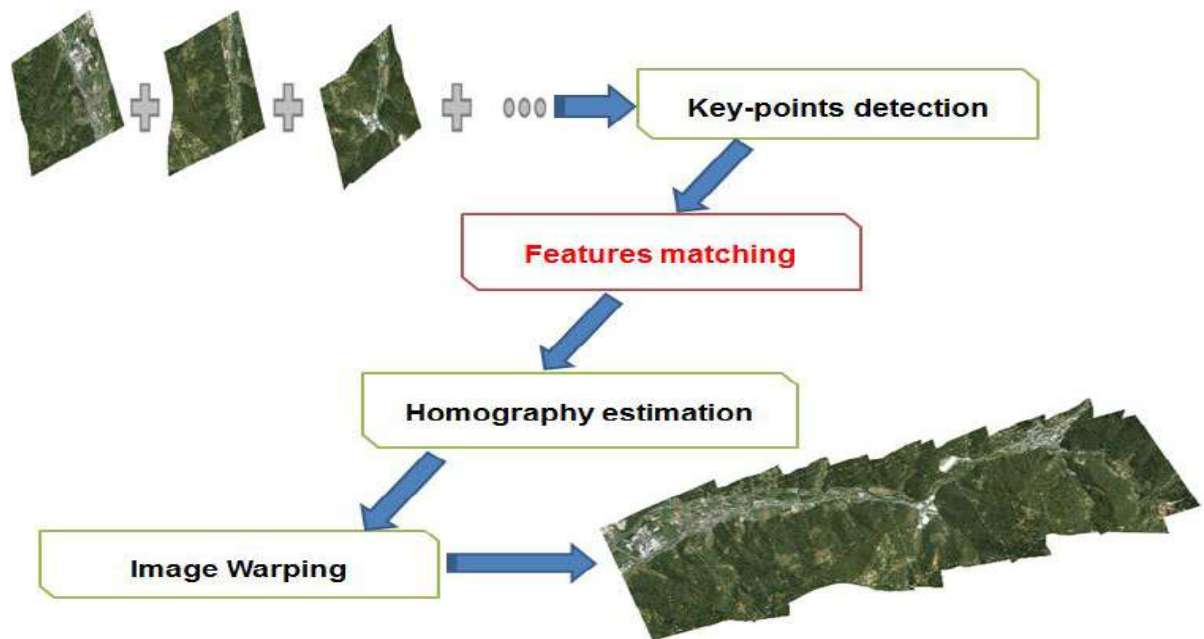


Figure IV-1: The various stages of image mosaicing algorithm.

The existence of overlapping region between successive images is necessary condition in our algorithms, because creating an image mosaic requires establishing correspondences based on that overlapping. Finding correspondences may be reached by several features matching techniques; in which false associations form great problem in most of the developed methods. As discussed in the previous chapter, we have involved fuzzy logic theory to overcome that problem in three different ways.

Matlab is a powerful software platform which can be used for the development of several applications. In our case, due to the provided image processing predefined functions with Matlab toolbox; Matlab software is suitable for the development of complex algorithms such as image mosaicing algorithm. Visual Studio Microsoft is another software platform which can be used for the creation of an image mosaic because it is compatible with the most useful libraries of computer vision.

IV.2. Simulation Results

Most of the results are published in proceedings of international conferences or journals; these scientific papers are cited in the previous chapter and also in this one. Our contributions were focused on features matching stage and on how to eliminate false matches called outliers. For features detection; we have used and compared between corners and SIFT detectors, for features matching; we have tested the proposed fuzzy approaches and compared them with recent works in the literatures using important performance metrics. Homography matrix is estimated using DLT technique and finally images are warped via backward method and blended using bilinear interpolation technique.

To test the proposed image mosaicing algorithms, we have used Matlab running on a computer that disposes 4 GB of RAM, CPU of Intel i7 generation and Intel graphic card; we tested our mosaicing approaches on images of real aerial data set [99].

IV.2.1. Image Acquisition

Figure IV-3; shows the tested overlapping aerial images, which are real images captured by UAV flying at high altitude above a forest as illustrated in **Figure IV-2**.



Figure IV-2: Capturing of aerial images by UAV.



(a)

(b)

Figure IV-3: (a) and (b) Two successive images seen by a camera embedded on an UAV.

We have started testing our algorithms on aerial images, then we have tried with other types of images (i.e indoor images, medical images, smart phone images). Images that we have used for our test are colored images (three channel RGB images), but the used techniques in our algorithms (features detection and matching and homography estimation) deal with images as gray scale images, which are one dimension (channel) images, and their intensity values are derived from RGB images using the **equation (IV-1)** [100]:

$$\text{Gray - Scale - Image} = 0.299 * R + 0.587 * G + 0.114 * B \quad (\text{IV} - 1)$$

But in the last stage of image mosaicing (image warping), the three channel RGB images of overlapping views are warped together to give colored image mosaic. In most cases, some blending techniques are needed in order to make the mosaic seamless. In our work; we have used the blending technique discussed in section (III-6-4), and we got accurate results.

IV.2.2. Evaluations of Harris/ SIFT based features detection

Figures IV-4 and **Figure IV-5** show the detected points based features on the overlapping images; using Harris and SIFT detectors respectively:

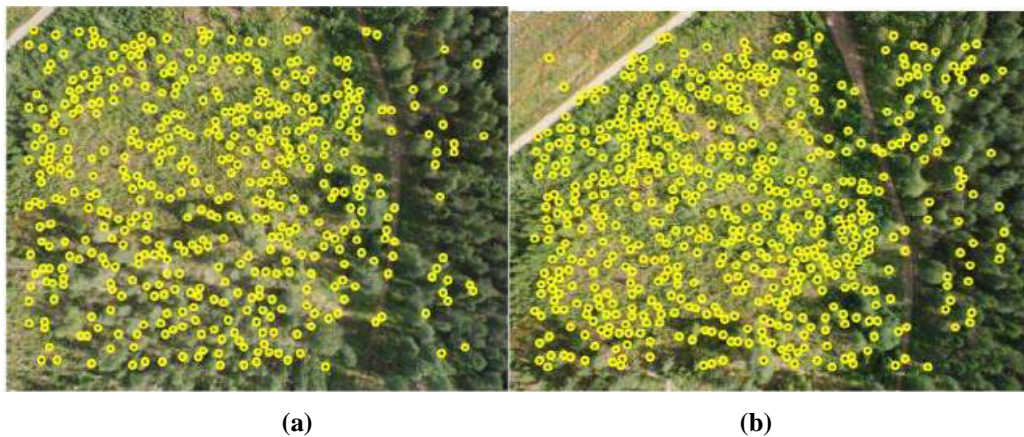


Figure IV-4: a) and b) Features detected in both images by Harris detector.

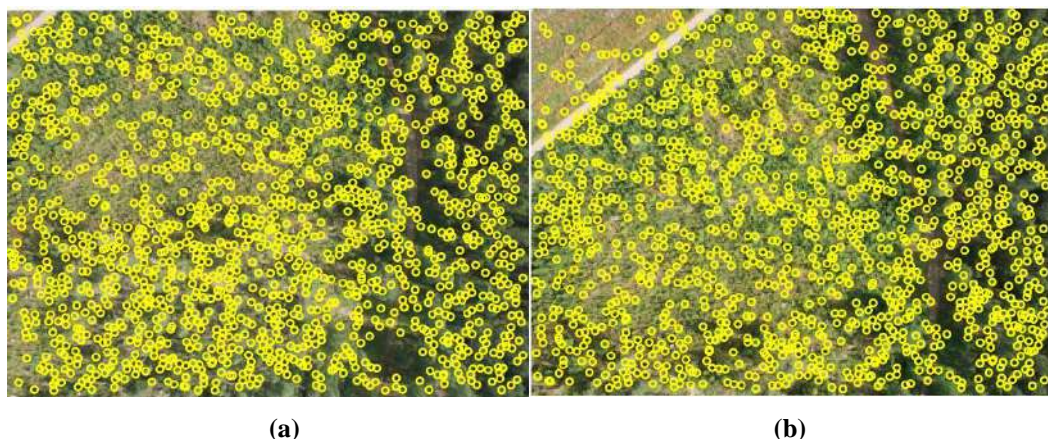


Figure IV-5: a) and b) Features detected in both images by SIFT detector.

The above figures show the detected features in the two images using two different detectors, in which we can see that repeatability condition is well verified using these types of points based detectors. Harris detector gives good results under rotation and small scale changes, however; SIFT performs the best under scale and rotation changes, but the main drawback of SIFT detector is illumination change, which was not considered in our tests. This drawback was considered in other works by various filtering techniques.

For illustrating the dependence between the threshold and the number of detected corners, we vary the threshold in the range [250-5000]; high threshold is frequently used in order to guarantee a minimum number of detections with short processing time. For contrasted regions; some particularly sharp scenes may feature a large number of detections even for high thresholds. For images 1 and 2 which are of size (390 × 420), we have varied the threshold and we got results of **Table IV-1**:

Table IV-1: Effect of Harris threshold on number of detected corners.

Threshold	Features in Image 1	Features in Image 2
5000	358	239
4000	411	484
3000	583	605
2000	680	682
1000	722	730
500	726	734
250	728	734

For SIFT detector; the selection of sigma-parameter of the Gaussian (σ_1) may not have a great effect, as the number of scales per octave (K) which is the most effective parameter in the SIFT algorithm (usually set to 3), in which, increasing K usually gives more key points, but may make key point detection unstable due to noises in image. Since the used images in our test are of full texture with size (390 × 420), they give rise to about 2000 SIFT key points with the proposed adequate number of octave by David Lowe ($k=1.6$) [55]. That choice is efficient only for images with suitable amount of texture, for low frequency images (seas, deserts...) only few features are detected, while, for high frequency images (spatial, building...) SIFT algorithm leads to lots of features, which are not suitable for several image processing algorithms, As a solution to this problem, an adaptive scale representation with an adaptive factor k was proposed [23] in order to give few robust features that are enough for features matching purpose.

➤ Repeatability

Repeatability represents the ability to locate the same key point in overlapping region between two images. This parameter can be affected by lighting changes and imaging noise [101]. The value of repeatability can be calculated by **equation (IV-2)**:

$$\text{Repeatability} = \frac{\text{Correspondence}}{\text{Query Features}} \quad (\text{IV} - 2)$$

Figure IV-6 shows the effect of increasing scale of images on the repeatability of the used features detector, here; we have compared between SIFT and Harris detectors. The higher value of repeatability represents the better performance of detector.

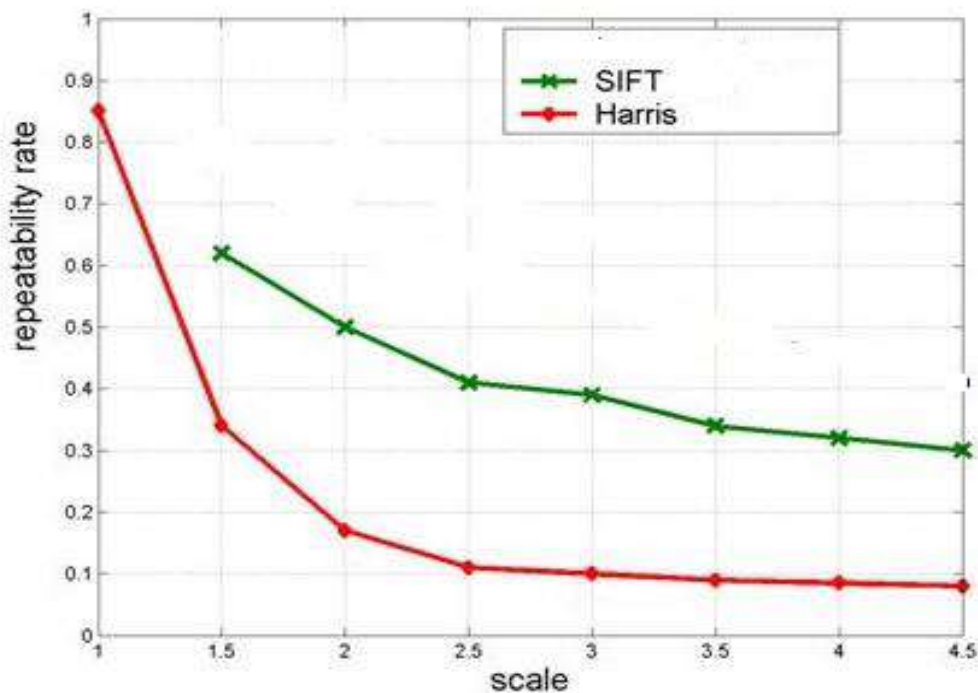


Figure IV-6: Evaluation of SIFT and Harris detectors under different scale changes.

From the above curve, it is clearly notable that SIFT detector performs better than Harris corner detector under large scales; however, the used images in our test are almost of the same scale. The used detector in our algorithm is not of importance as the matching method.

IV.2.3. Evaluations of Fuzzy Features Matching

The purpose of using fuzzy outliers rejection in finding matches; is to guarantee estimating homography matrix from only the inliers, because the existence of outliers in the used set of features for homography estimation deforms the resulted image mosaic. In the following sections; we will show the obtained results before and after applying the different methods.

Figure IV-7 shows the results of correspondence using SAD based correlation criterion using matching window of size (3x3), where **Figure IV-8** shows the results of applying fuzzy correlation method which was discussed in previous chapter.

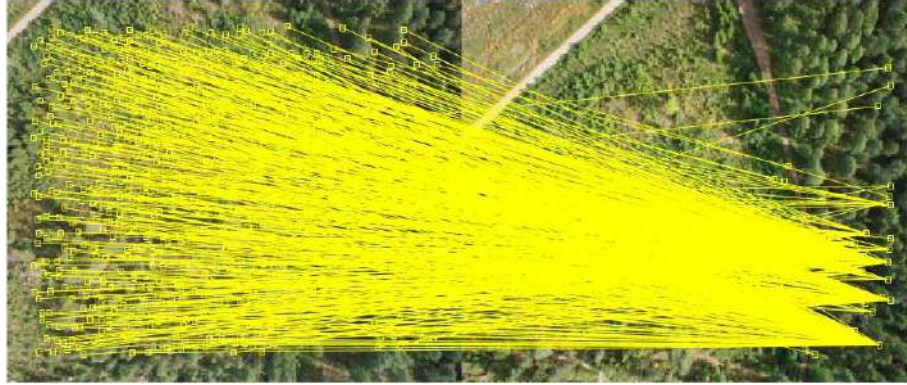


Figure IV-7: Feature matching using correlation method (SAD).



Figure IV-8: Outliers rejection using fuzzy correlation based method.

From **Figure IV-7**, huge number of false matches is obtained; this refers to the correlation window size and the similar textures in the whole images. In **Table IV-2**; we present the effect of changing matching window on the number of good matches and the execution time:

Table.IV-2: Effect of window size value on features matching.

Window	Good matches	Time (s)
3×3	3	0.6028
10×10	8	0.6722
22×22	11	0.9019
25×25	26	1.0188
30×30	24	1.3903

So to get enough number of correct matches, large size of correlation window should be chosen; but this requires long computation time. Fuzzy based correlation method which is discussed in section (III-3); is used to overcome this drawback. Our approach is based on calculating three different correlation criteria; using a small correlation window; this provides good matching results as shown in the **Figure IV-8**. The main disadvantage of fuzzy correlation technique is number of matches; which can be in some cases of small overlapping insufficient for estimating the transformation model.

The second proposed fuzzy matching method is based on Improved LBP descriptors [91], **Figure IV-9** and **Figure IV-10** show the obtained results of features matching using both Improved LBP method and fuzzy based ILBP method respectively:

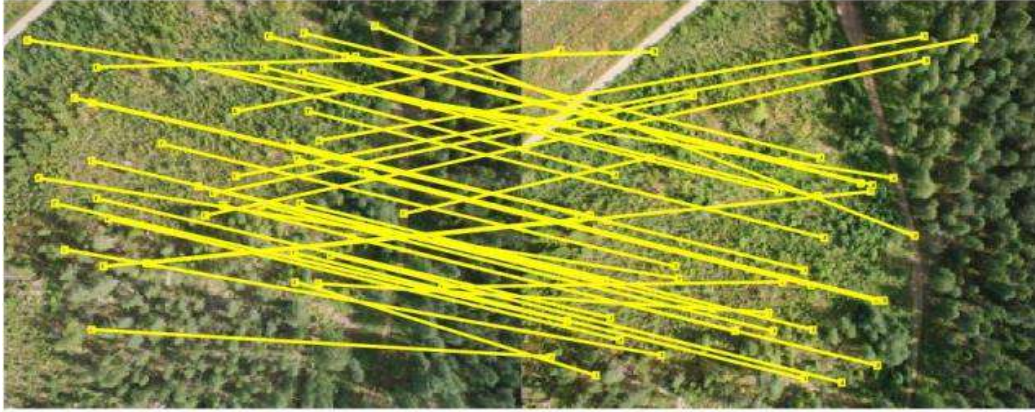


Figure IV-9: Feature matching using ILBP descriptor.

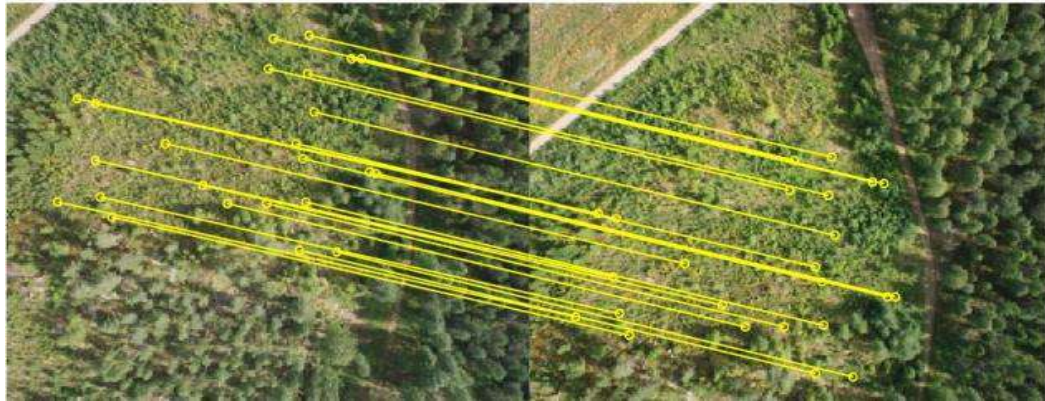


Figure IV-10: Outliers rejection using fuzzy based LBP method.

Table IV-3 gives the effect of length of ILBP descriptors ($N \times 8$) on the number of good and false matches; also the execution time is stated for each case:

Table IV-3: Important statistics of the obtained ILBP results.

Length (N)	Features in image 1	Features in image 2	Matches	Good Matches	False Matches	Time (s)
N=1	358	239	101	03	98	0.1029
N=2	358	239	87	13	74	0.3266
N=3	358	239	64	19	45	0.7088
N=4	358	239	51	23	28	1.201

From the above table; we can notice clearly that increasing the length of LBP descriptors produces better matching results but takes longer time. The proposed fuzzy based ILBP technique removes all false matches using few simple fuzzy rules. This method overcomes drawback of fuzzy correlation technique and gives better results as shown in **Figure IV-10**.

The last proposed fuzzy matching technique is based on using bidirectional and RANSAC approaches for removing false matches. **Figure IV-11** shows the matching results of LBP technique and **Figure IV-12** shows the result of RANSAC based outliers rejection.



Figure IV-11: Feature matching using LBP descriptor.

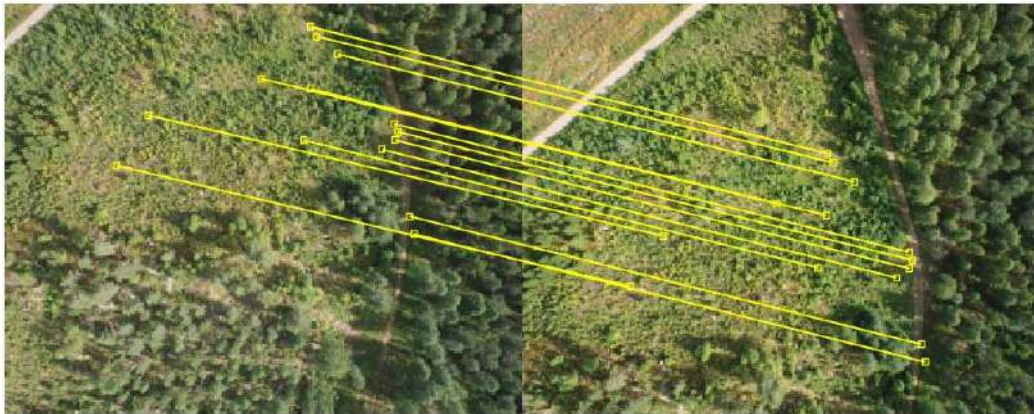


Figure IV-12: Outliers rejection using fuzzy RANSAC based method.

We can notice the existence of a lot of incorrect matches in **Figure IV-11**, but with the fuzzy based outliers rejection; we can visually notice that this approach removes all of them as shown in **Figure IV-12**. Fuzzy RANSAC based outliers rejection technique can be applied after any features matching methods, thus; it is better than fuzzy correlation and ILBP approaches. Therefore; some numerical evaluations are done on it for proving its performance with comparison with other works in recent literatures [94].

IV.2.3.1. Performance Measures

Image mosaicing relies mainly on approaches of performing registration, visual results are not sufficient to appreciate research works, therefore, some objective metrics must be used to evaluate the obtained results. We will focus on two metrics widely used called RMSE (Root Mean Squared Error) [102], recall and precision [103].

i. RMSE

Having coordinates of a pair of matched points, (x_i, y_i) in the first image and (u_i, v_i) in the second image and H is the homography matrix relating the two images, then we can get (U_i, V_i) which is the coordinate (u_i, v_i) in the frame of image 1 by **equation (IV-3)**:

$$(U_i, V_i, 1) = H(u_i, v_i, 1) \quad (\text{IV-3})$$

The distance Dis_i between a point in the first image and the corresponding point after transforming the second image is given by **equation (IV-4)**:

$$Dis_i = \left[(U_i - x_i)^2 - (V_i - y_i)^2 \right]^{1/2} \quad (\text{IV-4})$$

If N is the total number of matches between images, RMSE is calculated by **equation (IV-5)**:

$$RMSE = \sqrt{\frac{1}{N} \left(\sum_{i=1}^N \left[(U_i - x_i)^2 - (V_i - y_i)^2 \right] \right)} \quad (\text{IV-5})$$

ii. Recall

This evaluation criterion depends on number of correct matches and the number of false matches obtained for the image pair. It can be given by **equation (IV-6)**:

$$recall = \frac{\text{number of correct matches}}{\text{total number of correspondence}} \quad (\text{IV-6})$$

Ideal recall value is 1; in that case all matches are inliers; and no existence of outliers.

iii. Precision

This parameter counts the number of correct matches as well as the number of false matches as illustrated by **equation (IV-7)**:

$$1 - precision = \frac{\text{false matches}}{\text{all matches}} \quad (\text{IV-7})$$

Good matching methods give few numbers of false matches, thus precision value tends to 1. So the goal is to find the feature matching algorithms that make it possible to maximize the correct match rate while minimizing the incorrect match rate. Other performance metrics were used in some literatures, in which, correct and false matches are categorized into four possible outcomes based on the matches' natures namely:

- TP: obtained when an algorithm's outcome is a correct match;
- FP: obtained when an algorithm reports a result but that result is an incorrect match;
- TN: obtained when an algorithm reports a failure when a point in the first image is not matched because there is no corresponding point in the second image;

- FN: obtained when an algorithm reports a failure when the corresponding point exists in the second image but was not matched.

Even though; these metrics are good indicators of good or false matches, there are no comparisons using them in the literatures.

IV.2.4. Linear Estimation of Homography Parameters

From the obtained N matched features, a least square technique was used to estimate the homography matrix. Where, the structure of A , b and h are illustrated in the previous chapter.

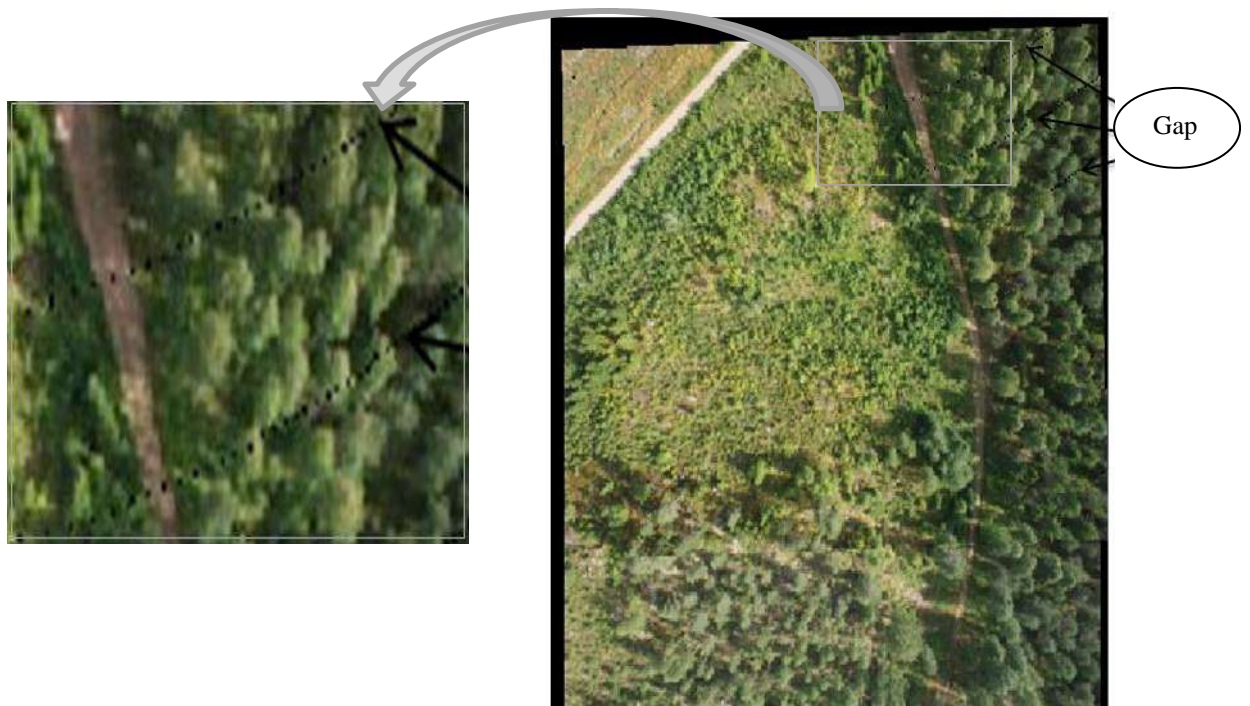
The used algorithm is summarized as follows:

$$\begin{aligned} A_{2N \times 8} \times h_{8 \times 1} &= b_{2N \times 1} \\ A_{8 \times 2N}^T \times A_{2N \times 8} \times h_{8 \times 1} &= A_{8 \times 2N}^T \times b_{2N \times 1} \\ (A^T \times A)_{8 \times 8} \times h_{8 \times 1} &= (A^T \times b)_{8 \times 1} \\ h_{8 \times 1} &= (A^T \times A)^{-1} (A^T \times b) \end{aligned}$$

The minimal number of pairs required to solve the system is $N=4$. For $N < 4$ pairs, h will not have an exact solution.

IV.2.5. Backward Image Warping and Interpolation Blending

After homography estimation, this transformation was used to warp images, and bilinear interpolation technique was used to get seamless image mosaic as shown in **Figure IV-13**.



(a)



(b)

Figure IV-13: Image mosaic (a) after geometric registration, (b) after blending.

After applying the interpolation blending technique; gapes have been completely removed. To test the visual and numerical performances of our algorithm, we have used different aerial images captured from different locations with different percentage of overlapping. The following figures show the used input images and the obtained image mosaic after applying our mosaicing algorithm for different aerial scenes “**Figures IV (14-15-16)**”:

IV.3. Tests of Mosaicing Aerial Images

i. Scene 1: “Mosaicing of overlapped monain images”



(a)

(b)



Figure IV-14: a) Left side of montain, b) Right side of montain, c) Image mosaic of the two images.

ii. Scene 2: “Mosaicing of overlapped road images”



(a)

(b)



(c)

Figure IV-15: a) Lower side of road, b) Upper side of road, c) Image mosaic of the two images of road.

iii. Scene 3: “Mosaicing of overlapped bridge images”



(a)

(b)



(c)

Figure IV-16: a) Left side of bridge, b) Right side of bridge, c) Image mosaic of the two images of bridge.

By looking to the above results, we can notice that our image mosaicing algorithm succeeds in a wide range of overlapping images, including difficult visually sparse and self-similar regions. However, only visual performance needs some numerical criteria to prove the efficiency of our proposed algorithm.

IV.4. Tests of Mosaicing Different Images (Not aerial images)

After testing our algorithm on aerial images from known data set; and we got good results; we have tested the proposed technique on real images captured by our smart phone, to show that our algorithm is efficient for all types of images. The following figures illustrate the used images with the obtained results “**Figures IV (17-18)**”:

i. Test 1: “Two overlapped images taken inside our laboratory”

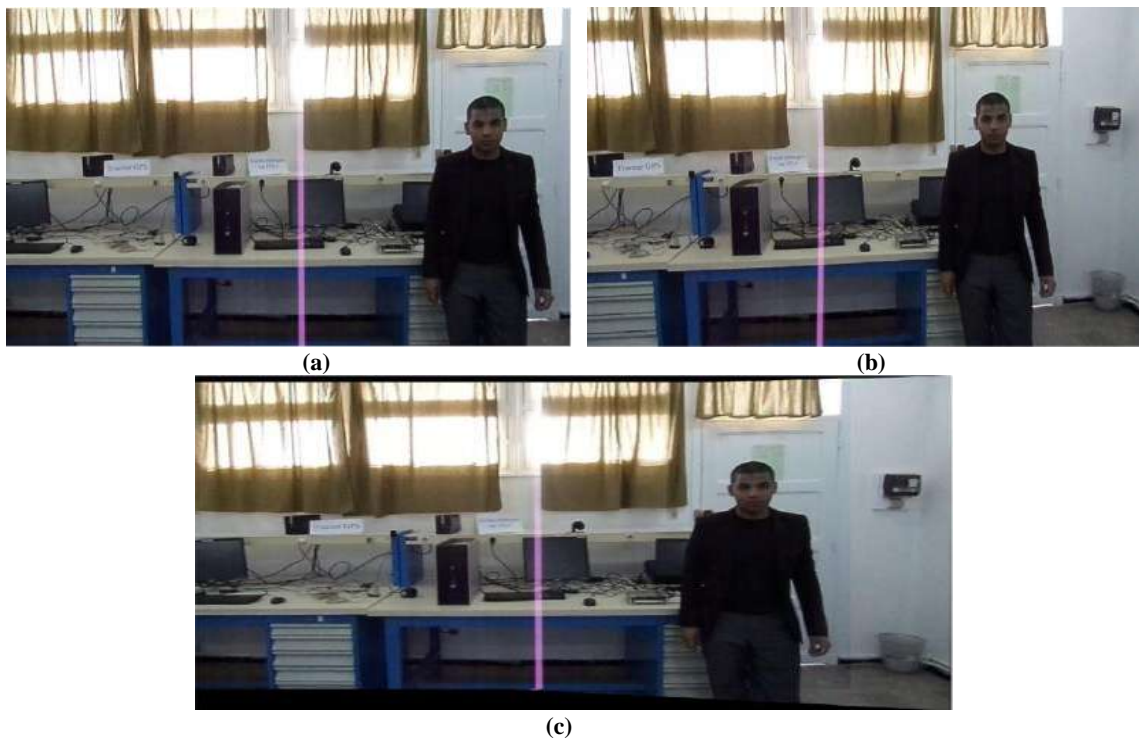


Figure IV-17:a) Left image inside laboratory, b) Right image inside laboratory, c) Obtained image mosaic.

ii. Test 2: “Two overlapped images taken in front of our faculty”





(c)

Figure IV-18: a) Left image in front of faculty, b) Right image in front of faculty, c) Obtained mosaic.

The performance and efficiency of our proposed algorithm were validated using images of different scenes; these images were collected using camera of smart phone in different conditions. On these tests, our application gave generally very satisfying results.

Table IV-4 gives some statistical details; which are helpful for doing some numerical evaluations using the stated performance metrics.

Table IV-4: Important statistics of the obtained fuzzy RANSAC results.

Data set	Features in image 1	Features in image 2	Matched features	Verified bidirectional	Verified RANSAC	Inliers
Scene # 1	257	268	110	102	93	83
Scene # 2	321	293	141	130	116	105
Scene # 3	403	306	162	129	148	116
Test # 1	206	199	65	59	55	50
Test # 2	189	152	91	80	74	67

From the above table; we can notice clearly that checking the bidirectional condition eliminates some incorrect matches, and applying RANSAC with predefined threshold eliminates more wrong matches, this lead to obtaining a set of good matches that were verified twice by the proposed fuzzy inference system.

IV.5. Comparison with Literatures

To compare the performance of the proposed method with other works, visual comparisons can be subjective, thus, a numerical evaluation of the algorithms was compared with some other methods in the literature.

As an indicator to efficiency of outliers rejection methods, RMSE value is a good criterion for this purpose; in which low RMSE value ensures good performance of the method, while high RMSE value ensures the bad performance of the applied approach. **Table IV-5** summarizes comparisons of the proposed method to other works using RMSE value:

Table IV-5: Comparison of RMSE values of some related works.

Method	RMSE
Literature [84]	1.9
Literature [79]	1.8
Scene 1	1.2
Scene 2	1.4
Scene 3	1.5
Test 1	0.39
Test 2	0.80

By comparing the obtained RMSE of our algorithm with other methods in the state of the art, we can notice that our method gives very efficient results. RMSE value is reduced in our algorithm because SIFT detector combined with LBP descriptors gives good matches, moreover; we have used two outliers rejection approaches controlled by robust fuzzy logic rules.

We have also evaluated the performance of our approach using recall measure. **Table IV-6** shows the comparison of evaluation results with existing methods.

Table IV-6: Comparison of recall values with literatures.

Method	Recall
Literature [55]	0.62
Literature [87]	0.71
Literature [104]	0.27
Literature [105]	0.60
Scene 1	0.76
Scene 2	0.75
Scene 3	0.72
Test 1	0.77
Test 2	0.74

From the comparison results, it clearly demonstrates that our approach has high recall compared to other methods, and this refers to the efficiency of our proposed fuzzy technique. Since, texture information extracted using LBP is robust to illumination variation and geometric deformation, it helps for enhancing the matching accuracy, furthermore, the proposed fuzzy based outliers rejection method improve more the matching results, thus recall value will be good enough.

The time cost of our proposed method is reduced compared to other image mosaicing algorithms, because of the use of binary descriptors minimizes the computation time, and the proposed fuzzy outliers rejection technique consumes less time contrary to other techniques. **Table IV-7** compares the computation time of our algorithm to other works:

Table IV-7: Comparison of time cost of the proposed algorithm with other methods.

	Images size	Mosaic time (s)
Literature [79]	408 × 336	4.10
Literature [106]	381 × 334	4.64
Scene # 1	420 × 520	2.98
Scene # 2	390 × 420	2.66
Scene # 3	390 × 420	3.22
Test # 1	480 × 570	3.17
Test # 2	620 × 430	3.09

➤ Discussion of Performances

Our proposed algorithms were compared visually and numerically with recent state-of-the-art related works in the literatures, the fuzzy outliers rejection methods provide good RMSE and recall values compared to other outlier rejection methods, apart from these metrics, the flexibility of the proposed method allows us to tune parameters to a level where recall remains high and RMSE remains low, moreover, for other methods, removing outliers often involves discarding a large percentage of inliers, but our technique with good threshold values guarantee keeping all good matches. Also the execution time has been improved when comparing our technique with sequential execution on the images.

After applying our proposed algorithm on different sequence of images, we have achieved high mosaicing accuracy and good performance evaluations; all of these ensure the efficiency and success of our algorithms.

IV.6. LabVIEW Implementation

IV.6.1. LabVIEW Platform

To implement color imaging systems, there are a lot of programming languages, in which we need to know deeply programming information for many image analysis algorithms. But the LabVIEW platform gives an opportunity for better image processing applications than other programming languages, because LabVIEW tools can be helpful for obtaining the most useful measurement results. LabVIEW is the abbreviation for Laboratory Virtual Instrumentation Engineering Workbench [107], which is a graphical programming language, used for instrument control and automation on different platform as Linux or windows. The code files have the extension “.VI”; which is an abbreviation of Virtual Instrument. **Figure IV-19** shows the front panel of image compression.

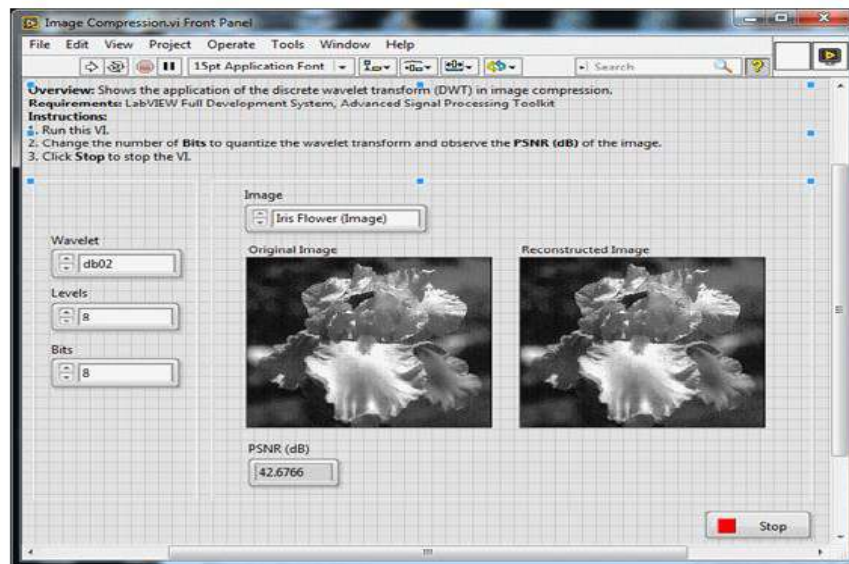


Figure IV-19: Front panel of LabVIEW of image compression algorithm,

The front panel is the programming part of LabVIEW for which where the programmer may enter data in software, it is provided with important visual tools as indicators and graphics for watching the outputs on screens. Having visual elements in this panel, software interfaces can be implemented in short time.

Figure IV-20 the block diagram of LabVIEW, with illustrating the functions of virtual elements. The block diagram is the area for programming different operation in LabVIEW. The programmer can run the source codes in this place by using the links between virtual elements. The resulted outputs can be seen on the front panel after necessary processing. All virtual elements which have input and output ports can be seen as an icon, and combining some icons lead to creation of block diagram

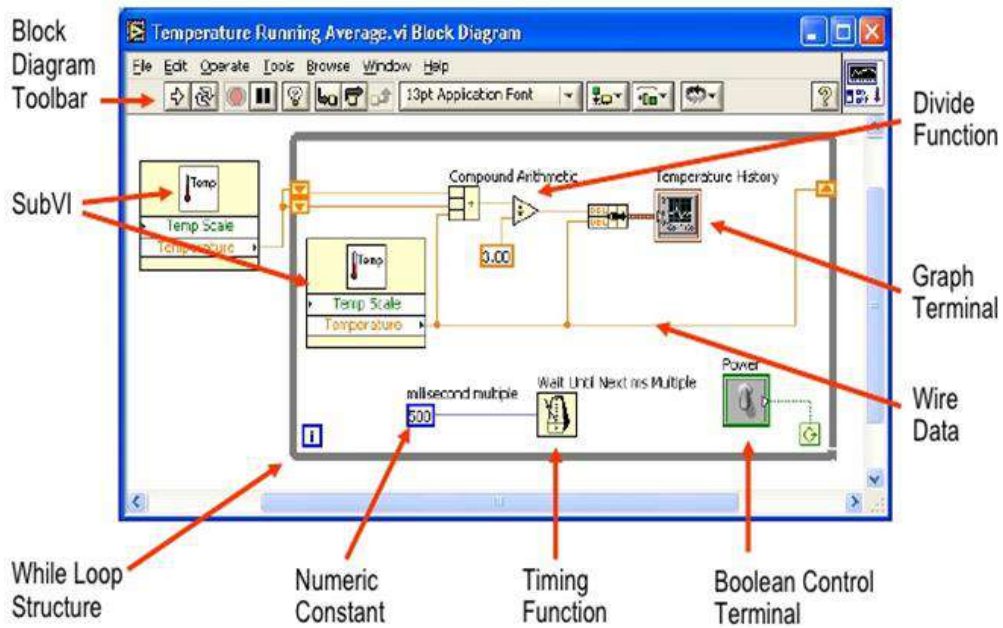


Figure IV-20: General block diagram of LabVIEW.

RIO technology is a National Instruments of LabVIEW for FPGA development, which is a set of software tools that simplifies the development of embedded systems using FPGA-based devices [108]. The simplification arises because IRIO defines three main elements: a data acquisition and processing architecture for the FPGA, a software layer interfacing. LabVIEW-FPGA module should be integrated on FPGA kit to be able to do the implementation. As shown in **Figure IV-21**; LabVIEW implementation is the only phase that needs to be created by the programmer; while the other phases can be automatically generated.

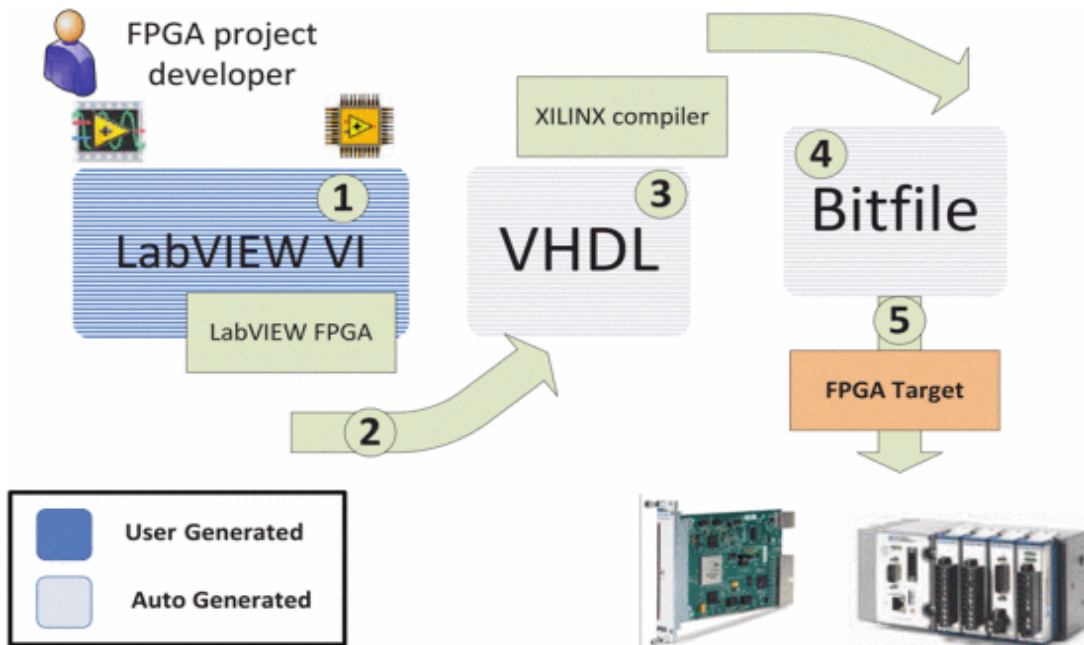


Figure IV-21: Necessary steps for performing LabVIEW-FPGA embedded system.

We have worked on implementing our algorithms on FPGA through LabVIEW tool that is why; we implemented all stages of our application on LabVIEW; but unfortunately; we missed hardware interface to allow charging our codes from LabVIEW to Xilinx kit.

IV.6.2. Implementation of image mosaicing on LabVIEW

To build a single image with a wide view from two overlapped images, we design a LabVIEW VI program which allowed us to obtain a mosaiced image. To being able to test our system, and verify some results given in this document, we design an execution interface on LabVIEW. This allowed the user to upload two overlapping images furthermore, we give the user the ability to select the type of corners detector (FAST or Harris) and its threshold value. Also, the user will be able to choose between Fast REtinA Key points (FREAK) descriptors [109] and Binary Robust Invariant Scalable Key points (BRISK) descriptors [110] for the matching purpose. As a result, the mosaiced image, the detected corners in both images and their matching are shown to the user, with some essential information:

- Number of features detected in both images.
- Number of matched points.
- Type of the transformation matrix (Homography matrix).
- Method of image re-projection.

With one click; the created LabVIEW interface can be executed, and the following figures are some screen shots of our LabVIEW interface (Front Panel). **Figure IV-22** gives the user the ability to upload two overlapping images even from different trajectories in PC.

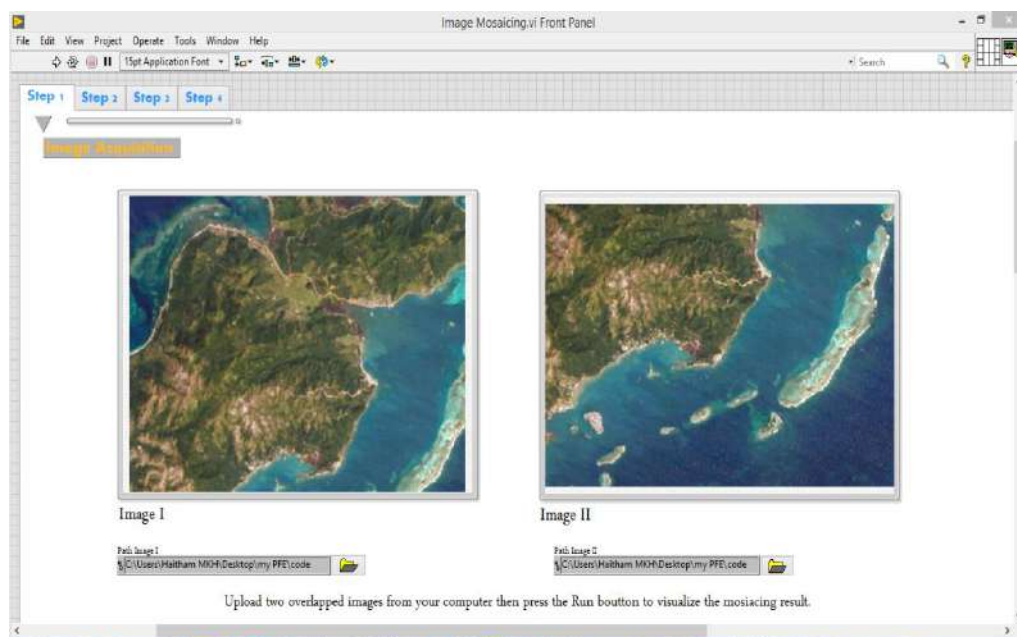


Figure IV-22: Acquisition of the overlapped satellite image.

Figure IV-23 shows the detected key points, here the user may choose between Harris or FAST corner detector; also he can change the threshold value to control the number of detected features.

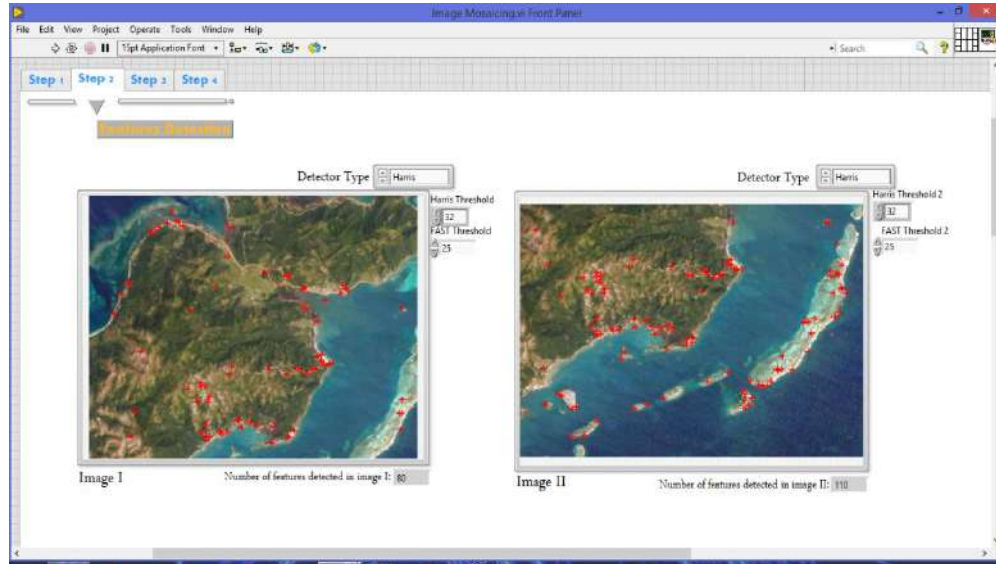


Figure IV-23: Features detection by Harris detector.

For features matching, the user may choose between two recent binary descriptors, which are FREAK and BRISK, with these two descriptors; Hamming distance is used as matching distance with small threshold value to get good matches. **Figure IV-24** shows the results of features matching with the type of chosen descriptors and coordinates of all matches.

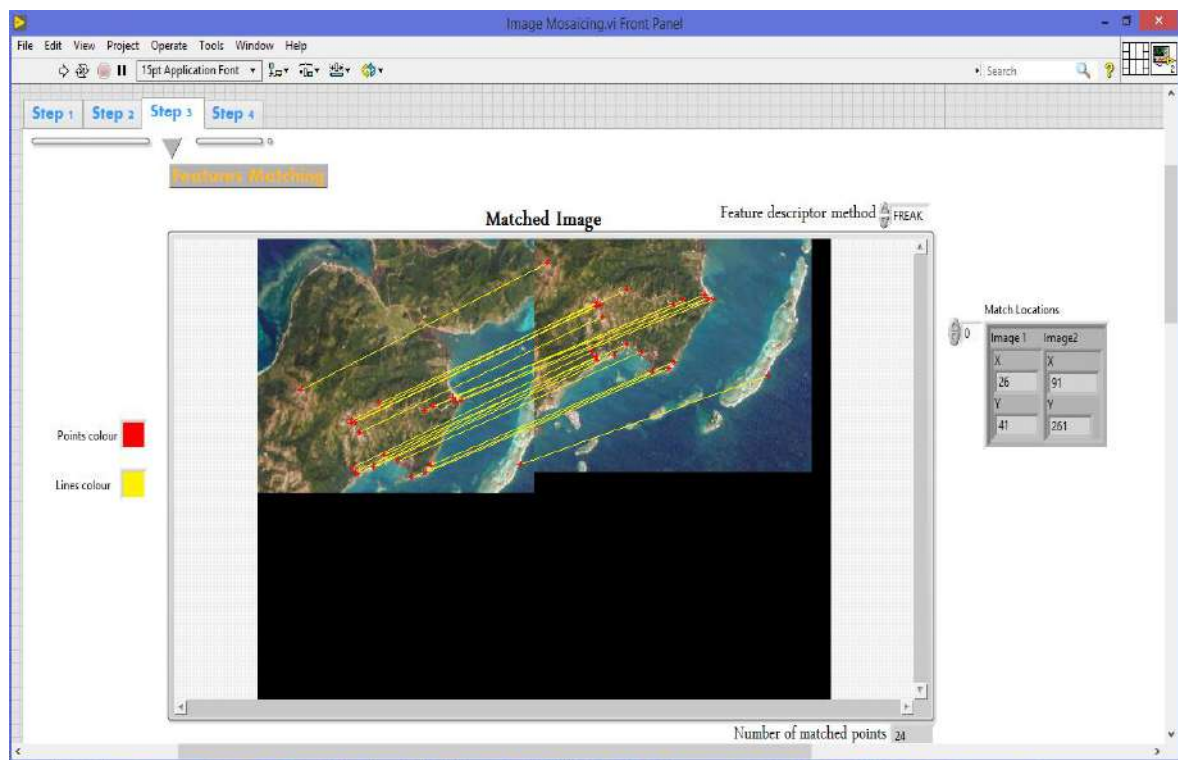


Figure IV-24: Features matching using FREAK descriptors.

After finding enough number of good matches, parameters of homography matrix are estimated using direct linear algorithm. **Figure IV-25** shows the obtained image mosaic with summary for all executed steps.

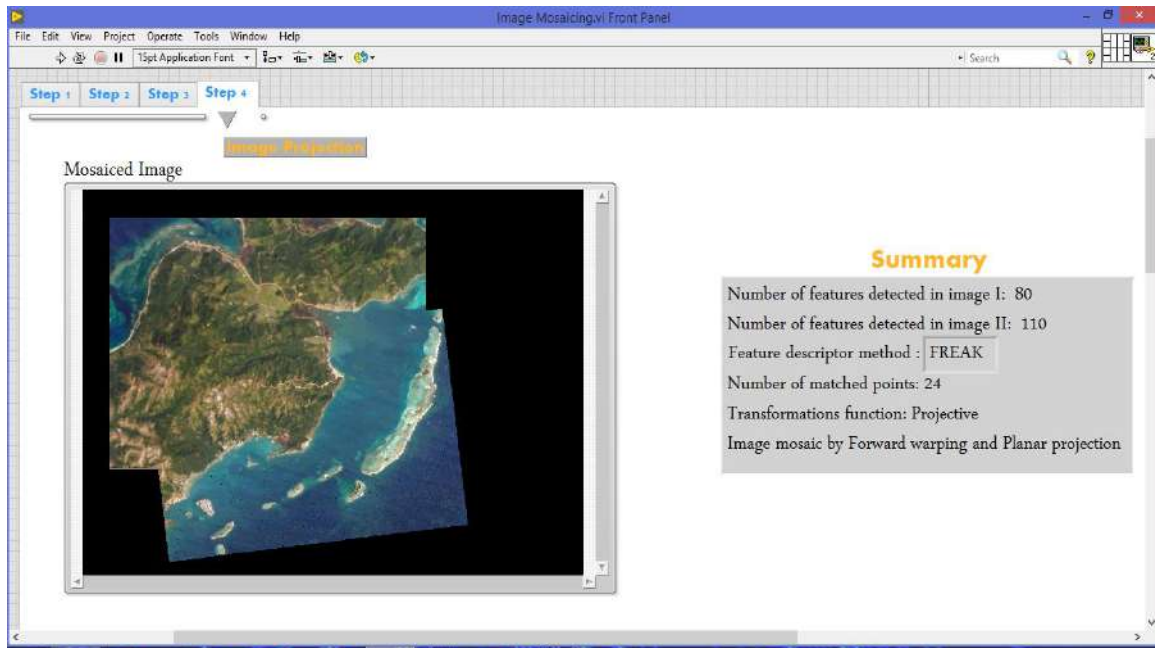
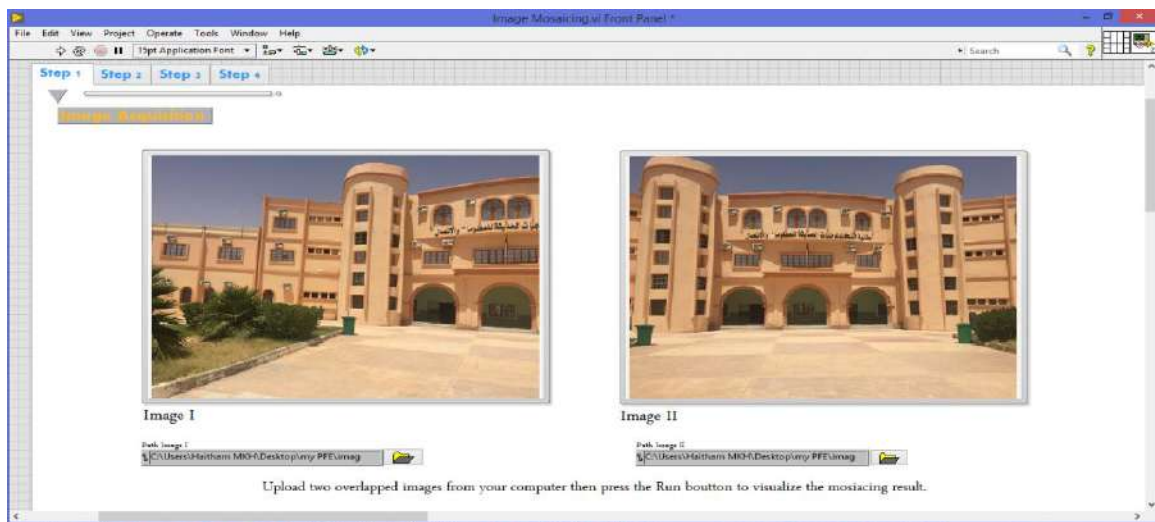


Figure IV-25: Image mosaic by applying backward warping.

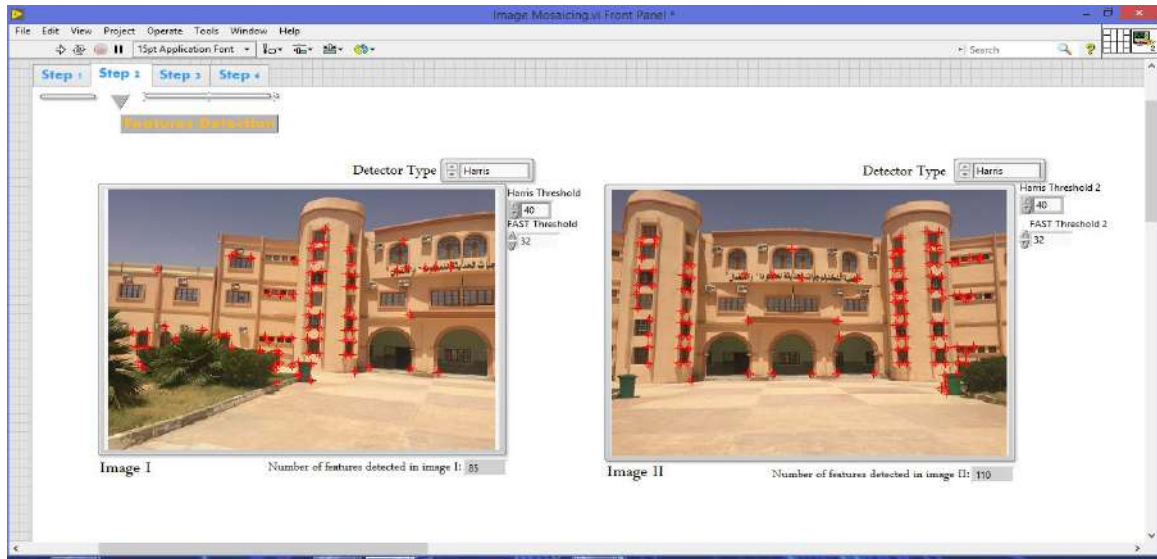
After all, for testing the results of our LabVIEW application, we are going to present in the flowing tables different categories of images sources outputs: satellite, aerial images (from UAV) and medical images.

IV.6.2.1. Test 1: Smart phone images

We captured two overlapping images using our smart phone in front of the faculty, those images are of large size; therefore they have been resized using '*imresize*' Matlab function. **Figures IV-26** show overlapping images and all steps for creating the image mosaic.



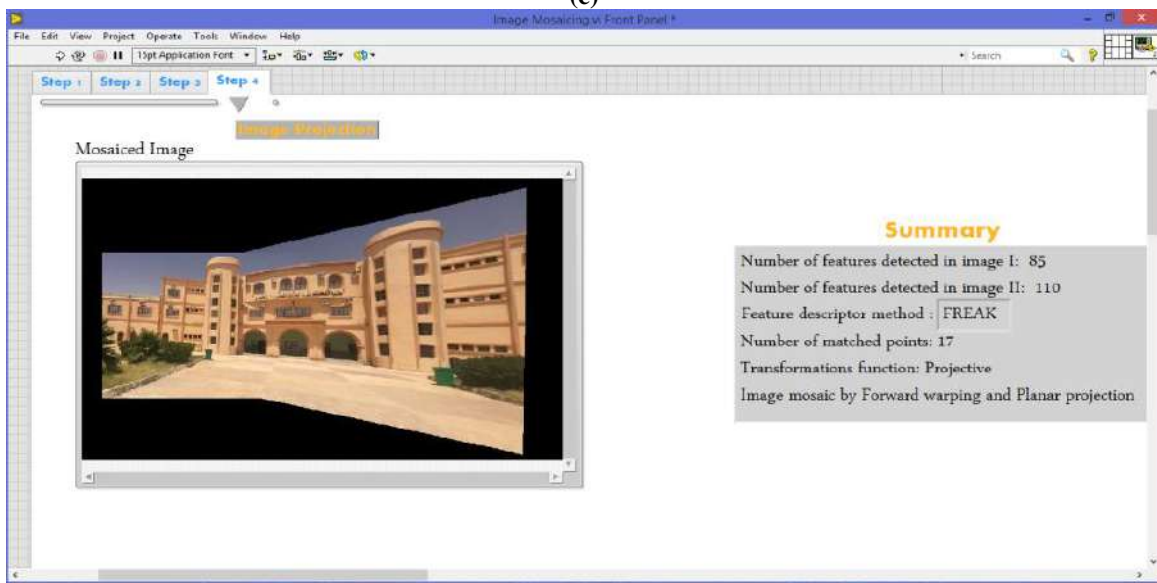
(a)



(b)



(c)



(d)

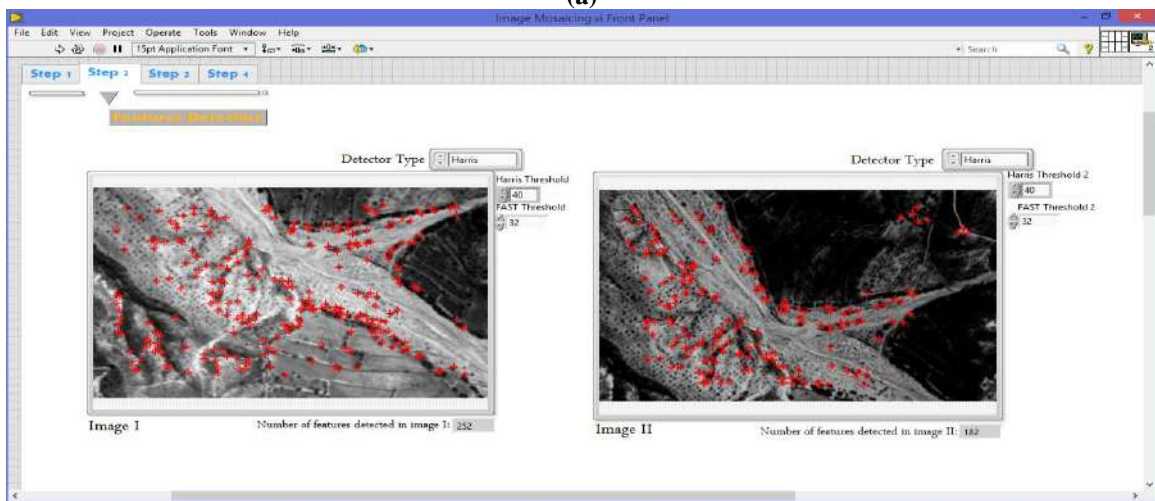
Figure IV-26: (a) overlapping smart phone images, (b) features detection by Harris detector, (c) finding correspondences using FREAK descriptors, (d) the obtained image mosaic and details.

IV.6.2.2. Test 2: Medical images

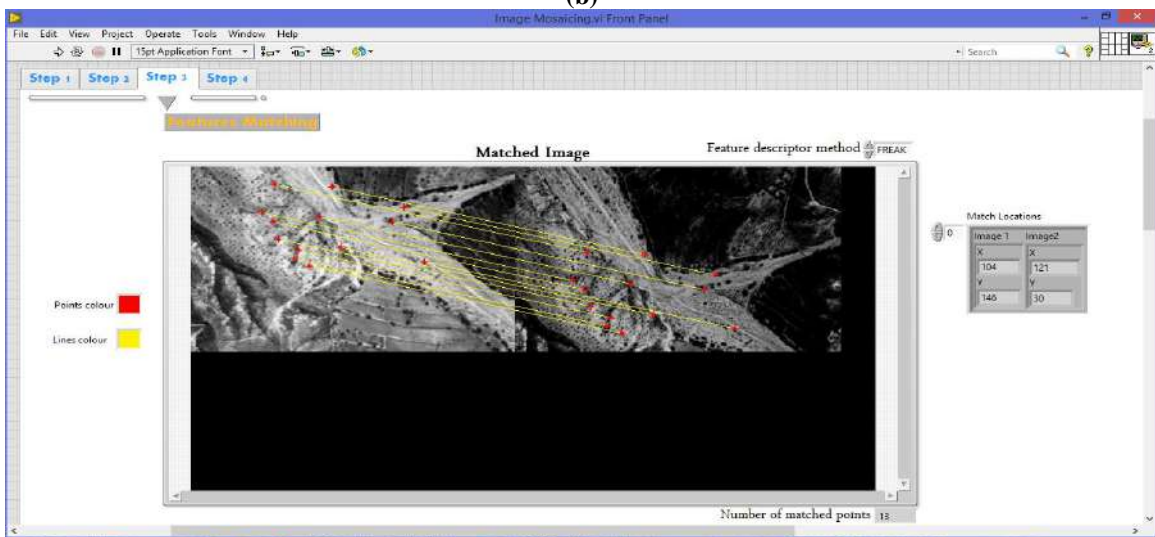
We have tested two remotely sensed overlapping images, these images are of gray level type; therefore RGB to gray level is not necessary in Harris or FAST algorithms. Those images are obtained from [84]. **Figures IV-27** shows all steps for creating the mosaic.



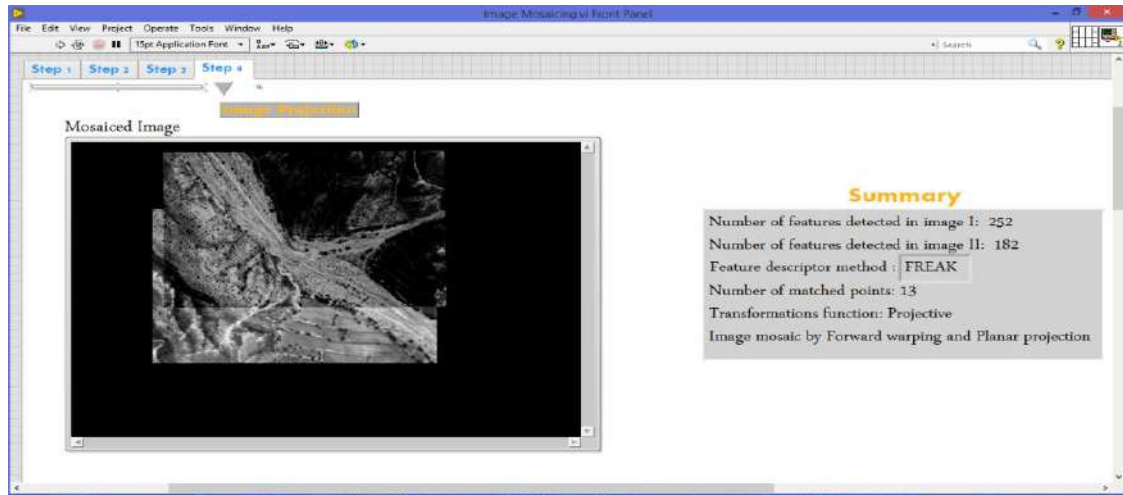
(a)



(b)



(c)

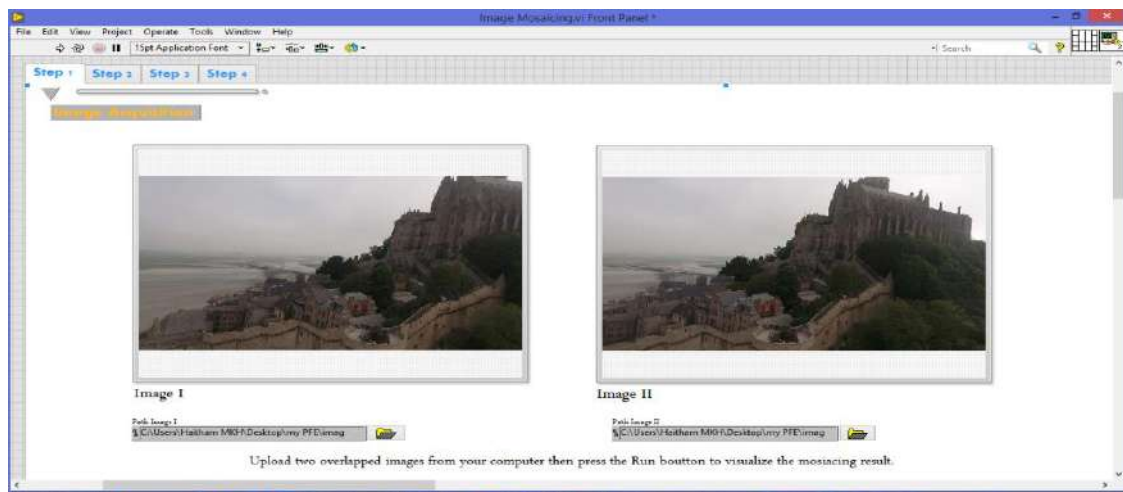


(d)

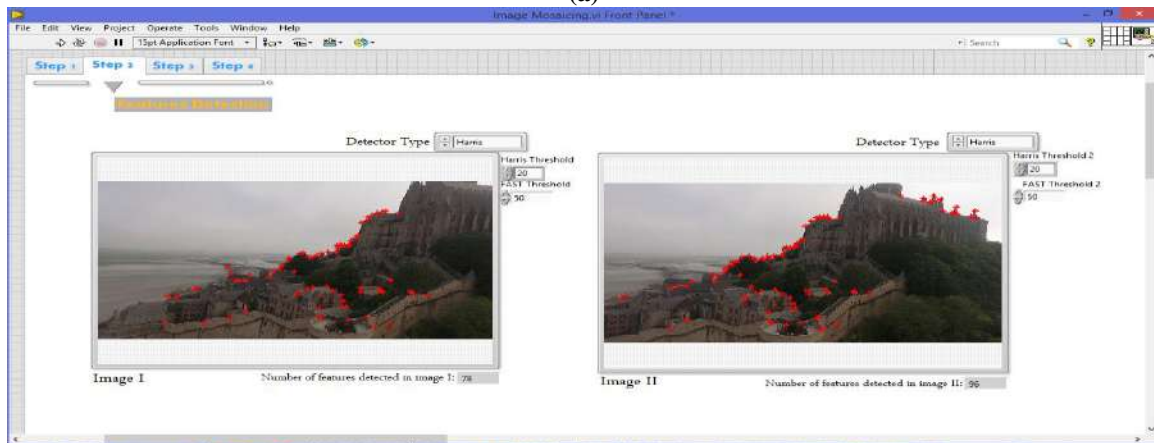
Figure IV-27: (a) overlapping medical images, (b) features detection by Harris detector, (c) finding correspondences using FREAK descriptors, (d) the obtained image mosaic and details.

IV.6.2.3. Test 3: UAV images

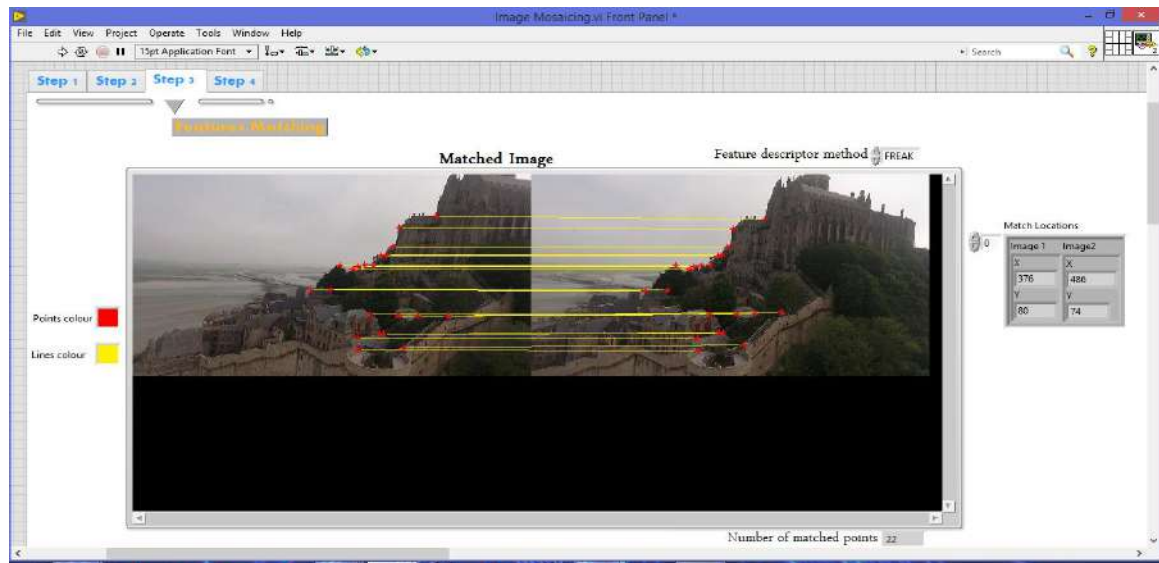
These images are captured by Los Angeles-based French photographer called Serge Ramelli, he uses the DJI Phantom 4 drone to capture aerial images [111]. Figures IV-28 shows all steps for constructing the panoramic mosaic.



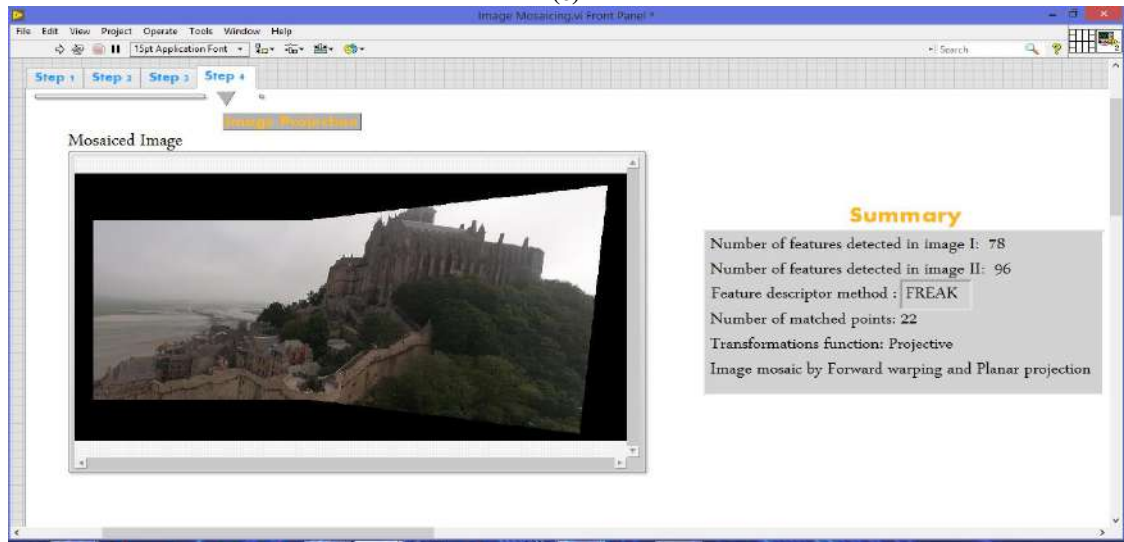
(a)



(b)



(c)

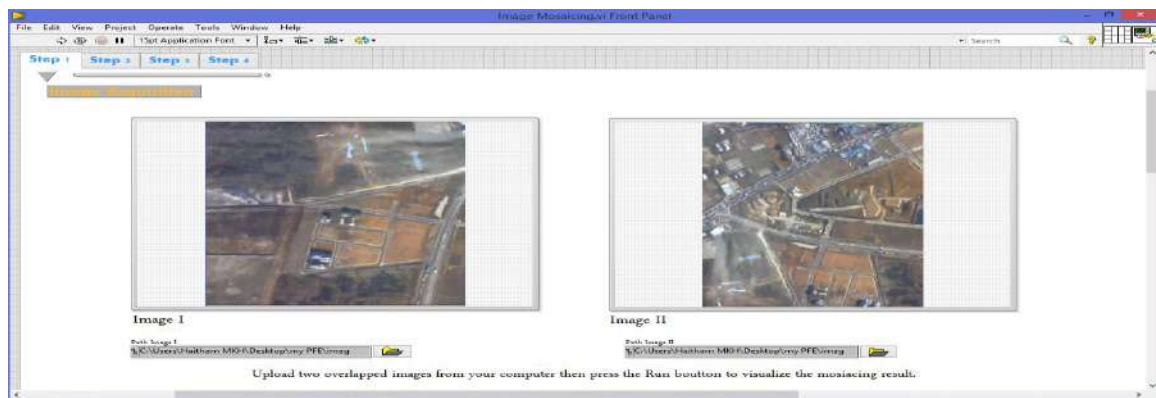


(d)

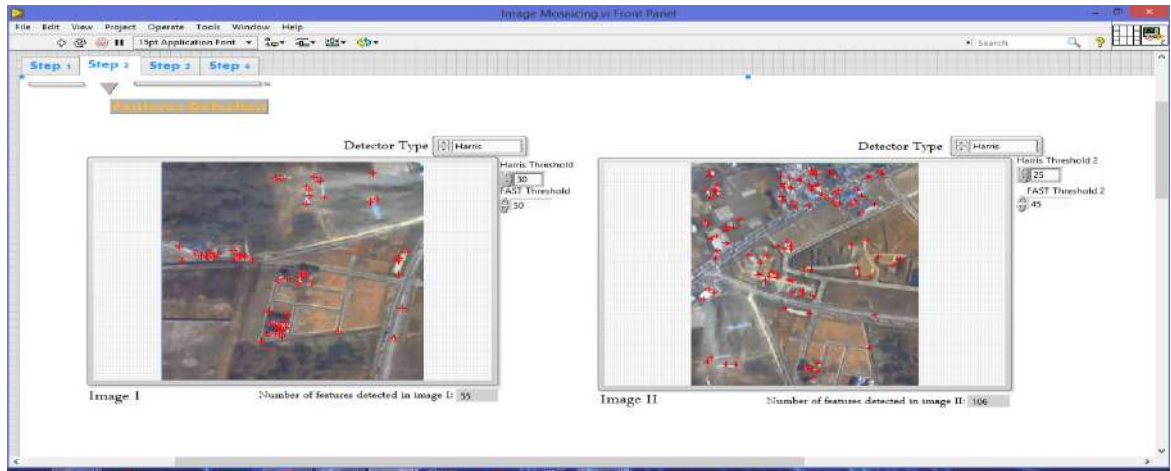
Figure IV-28: (a) overlapping images of drone, (b) features detection by Harris detector, (c) finding correspondences using FREAK descriptors, (d) the obtained image mosaic and details.

IV.6.2.4. Test 4: Satellite images

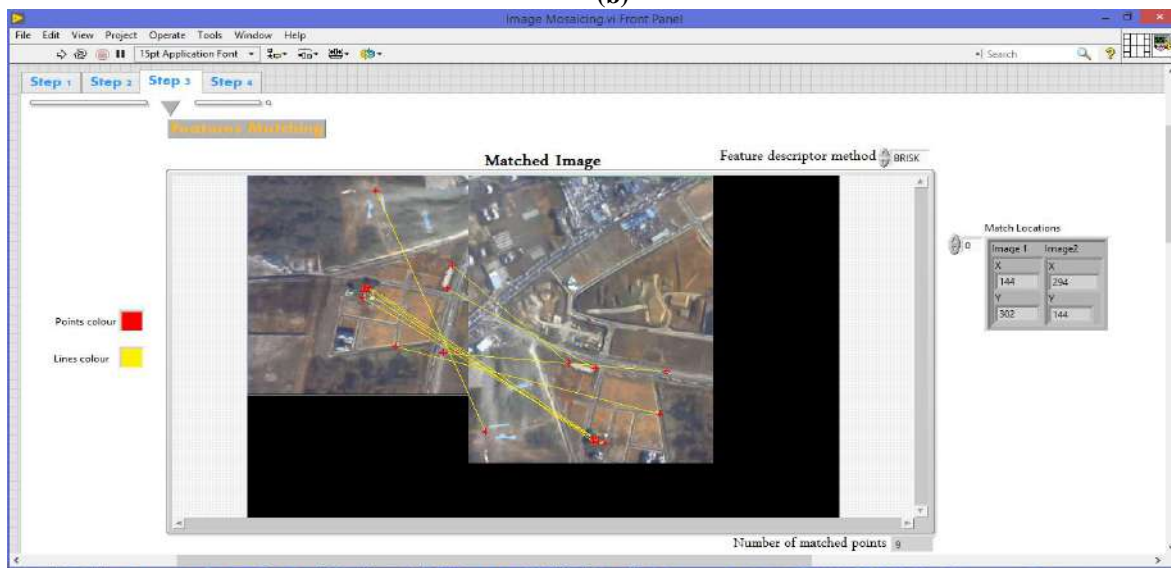
Satellite images with large overlapping are used here, they are taken from high altitude [112]. Figures IV-29 shows all steps for creating the aerial image mosaic.



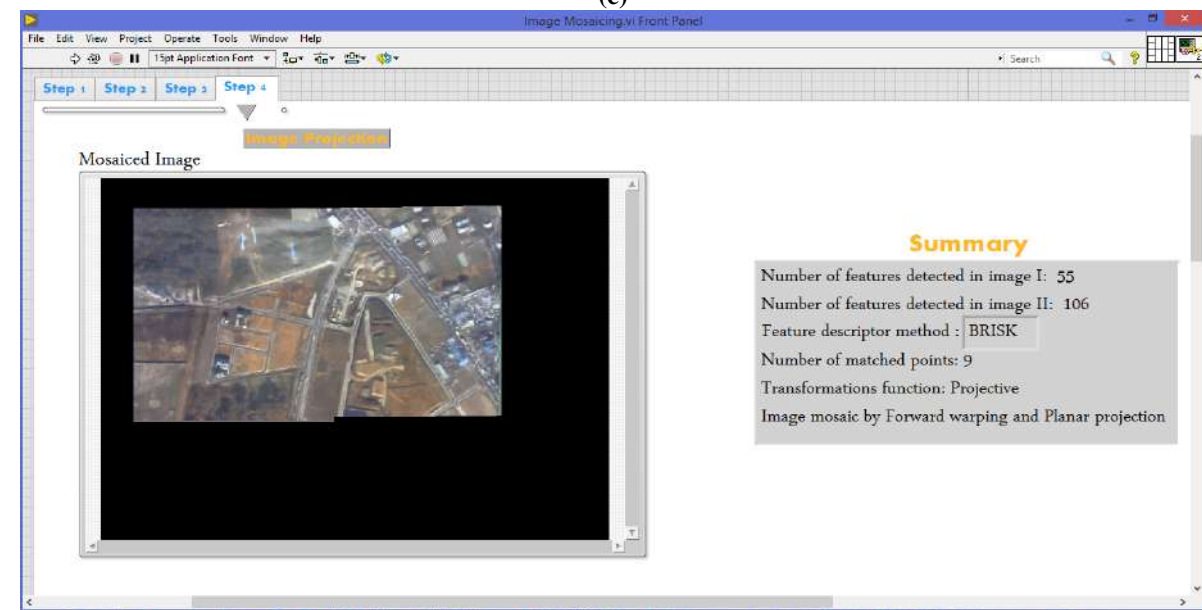
(a)



(b)



(c)



(d)

Figure IV-29: (a) overlapping satellite images, (b) features detection by Harris detector, (c) finding correspondences using BRISK descriptors, (d) the obtained image mosaic and details.

The performance and efficiency of our proposed algorithm were validated using different data set, these data set are collected using different camera types in different conditions. On these tests, our application gives generally very satisfying results.

IV.6.3. Implementation of Features based object tracking on LabVIEW

Object tracking algorithm is designed to locate and keep a steady watch on a moving object or many moving objects over time in a video stream or image sequences. This algorithm is an important component of many computer vision systems, and it is widely used in video surveillance, robotics, medical imaging, and human computer interface.

IV.6.3.1. State of The Art about Object Tracking

The work presented in [113] was designed to follow a moving object by a mobile robot, authors used mobile camera to capture image of the colored moving object and processed those images to get coordinate of both the moving object and robot. Global features of the moving object such as color and shape information of the target were used to track the moving object. In [114], mean shift algorithm was used for object tracking, in this algorithm current location was searched based on the histogram of the object in the previous image frame and result of mean shift was used to find the peak of probability density function near the object old position. Implementation of the algorithm on LabVIEW for different moving objects showed that it is suitable for real data analysis. Another work [115] used color features for implementing stereo vision tracking system using LabVIEW, the algorithm was based on detecting the tracked object in both web cameras images and maintaining the middle point between the cameras in the center of the image and at the same time; images were used to estimate the distance between the object and the stereo vision system, the advantage of the proposed algorithm is that other types of global features as shape or size can be used for object detection. The proposed system in [116] is generally applied for face detection and tracking process, the used webcam detected the color which was fed by the Region of Interest (ROI) coordinates to be tracked in the program, in that color tracking system, the camera was taking the color value and the setup of the camera was working as desired.

By looking to the above discussed literatures, we can easily recognize that most of developed object tracking algorithms are based on global features as size, color and shape, and these algorithms need processing all image for tracking purpose, therefore; we have proposed a robust tracking algorithm based on local features rather than global features.

IV.6.3.2. Object Tracking Results on LabVIEW

Tracking of an object pre-selected by the user or recognizing the specific object of interest and its tracking can be applied in public transportation, traffic, military and rescue systems etc. In recent decades several studies are conducted on image processing or object recognizing and tracking through different scientific and experimental methods. Our strategy to achieve this algorithm firstly, we pass through the same three stages(feature extraction and feature matching then the homography estimation) ,then we multiple the four corners coordinates of the template image with the homography matrix ,then we obtain new four coordinates which represent the corners of the rectangular target tracked. **Figure IV-30** shows the flow chart for the essential steps of the object tracking algorithm applied.

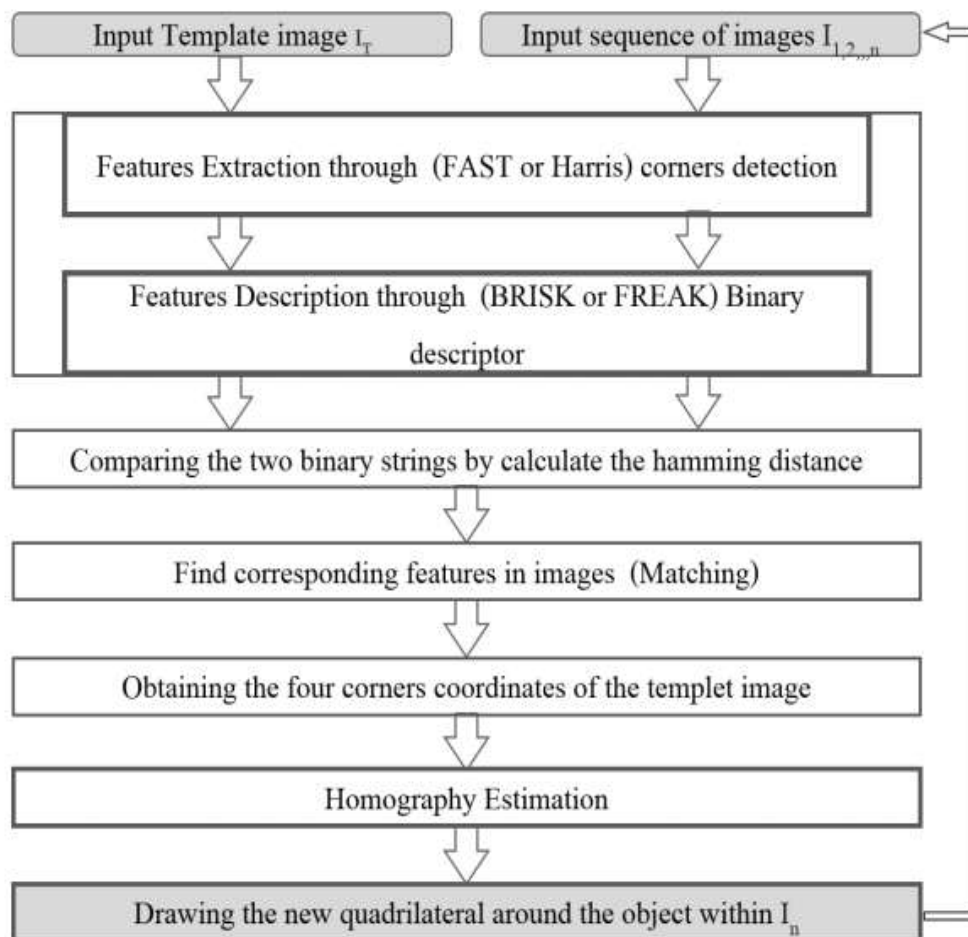


Figure IV-30: The method proposed for object tracking flowchart.

The created LabVIEW interface of object tracking is based on choosing locations of reference image and template one for identifying the tracked object; with knowing the time delay between them, our algorithm can be executed with one click. **Figure IV-31** shows the built interface which is for tracking Arduino kit:

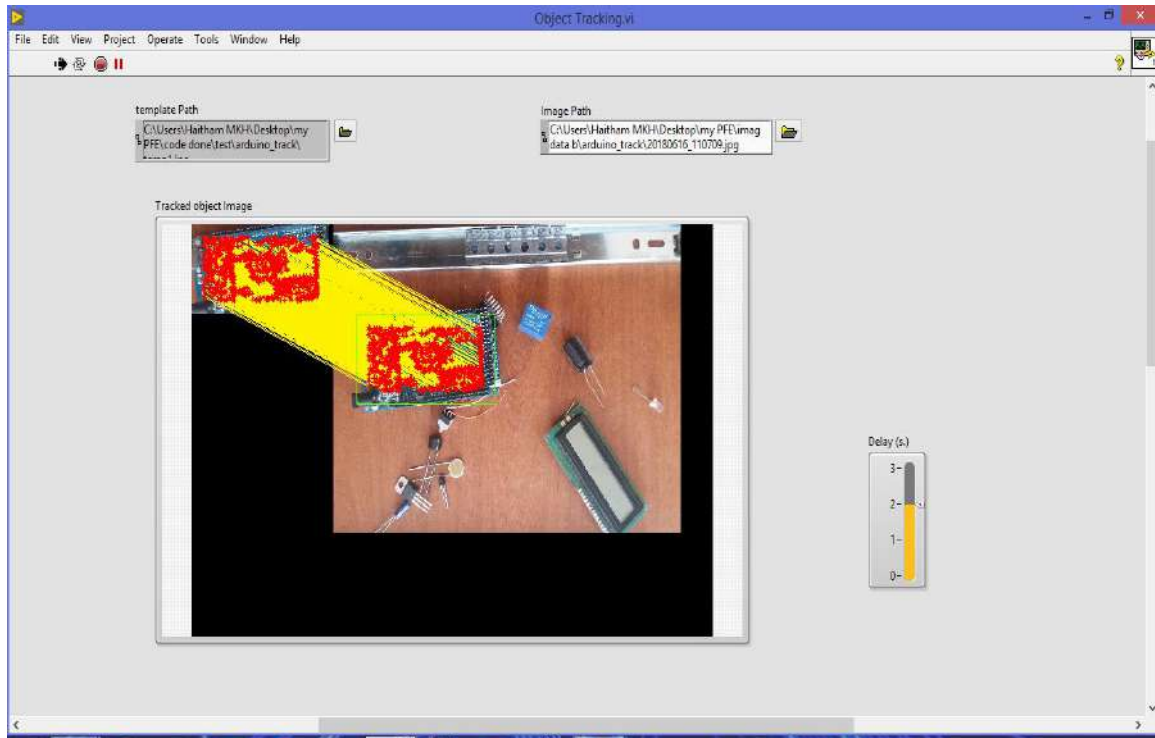


Figure IV-31: Interface of features based object tracking.

Some results of this algorithm are shown next in **Figures (IV-32 and IV-33)**:

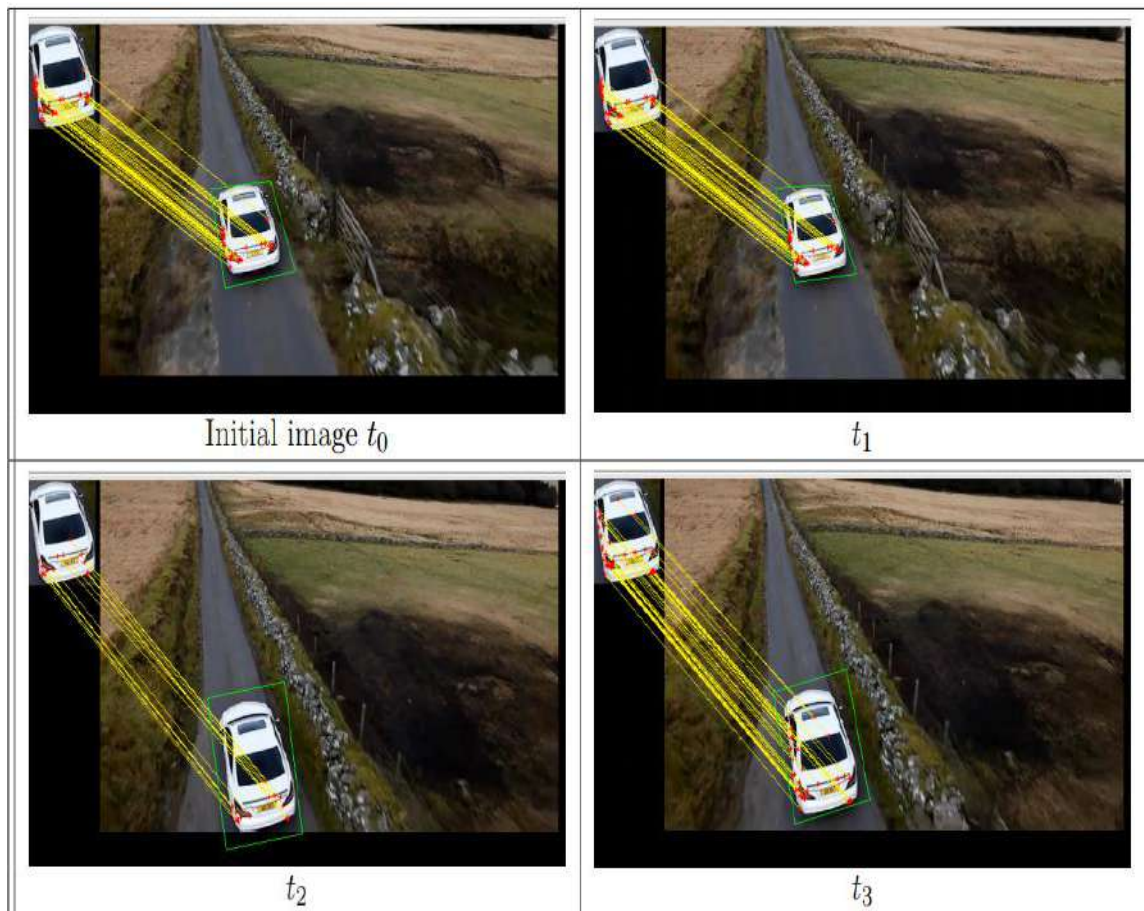


Figure IV-32: Car tracking (detected object within green trapezium).

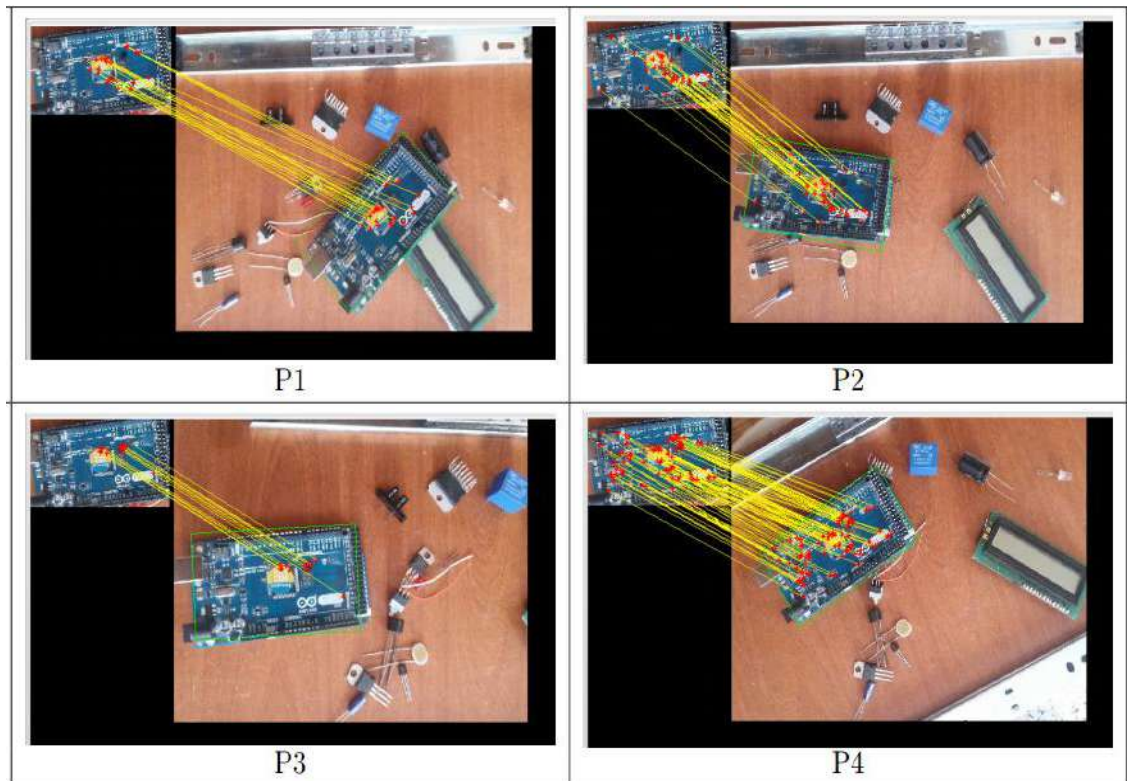


Figure IV-33: object (Arduino) detection and tracking.

Key points-based tracking is illustrated in two tests, the first one shows the result of tracking a moving car in a sequence of video (filming by UAV) and the second test shows the results of object (Arduino) detection and tracking using a fixed camera. In both results, of which four are shown here. A green trapezium has been drawn around the template target in each frame and the parameters of this trapezium are delivered by the tracking algorithm. As the object or camera moves, the position of the rectangle is centered on the car and the width and angles of the rectangle changes as the car's motion. From this, we can then analyze the target and their motion; we can conclude that these algorithms could be useful in public transportation, traffic, military and robotic domains.

By applying our features based tracking algorithm on the two above examples (Arduino and car); we got excellent results, in which the object will be kept tracked while it is in the appearance of the camera. Advantages of our algorithms are the following:

- 1) The algorithm is based on local features (points) contrary to other algorithms [113, 114, 115, 116] that used global features (shape, color... etc.).
- 2) Tracking of objects can be done by using single or different cameras.
- 3) The created LabVIEW interface is practical for real time application.

IV.7. Conclusion

In this chapter, image mosaicing of overlapping images has been introduced. The general scheme of the algorithm includes steps of image features detection, defining the overlapping region, finding the appropriate transformation and projecting the images. These steps will work even if they were implemented in different methods, but our method overcome drawbacks of the other method. From the obtained results, it can be concluded that SIFT or Harris detector combined with LBPDs produce simple and accurate detection and description for images key points, and in order to eliminate the wrong matches, three techniques were considered to be fuzzy sets, then; these fuzzy sets were linked according to fuzzy rules. Our tests were performed on real images from famous data base, since there is no evaluation criterion available in some literatures to evaluate the mosaic results, we compared the results visually and for other works, we attempt to evaluate the mosaicing results by using well known performance metrics. All the evaluation measures confirm that the proposed algorithm is robust and efficient for mosaicing aerial and non-aerial images and can be used for aerial navigation, visual mapping and other robotic applications.

LabVIEW implementation of image mosaicing algorithm was developed at the end of this chapter, but unfortunately; because of the missing hardware interface between LabVIEW and FPGA kit; the embedded system could not be established. The template object tracking algorithms described in this chapter can detect and track any kind of object, at various distances even if the object is moved, rotated or flipped. And it can be useful in many domains such as surveillance, traffic, military, biometry and robotics etc. Both of our VI executable for image mosaicing and object tracking are based on point's features, Those VIs give good outputs results with different images from different sources in many domains.

General Conclusion

General Conclusion

➤ Conclusions About Thesis

Most of robotic vision applications, such as obstacle avoidance, object tracking and pose estimation require robust image feature matching techniques, but, even though several algorithms were developed for that purpose; they cannot accommodate large changes in viewpoint. This problem is caused by either the absence of correct correspondences or their portion is insufficient for fitting methods to work correctly. The aim of this thesis is to propose a solution to UAV images of small field of view; through combining overlapping images to form a big mosaic. Features based image mosaicing is an important vision algorithm that was used since a long time for different tasks. This algorithm requires proceeding successive steps; in which, features matching is the most critical stage, and false associations problem is its big challenge, these type of matches are known as outliers and they affect negatively on the quality of constructed mosaic. Researchers in image processing domain suggested several solutions, but more improvements are still needed. In our work, we proposed efficient fuzzy techniques for finding good correspondences between images.

In our thesis; a number of important topics concerning aerial vehicles applications has been studied; especially in imaging domain, therefore; we have started by introducing history of UAVs, how they may be classified according to size or flying properties, and their uses in military or civilian tasks. Some UAV vision based systems were discussed also to show the advantages of them in several aerial robotic navigation algorithms. Then, we have passed to give a general scheme of image mosaic constructions, with explaining each step in details. Based on vast research in literatures; recent related image mosaicing works were discussed in order to introduce the main drawbacks of them. After that, proposed outliers rejection approaches based on fuzzy logic theory were stated. Finally, simulation tests using real data have illustrated the robustness and efficiency of the proposed algorithms to remove false associations and construct a large image mosaic of a scene.

The presented work has been virtually divided into five integrated contributions. First, an enhancement to classical LBP technique was developed to overcome interpolations errors in constructing the LBP descriptors. Second, fuzzy inference system based mainly on hamming distance was proposed to improve the matching results of these binary descriptors. Third, classical similarity measures with their calculated scores were used as fuzzy inputs to

eliminate false matches produced by correlation based features matching. Fourth, another fuzzy inference system was proposed for removing outliers using RANSAC and bidirectional techniques. Fifth; a sophisticated LabVIEW interface for image mosaic constructions was created to facilitate acquiring images and algorithm execution to users. Based on the same procedures, features based object tracking algorithm was implemented on LabVIEW and executed using different scenarios.

➤ **Perspectives for Futures Works**

As every scientific research work, this thesis had some limitations and furthermore works to add, these could be because of time or funds. Thus, a number of research challenges have been identified and proposed for future investigation. As a critical criterion to all image processing algorithms; the complexity and computation time form the principal real time constraints, this why it is very important to select the suitable algorithm for real time tasks. We propose using other types of images as thermal images or remote sensed ones, also we recommend looking for implementing the proposed algorithms on embedded systems.

References

References

- [1] Wierzbicki D, Kedzierski M and Fryskowska A . "Assesment of the influence of uav image quality on the orthophoto production." The International Archives of Photogrammetry, Remote Sensing and Spatial Information Sciences 40.1 ,2015.
- [2] Sieberth T, Rene W, and Jim HC. "UAV image blur–its influence and ways to correct it." 2015.
- [3] Sachs, David, Steven N, and Daniel G. "Image stabilization technology overview" . InvenSense Whitepaper, 2006.
- [4] Gupta S.G, Ghonge M. M and Jawandhiya P.M. “ Review of unmanned aircraft system (UAS)” . International journal of advanced research in computer engineering & technology (IJARCET), 2(4), 1646-1658. 2013.
- [5] Gonzales D and Harting S.“ Designing Unmanned Systems with Greater Autonomy, Using a Federated, Partially Open Systems Architecture Approach”. ISBN: 978-0-8330-8606-8 . Published by the RAND Corporation, Santa Monica, Calif. 2014 .
- [6] Cummings M.L, da Silva F.B and Scott S.D. “Design Methodology for Unmanned Aerial Vehicle (UAV) Team Coordination” . Massachusetts Institute of Technology* Prepared For Boeing Phantom Works HAL2007-05 .2007.
- [7] Gertler J .“U.S. Unmanned Aerial Systems” . Library of Congress Washington DC Congressional Research Service .2012.
- [8] Dobbing M and Cole C. “ Israel and the drone wars - Examining Israel’s production, use and proliferation of UAVs”. Published by Drone Wars UK . 2010.
- [9] John F. K and Stephen S. C. “ A Brief History of Early Unmanned Aircraft” Johns Hopkins Apl Technical Digest, Volume 32, Number 3 . pp 558-571. 2013.
- [10] Therese S. “ Unmanned Aircraft Systems for civilian Missions” .Brandenburg Institute for Society and Security gGmbH BIGS Policy Paper No. 1 .2012.
- [11] Ivan A.S, Christopher J.N and Mark A.S. “Civil UAV Capability Assessment” Prepared for Lawrence Camacho UAV Vehicle Sector Manager-Vehicle Systems Program NASA Aeronautics Research Mission Directorate . 2004.
- [12] Freed M, Harris R and Shafto M. “Comparing methods for UAV-based autonomous surveillance”. Submitted to the National Conference on Artificial Intelligence of NASA Ames Research Center.2004.

- [13] Adams, S.M and Friedland, C.J. “A survey of unmanned aerial vehicle (UAV) usage for imagery collection in disaster research and management”. In 9th International Workshop on Remote Sensing for Disaster Response (Vol. 8). 2011.
- [14] Segor F, Bürkle A, Kollmann M and Schönbein, R. “Instantaneous autonomous aerial reconnaissance for civil applications”. In Proceedings of the Sixth International Conference on Systems (pp. 72-76). 2011.
- [15] Abdessameud A and Abdelhamid T . “Motion Coordination for VTOL Unmanned Aerial Vehicles: Attitude Synchronisation and Formation Control” . 196 Pages | ISBN: 1447150937. 2013.
- [16] Arthur D. A and Eveker, K . “Alternatives for modernizing US fighter forces.” Government Printing Office. p. 38. 2009.
- [17] Yang X., Wang, T., Liang, J., Yao, G., and Liu, M.. “Survey on the novel hybrid aquatic–aerial amphibious aircraft: Aquatic unmanned aerial vehicle (AquaUAV)”. Progress in Aerospace Sciences, 74, pp.131-151. 2015.
- [18] M Saska , Z Kasl and L Preucil “Motion Planning and Control of Formations of Micro Aerial Vehicles”. In Proceedings of The 19th World Congress of the International Federation of Automatic Control . PP 1228- 1233.South Africa. 2014.
- [19] Bills, C., Chen, J., Saxena, A. “Autonomous MAV flight in indoor environments using single image perspective cues.” In: IEEE International Conference on Robotics and Automation. 2011.
- [20] Ng, W.S and Sharlin E. “Collocated interaction with flying robots”. Technical Report 2011-998-10, Dept. of Computer Science, University of Calgary, Canada .2011.
- [21] Theys, B., Notteboom, C., Hochstenbach, M., and De Schutter, J. “Design and control of an unmanned aerial vehicle for autonomous parcel delivery with transition from vertical take-off to forward flight”. International Journal of Micro Air Vehicles, 7(4), p395-405. 2015.
- [22] Lin F “Development and Applications of a Vision-Based Unmanned Helicopter”. A thesis submitted for the degree of doctor of philosophy department of electrical & computer engineering (PhD) . Beihang University, China . 2010.
- [23] Nemra A. ‘Robust Airborne 3D Visual Simultaneous Localisation And Mapping’, PhD thesis, Cranfield University.2010.

- [24] Mejias, S. Saripalli, P. Cervera and Sukhatme G. S. “Visual servoing of an autonomous helicopter in urban areas using feature tracking,”*Journal of Field Robotics*, vol. 23, pp. 185-199, 2006.
- [25] Sattigeri R., Johnson E., Calise A. and Ha J. “Vision-based target tracking with adaptive target state estimator,”*Proceedings of the AIAA Guidance, Navigation and Control Conference and Exhibit, Hilton Head, , pp. 1-13, USA. 2007.*
- [26] Wagter C. D., Proctor A. A. and Johnson E. N. “Vision-Only aircraft flight control,”*Proceedings of the 22nd Digital Avionics Systems Conference, India, 2003.*
- [27] Proctor A. A. and Johnson E. N. “Vision-Only Aircraft Flight Control Methods and Test Results,”*Proceedings of the AIAA Guidance, Navigation, and Control Conference, Providence, Rhode Island, pp. 1-16, 2004.*
- [28] Shakernia O, Ma Y., Koo T. J. and Sastry S. “Landing an Unmanned Air Vehicle: Vision Based Motion Estimation and Nonlinear Control,”*Asian Journal of Control*, vol. 1 pp. 128–204, 1999.
- [29] Kumar K.S, Kavitha G and Subramanian R. ‘Image Fusion of Video Images and Geolocalization for UAV Applications’ . *ACEEE Int. J. on Information Technology*, Vol. 01, No. 02. India 2011.
- [30] Louvat B, Bonnaud L, Marchand N and Bouvier G. “ Suivi d’objets pour une camera embarquée dans un drone” *Colloque GRETSI*, PP 681-684 . Troyes. France 2007.
- [31] Porikli F. “Achieving real-time object detection and tracking under extreme conditions,”*Journal of Real-Time Image Processing*, vol. 1, pp. 33-40, 2006.
- [32] He Z, Venkataraman R and Chandler P. “Vision-based UAV flight control and obstacle avoidance”. In *Proceeding of IEEE American Control Conference*. 2006.
- [33] Feng, Y., Zhang, C., Baek, S., Rawashdeh, S., and Mohammadi, A. “Autonomous Landing of a UAV on a Moving Platform Using Model Predictive Control”. *Drones*, vol. 2, no 4, p. 34. 2018.
- [34] Ivan F, Miguel A and Campoy P, Martinez, Carol M and Mejias L. “Unmanned Aerial Vehicles UAVs attitude, height, motion estimation and control using visual systems” .*Autonomous Robots*. (In Press). Spain .2010.
- [35] Omkar S.N., Tripathi S, Gaurav K and Itika G. “Vision Based Obstacle Detection mechanism of a Fixed Wing UAV” *International Journal of Advanced Computer Research* (ISSN (print): 2249-7277 ISSN (online): 2277-7970) Volume-4 N-1 Issue-14 .2014.

- [36] Hrabar S., Sukhatme G. S., Corke P., Usher K. and Roberts J. “Combined optic-flow and stereo-based navigation of urban canyons for a UAV,”IEEE/RSJ International Conference on Intelligent Robots and Systems, pp. 3309-3316, 2005.
- [37] Wendel, A., Maurer, M., Katusic, M., and Bischof, H. “Fuzzy visual servoing for micro aerial vehicles”. na. 2012.
- [38] Al-Kaff, A., García, F., Martín, D., De La Escalera, A., and Armingol, J. “Obstacle detection and avoidance system based on monocular camera and size expansion algorithm for UAVs. Sensors”, vol. 17, no 5, p. 1061. 2017.
- [39] Milford, M. J., Schill, F., Corke, P., Mahony, R., and Wyeth, G. “Aerial SLAM with a single camera using visual expectation”. In IEEE International Conference on Robotics and Automation (pp. 2506-2512). IEEE. 2011.
- [40] Bheda D., Joshi M. and Agrawal V. “ A Study on Features Extraction Techniques for Image Mosaicing ”. International Journal of Innovative Research in Computer and Communication Engineering.Vol 2. Issue 3. Pages 3432–3437. India. 2014.
- [41] Joshi H. and Sinha K. “ A Survey on Image Mosaicing Techniques International Journal of Advanced Research in Computer Engineering Technology . Vol 2. Issue 2. ISSN 2278-1323 . Pages 365–369. India. 2013.
- [42] Shum H.Y and Szeliski R.“ Panoramic Image Mosaics ”. Published in Proceedings of the 24th annual conference on Computer graphics and interactive techniques (SIGGRAPH '97) . Pages 251-258. New York , USA .1997.
- [43] Jae-Neung L and Keun-Chang K. “Trends Analysis of Image Processing in Unmanned Aerial Vehicle”. International Journal of Computer, Electrical, Automation, Control and Information Engineering Vol:8, No:2, pp 271-274. 2014.
- [44] Carnie R, Walker R and Corke P. “Image Processing Algorithms for UAV “Sense and Avoid”,” in ICRA, International Conference, pp. 2848-2853, 2006.
- [45] Lee J.N and Kwak K.C, “A Trends Analysis of Domestic Research in Unmanned Aerial Vehicle image Processing,” Proceedings of KISM Fall Conference , vol. 2, pp. 221-224, 2013.
- [46] Cheng X , Jinling W and Yaming X . “A Method for Building a Mosaic with UAV Images”. International Journal in Information Engineering and Electronic Business (MECS). PP 9:15.2010.
- [47] Sk SA ‘Image Mosaicing, its techniques, algorithms, implementations and applications ’.Roll No:02..M tech computer science and eng.2014.

- [48] Goshtasby A.A. “ 2-D and 3-D Image Registration for Medical, Remote Sensing, and Industrial Applications ” . Published by John Wiley & Sons, Inc., Hoboken, New Jersey. Published simultaneously in Canada. 2005.
- [49] Alhichri H.S. and Kamel M. “ Virtual circles: a new set of features for fast image registration. Pattern Recognition Letters. pp 1181–1190 . 2002.
- [50] Canny J, “ A computational approach to edge detection ”. In Proceeding of IEEE ,Transactions on Pattern Analysis and Machine Intelligence. 1986.
- [51] Tuytelaars T and Mikolajczyk K. “ Local Invariant Feature Detectors: A Survey ” .Foundations and Trends Rin Computer Graphics and Vision, Journal of Intelligent & Fuzzy Systems. Pages 41-50. 2008.
- [52] Rosten E. “ FAST Corner Detection Homepage ”. <http://svr-www.eng.cam.ac.uk/er258/work/fast.html>. 2011.
- [53] Harris, C. G., and Stephens, M. “A combined corner and edge detector”. In Alvey vision conference (Vol. 15, No. 50, pp. 10-5244). 1988.
- [54] Stoica A.R. “ Delaunay Diagram Representations For Use in Image Near-Duplicate Detection ”. Senior Project submitted to The Division of Science, Mathematics & Computing Of Bard College . Annandale-on-Hudson. New York. 2011.
- [55] Lowe D. “ Distinctive Image Features from Scale-Invariant Keypoints ”. Accepted for publication in the International Journal of Computer Vision. Pages 1-28. 2004.
- [56] V.S Bind, P.R Muduli and U.C. Pati, “ A Robust Technique for Feature-based Image Mosaicing using Image Fusion ”. International Journal of Advanced Computer Research;, Vol 3 Issue 1. Pages 263 . 2013.
- [57] D. Capel and A.Zisserman, “Automated Mosaicing with Super-resolution Zoom”.Robotics Research Group ,Department of Engineering Science .University of Oxford Oxford OX1 3PJ, UK.1998.
- [58] J. Zhao, S. Zhu, and X. Huang, “ Real-Time Traffic Sign Detection Using SURF Features on FPGA ”. In IEEE , High Performance Extreme Computing 'HPEC' .2013.
- [59] S. Adam, M. Kraft, M. Fularz and Z. Domagała, “ The Comparison of Point Feature Detectors and Descriptors in the Context of Robot Navigation ”. Workshop on Perception for Mobile Robots Autonomy. 2012.
- [60] S. Chambon and A. Crouzil, “ Evaluation et comparaison de mesures de corrélation robustes aux occultations ”. Rapport de recherche. Université PaulSabatier, Toulouse, France. 2002.

- [61] Minoru, M., Kunio, K.: Fast Template Matching Based on Normalized Cross Correlation Using Adaptive Block Partitioning and Initial Threshold Estimation. In: IEEE International Symposium on Multimedia, pp. 196–203. IEEE Press. 2010.
- [62] Alhwarin, Faraj. Fast and robust image feature matching methods for computer vision applications. University of Bremen, 2011.
- [63] J. Shiand et C. Tomasi, “ Good features to track ” .In Proceeding of IEEE Conference on Computer Vision an Pattern Recognition, Seattle. Pages 593–600. 1994.
- [64] R. Hartley and A. Zisserman, “ Multiple View Geomerty in Computer Vision ”. Cambridge University Press, second edition. 2003.
- [65] J-K Kamarainen and P. Paalanen, “ Experimental study on fast 2d homography estimation from a few point correspondences ”. ISBN 0978-952-214-773-8. ISSN 0783-8069 . Page 1-20 . Lappeenranta .2009.
- [66] Dubrofsky, Elan. "Homography estimation." Diplomová práce. Vancouver: Univerzita Britské Kolumbie. 2009.
- [67] HarshalPatil and S.S. Deshmukh, “ Homography Estimation Using RANSAC ”. International Journal of Research in Engineering & Advanced Technology (IJREAT), Volume 1, Issue 3, ISSN: 2320 – 8791. 2013.
- [68] Botterill, T., Mills, S., and Green, R. D. “New Conditional Sampling Strategies for Speeded-Up RANSAC”. In BMVC (pp. 1-11). 2009.
- [69] Renuka D-S ‘Image Mosaicing Using Phase Correlation And Feature Based Approach: A Review ‘.ECE Dept, G. Narayanamma Institute of Technology& Science Shaikpet ,Hyderabad, India.2016.
- [70] Adel, Ebtsam, Mohammed Elmogy, and Hazem Elbakry. "Real time image mosaicing system based on feature extraction techniques." *2014 9th International Conference on Computer Engineering & Systems (ICCES)*. IEEE, 2014.
- [71] Arya Mary K J , Dr. Priya S ‘Panoramic Image Stitching based on Feature Extraction and Correlation’. International Journal of Innovative Research in Science, Engineering and Technology (IJIRSET). Volume 6, Special Issue 6, 2017.
- [72] Ghannam, Sherin, and A. Lynn Abbott. "Cross correlation versus mutual information for image mosaicing." *International Journal of Advanced Computer Science and Applications (IJACSA)*2013.

- [73] Rankov, Vladan, et al. "An algorithm for image stitching and blending." *Three-Dimensional and Multidimensional Microscopy: Image Acquisition and Processing XII*. Vol. 5701. International Society for Optics and Photonics, 2005.
- [74] Liu, Changying, et al. "Normalized cross correlation image stitching algorithm based on minimum spanning tree." *Optik* 179 . pp 610-616.2019.
- [75] S.P Mallick , “ Feature Based Image Mosaicing ” . Department of Electrical and Computer Engineering, University of California, San Diego.
- [76] Z. Zhang , R. Deriche , O. Faugeras & Q. Luong, “ A robust technique for matching two uncalibrated images through the recovery of the unknown epipolar geometry ”. *Artificial Intelligence Journal*. pp 78-87. 1995.
- [77] T.A.S Coito , “ Building and Evaluation of a Mosaic of Images using Aerial Photographs”. Dept. Engenharia Mecânica, Instituto Superior Técnico . 2012.
- [78] H. Djebli, “ La mosaïque d’images ”. Thème de Magister, l’Ecole Nationale Supérieure d’Informatique . Algerie . 2012
- [79] Ming Li ,Deren Li , Dengke Fan (A Study on automatic UAV image mosaic method for paroxysmal disaster). *International Archives of the Photo grammetry, Remote Sensing and Spatial Information Sciences*. Melbourne, Australia. 2012.
- [80] Cheng-Chuan Chou , Shih-Ming Huang and Ching-Chun Huang. “Image Registration among UAV Image Sequence and Google Satellite Image Under Quality Mismatch” *The 12th International Conference on ITS Telecommunication*. pp 311-315. 2012
- [81] Hadrović, E., Osmanović, D and Velagić J. “Aerial image mosaicing approach based on feature matching”. In *International Symposium ELMAR* (pp. 177-180). IEEE. 2017.
- [82] Botterill, T., Mills, S., and Green, R. “Real-time aerial image mosaicing”. In *25th International Conference of Image and Vision Computing New Zealand* (pp. 1-8). IEEE. 2010.
- [83] LI, Xinghua, HUI, Nian, SHEN, Huanfeng, et al. ‘A robust mosaicking procedure for high spatial resolution remote sensing images’. *ISPRS journal of Photogrammetry and Remote Sensing* , vol. 109, pp 108-125. 2015
- [84] S. Ait-Aoudia, R. Mahiou, H. Djebli, E. Guerrou, ‘Satellite and Aerial Image Mosaicing - A Comparative Insight’, *16th International. Conference on Information Visualisation*, Montpellier, France, 2012.

- [85] Panchal, P. M., Panchal, S. R., and Shah, S. K. "A comparison of SIFT and SURF". *International Journal of Innovative Research in Computer and Communication Engineering*, 1(2), 323-327. 2013.
- [86] Bu, S., Zhao, Y., Wan, G., and Liu, Z. 'Map2DFusion: Real-time incremental UAV image mosaicing based on monocular slam'. *Intelligent Robots and Systems (IROS'16), IEEE/RSJ International Conference on. IEEE*, pp 4564-4571 .2016
- [87] Nagaraja, S., Prabhakar, C.J., and Praveen Kumar, P.U. 'Parallax effect free mosaicing of underwater video sequence based o texture features' . *Signal & Image Processing: An International Journal (SIPIJ) Vol.5, No.5*. 2014.
- [88] Beckouche, S., Leprince, S., Sabater, N., & Ayoub, F. ' Robust outliers detection in image point matching'. In *Computer Vision Workshops (ICCV Workshops), IEEE International Conference on IEEE* .pp. 180-187.. 2011.
- [89] Rabin J, Delon J, Gousseau Y, and Moisan L. 'Mac-ransac:a robust algorithm for the recognition of multiple objects'. In *3D'PVT*, 2010.
- [90] **Lati,A., Irki, Z.,Nemra,A., Sakhi, S., and Hamarlain, M., "Implementation of LBP based image mosaicing algorithm on FPGA using Nios II softcore." 2015 4th International Conference on Electrical Engineering (ICEE). IEEE, 2015.**
- [91] **Lati, A., Belhocine, M., and Achour,. "Adapted LBP Based Fast Image Mosaicing Algorithm for UAV Images." International Conference on Electrical Engineering and Control Applications. Springer, Cham, 2017.**
- [92] Lotfi A-Z ' Fuzzy Logic Systems: Origin, Concepts, And Trends' . *omputer Science Division Department of EECS UC Berkeley. Hong Kong* .2004.
- [93] **Lati, A., Belhocine, M., and Achour, N. Efficient Fuzzy based Image Mosaicing Algorithm for Overlapped Aerial Images. ICINCO. Volume 2, ISBN 978-989-758-321-6, pages 229-236. DOI: 10.5220/0006826702390246. 2018.**
- [94] **Lati, A, Belhocine M, and Achour N. "Robust aerial image mosaicing algorithm based on fuzzy outliers rejection." Evolving Systems. pp 1-13.doi.org/10.1007/s12530-019-09279-4. 2019.**
- [95] Yehu Sh, "Efficient normalized cross correlation calculation method for stereo vision based robot navigation",*Frontiers of Computer Science in China*, Volume 5, Issue 2, pp 227-235. 2011.

- [96] S. Ning, J.Zhenhai and Z. Cairong, " Gender classification based on local binary pattern ". Journal of Huazhong University of Science and Technology .Pages 177-181. Chinese. 2007.
- [97] Z. Zhou, " FPGA Implementation of Computer Vision Algorithm ". A thesis submitted in partial satisfaction of the requirement for the degree of Master of Science in Electrical Engineering. University of California (Riverside), 2014.
- [98] X. Zhou et al., Real-time joint landmark recognition and classifier generation by an evolving fuzzy system, IEEE International Conference on Fuzzy Systems, pp 1205-1212, 2006.
- [99] AerialRobotics Dataset. <ftp://www.aerialrobotics.eu/> accessed: 2014-03-30.
- [100] Saravanan, C. "Color image to grayscale image conversion." 2010 Second International Conference on Computer Engineering and Applications. Vol. 2. IEEE, 2010.
- [101] Mikolajczyk, Krystian, and Cordelia Schmid. "Indexing based on scale invariant interest points." International Conference on Computer Vision (ICCV'01). Vol. 1. IEEE Computer society, 2001.
- [102] Paalanen P, Kämäräinen J.-K and Kälviäinen H. 'Image Based Quantitative Mosaic Evaluation with Artificial Video', 16th Scandinavian Conference, SCIA, Oslo, Norway. pp 470-479. 2009.
- [103] Hassaballah, M., Abdelmgeid, AA., and Hammam, A.'Image Features Detection, Description and Matching'. Springer International Publishing Switzerland. 2016.
- [104] Reeff, M., Gerhard, F., Cattin, P. C., & Székely, G. . 'Mosaicing of Endoscopic Placenta Images'. GI Jahrestagung (1), , pp 467-474. 2006.
- [105] Laroze, M., Courtrai, L., & Lefèvre, S. . 'Human Detection from Aerial Imagery for Automatic Counting of Shellfish Gatherers'. In VISIGRAPP .(pp. 664-671). 2016.
- [106] Bhushan, R., & Sunkaria, R. K. . 'A novel technique of image mosaicing based on discrete wavelet transform and its performance evaluation'. International Journal of Computer Applications, 98(15). 2014.
- [107] Navaee, Shahnám. "Computing and programming with LabVIEW." age 9.2004.
- [108] Ruiz, Mariano, et al. "IRIO technology: Developing applications for advanced DAQ systems using FPGAs." 2016 IEEE-NPSS Real Time Conference (RT). IEEE, 2016.
- [109] Alahi, A., Ortiz, R., & Vanderghenst, P. Freak: Fast retina keypoint. In Computer Vision and Pattern Recognition (CVPR), 2012 IEEE Conference on (pp. 510-517). Ieee.2012.

- [110] Leutenegger, Stefan, Margarita Chli, and Roland Y. Siegwart. "BRISK: Binary robust invariant scalable keypoints", 2011 IEEE International Conference on Computer Vision (ICCV). IEEE, 2011.
- [111] Images data set :<https://www.imaging-resource.com/news/2016/08/12/serge-ramelli-takes-the-dji-phantom-4-for-a-spin-drone-photography>.
- [112] aseini, M.S. New Methods for Image Registration and Normalization using Image Feature Points. These Doctorat, University of Victoria, 2008.
- [113] Subramanian, T., Madbhavi, R., Potadar, S., D'souza, S. J., and Gangadharan, K. V. "Object Follower and Barrier Escaping Robot Using Image Processing", International Journal of Innovative Research in Science, Engineering and Technology, ISSN(Online) : 2319-8753, 2015.
- [114] Divya, M. "Single Object Tracking System By Using Labview." International Journal on Recent and Innovation Trends in Computing and Communication, pp 52-56. 2016.
- [115] Holonec, Rodica, et al. "Object Tracking System using Stereo Vision and LabVIEW Algorithms." Acta Electrotehnica 55.1-2 . 71-76. 2014.
- [116] Chaitra, J. M., & AV, R. K. "Smart Autonomous Camera Tracking System Using my RIO With LabVIEW". American Journal of Engineering Research (AJER). Volume-7, Issue-5, ISSN: 2320-0847. pp-408-413, 2018.

Scientific Products

Scientific Products

Most of the results presented in our thesis were validated by participating in international conferences and through publishing in Scopus journal. These papers have been published in proceedings of international libraries and cited in different sections of the rapport:

- Lati, A., Belhocine, M., and Achour,. "Adapted LBP Based Fast Image Mosaicing Algorithm for UAV Images." *International Conference on Electrical Engineering and Control Applications*. Constantine (Algeria), 2017.
- Lati A., Belhocine M., and Achour N. "Adapted LBP Based Fast Image Mosaicing Algorithm for UAV Images". In: Chadli M., Bououden S., Ziani S., Zelinka I. (eds) *Advanced Control Engineering Methods in Electrical Engineering Systems. ICEECA 2017. Lecture Notes in Electrical Engineering*, vol 522. pp 429-442. Springer, Cham. DOIhttps://doi.org/10.1007/978-3-319-97816-1_32.2019.
- Lati, A., Belhocine, M., and Achour, N. Efficient Fuzzy based Image Mosaicing Algorithm for Overlapped Aerial Images. *ICINCO*. Volume 2, ISBN 978-989-758-321-6, pages 229-236. DOI: 10.5220/0006826702390246. 2018.
- Lati, A, Belhocine M, and Achour N. "Robust aerial image mosaicing algorithm based on fuzzy outliers rejection." *Evolving Systems*. pp 1-13.doi.org/10.1007/s12530-019-09279-4. 2019.

Appendix :
Non-linear Algorithms
For Homography Estimation

Introduction

Typically, homographies are estimated between images by finding feature correspondences in those images. The most commonly used algorithms make use of point feature correspondences, though other features can be used as well, such as lines or conics. Linear algorithm for homography estimation was discussed in the second chapter, and in this appendix; we will discuss some non-linear algorithms which are based on minimizing some cost functions.

Different cost functions

In the case where there are more than 4 point correspondences available, the problem is to solve for a homography that minimizes a suitable cost function. The most cost functions that are used in practice are the following:

1. Algebraic distance

The simplest cost function is to minimize the algebraic distance. That is, we minimize the norm $\|\mathbf{A}\mathbf{h}\|$. To ensure that the \mathbf{h} that is selected isn't the zero vector we add the constraint that $\|\mathbf{h}\|=1$ (this 1 is selected arbitrarily).

The solution to this problem is the unit singular vector corresponding to the smallest singular value of \mathbf{A} . This can be found using Singular Value Decomposition (**SVD**) analysis.

While this is a simple linear cost function that is computationally cheap, its disadvantage is that the quantity being minimized is not geometrically meaningful.

2. Geometric distance

The geometric distance measures the Euclidian image distance between where the homography maps a point and where the point's correspondence was originally found. Another term for this is *the transfer error*. Assuming there are only errors in the second image, the total transfer error for a set of correspondences $x_i \rightarrow x_i'$ is:

$$\sum_i d(x_i', Hx_i)^2 \tag{A-1}$$

Where

- **H**: is the estimated homography.
- **d (, .)**: is the Euclidian image distance between two points.

In the more realistic case of there being errors in both images we minimize *the symmetric transfer error* where both the forward (H) and backward (H^{-1}) transformations are taken into account.

The symmetric transfer error is calculated as:

$$\sum_i d(x_i', Hx_i)^2 + d(x_i, H^{-1}x_i')^2 \quad (\text{A-2})$$

The estimated homography H will be the one for which equation (2) is minimized.

To minimize this or the following cost function, an iterative approach is required. While the results often are more accurate, iterative techniques have disadvantages compared to linear algorithms such the one for minimizing Algebraic distance. Iterative algorithms are slower, risk not converging and present additional problems such as picking initial estimates and stopping criteria.

3. Re-projection error

The re-projection error cost function aims to make a correction for each correspondence. The goal is to find the homography \hat{H} along with the set of correspondence points \hat{x}_i and \hat{x}_i' such that the following function is minimized:

$$\sum_i d(x_i', \hat{x}_i')^2 + d(x_i, \hat{x}_i)^2 \quad (\text{A-3})$$

Subject to $\hat{x}_i' = \hat{H}\hat{x}_i$

Minimizing this cost function is more complicated than geometric distance as it requires determining both \hat{H} and the set of correspondences \hat{x}_i' and \hat{x}_i as opposed to just finding H. The term re-projection error is used because this cost function is analogous to estimating a real world point \hat{X}_i from the originally found correspondence $x_i \leftrightarrow x_i'$ that is then re-projected to the estimated perfectly matched correspondence $\hat{x}_i \leftrightarrow \hat{x}_i'$.

4. Sampson error

The algebraic cost function is computationally cheap to compute but doesn't always provide intuitive results. On the other hand, the geometric and re-projection error cost functions provide very accurate results but their minimization algorithms are iterative and thus quite complex. The Sampson error cost function lies in between these two extremes in terms of computation cost and provides a close approximation to re-projection error.

A point correspondence $(x_i, y_i) \leftrightarrow (x'_i, y'_i)$ can be represented as a 4D point X_i . The re-projection error cost function can then be interpreted as finding the algebraic variety V_H that passes through the points X_i . An algebraic variety is a generalization to n dimensions of an algebraic curve so in this case we are looking for a curve in 4D. Since this will likely not exist due to errors in the correspondences, minimizing the re-projection error involves letting V_H be a variety corresponding to a homography transformation H , and for each X_i , letting \hat{X}_i be the closest point to X_i on V_H . The function to minimize then becomes:

$$\sum_i \| X_i - \hat{X}_i \|^2 \quad (\text{A-4})$$

As mentioned above, the vector \hat{X}_i can only be estimated via iteration. The Sampson error function estimates a first order approximation to \hat{X}_i using a Taylor expansion.



M LATI Abdelhai né le 14/02/1990 à El Oued, a obtenu son Baccalauréat série Sciences Expérimentales en 2008. Il est titulaire d'un diplôme d'ingénieur d'État en Génie Électrique et Electronique option Automatique de l'Institut de Génie Electrique et Electronique (Ex-INELEC) de l'Université M'hamed Bougara de Boumerdès en 2013. Il a obtenu son Magister en Automatique, option «Contrôle et Commande» de l'École Militaire Polytechnique (Ex-ENITA) en 2015. Il s'est inscrit depuis Décembre 2015 à l'USTHB pour une formation de Doctorat de Sciences en Electronique, option «Contrôle de Processus et Robotique». Son recherche est orientée vers les systèmes embarqués et la vision par ordinateur.

Abstract - The use of Unmanned Aerial Vehicles (UAVs) imagery for acquiring data is constantly evolving, due to the ease of use and low data acquisition costs. All of these made UAVs very popular and widely used in different purposes. For most cases, the acquired UAV images need further more processing before being analysed, and that because of changing illumination condition in aerial environment and fog generated with UAV flying speed. Image mosaicing is a practical solution for these problems; in which overlapping views of the same scene are combined to form a large image with high quality. The common problem associated with image mosaicing algorithms is the false associations (outliers) produced when defining the overlapping region between every two successive views. Our work presents image mosaicing algorithms based on efficient fuzzy techniques for outliers rejection. Our proposed methods are based on using classical features matching methods (correlation, LBP and RANSAC) with fuzzy inference systems in order to separate between inliers and outliers. The experimental results prove that the proposed methods have good performance for aerial images and give better results when compared to other techniques.

Keywords – *Aerial images, Image mosaicing, Features matching, Fuzzy outliers rejection.*

Résumé – L'utilisation de l'imagerie des UAV pour l'acquisition de données est en constante évolution, grâce à la facilité d'utilisation et les faibles coûts. Tous ces avantages ont rendu les UAV très populaires et largement utilisés à différentes besoins. Dans la plupart des cas, les images aériennes acquises nécessitent un traitement avant d'être analysées, car le changement des conditions d'éclairage dans l'environnement aérien et du brouillard généré par la vitesse de l'UAV. Le mosaïquage d'images est une solution pratique à ces problèmes, dans lequel des vues chevauchées sont combinées pour former une grande image de bonne qualité. Le problème commun associé aux algorithmes de mosaïquage d'image sont les fausses associations générées lors de la détermination de correspondances de primitives. Notre travail présente des algorithmes de mosaïquage d'images basés sur des techniques floues efficaces pour le rejet des fausses associations. Les techniques que nous proposons sont basées sur l'utilisation de méthodes classiques de correspondance de primitives (corrélation, LBP et RANSAC) avec des systèmes d'inférence floue afin de séparer les vrais et fausses associations. Les résultats expérimentaux prouvent que les méthodes proposées ont de bonnes performances pour les images aériennes et donnent de meilleurs résultats par rapport aux autres techniques.

Mots-clés - *Images aériennes, Mosaïquage des images, Correspondance des primitives, Rejet flou des fausse associations.*

ملخص - إن استخدام تصوير الطائرات بدون طيار هو في تطور مستمر. وذلك راجع لسهولة استعمالها و انخفاض تكاليفها. مما جعلها معروفة على نطاق واسع و مستخدمة في عدة اغراض. لكن في معظم الحالات تحتاج هذه الصور الى بعض المعالجة قبل تحليلها. و ذلك بسبب تغير شروط الاضاءة في البيئة الجوية و الضباب الناتج عن سرعة التحليق. فسيفساء الصورة هي حل عملي لهذه المشاكل. حيث يتم دمج صور متداخلة لنفس المشهد من اجل تشكيل صورة كبيرة ذات جودة عالية. المشكلة الشائعة و المرتبطة بخوارزميات فسيفساء الصور هي الارتباطات الخاطئة (القيم المتطرفة) الناتجة عند تحديد المنطقة المتداخلة بين كل صورتين متتاليتين. نعرض في عملنا هذا خوارزميات بناء فسيفساء معتمدين على تقنيات ضبابية فعالة لرفض القيم المتطرفة. حيث سنعتمد على طرق كلاسيكية لمطابقة النقاط الدالة بين الصور. ثم سنستخدم انظمة استدلال غامضة من اجل الفصل بين قيم الارتباط الصحيحة و المتطرفة. تثبت النتائج التجريبية أن الطرق المقترحة لها أداء جيد للصور الجوية وتعطي نتائج أفضل بالمقارنة مع تقنيات أخرى.

كلمات مفتاحية - *الصور الجوية ، صورة الفسيفساء ، مطابقة النقاط الدالة ، الرفض الغامض للقيم المتطرفة.*